

**Characterizing Sources and Identifying Pathways of Urban Metal Contamination at the  
Groundwater-Soil Interface**

by

**Angela Rena Mullins**

Bachelor of Science, The College of William and Mary, 2014

Submitted to the Graduate Faculty of the  
Dietrich School of Arts and Sciences in partial fulfillment  
of the requirements for the degree of  
Doctor of Philosophy

University of Pittsburgh

2020

UNIVERSITY OF PITTSBURGH

DIETRICH SCHOOL OF ARTS AND SCIENCES

This dissertation was presented

by

**Angela Rena Mullins**

It was defended on

October 9, 2020

and approved by

Mark Abbott, Professor, Geology and Environmental Science

Emily Elliott, Professor, Geology and Environmental Science

Anne Jefferson, Associate Professor, Kent State University, Department of Geology

Josef Werne, Professor, Geology and Environmental Science

Thesis Advisor: Daniel J. Bain, Associate Professor, Geology and Environmental Science

Copyright © by Angela Rena Mullins

2020

# **Characterizing Sources and Identifying Pathways of Urban Metal Contamination at the Groundwater-Soil Interface**

Angela Rena Mullins, PhD

University of Pittsburgh, 2020

Urban processes modify the landscape, disturbing natural groundwater flow and introducing chemical contaminants to the soil and groundwater. Therefore, urban groundwater can reroute contaminants, transporting metals and nutrients from surface runoff through the subsurface environment and reintroducing them to soils and rivers. Although groundwater connects surface runoff to receiving rivers and streams, few studies have documented the long-term impacts of urbanization on groundwater chemistry or the effects of contaminated groundwater on soil contamination patterns.

This dissertation examines metal contamination in both surface soils and near surface groundwater. The observed interaction between urban hydrology and legacy contamination reveals critical zone chemical dynamics with important implications for urban environments. In particular, the fate of urban metal contamination through the groundwater-soil interface in Pittsburgh, PA is examined by 1) exploring geochemical consequences of human interventions to reduce rapid runoff and associated hydrogeochemical impacts from green infrastructure installation, 2) analyzing transport of contaminants through urban groundwater systems using an elevational transect of discharging springs, and 3) examining the potential for soil metal accumulation at points of interaction between contaminated groundwater and soils.

This research revealed fundamental interactions between urban soils and groundwater: 1) Stormwater captured and introduced to shallow groundwater through road-side infiltration-based

green infrastructure changed water chemistry. The primary drivers were winter loadings of road de-icer and the formation of a reducing environment in the summer. 2) Groundwater spring chemistry is remarkably consistent across a series of strata aquifers despite substantial differences in distance from recharge zones. Further, this consistency in chemistry occurred even as silicon concentrations indicated the waters are a mix of short and long residence time waters. 3) Spring water discharge enriched with transition metals increases soil metal concentrations downslope of the springs. Using total, exchangeable, and pore water metal chemistries, records of legacy metal enrichment were found in soils receiving spring water over multiple time scales from months to decades. This pattern has the potential to create hot spots of soil metal contamination in urban landscapes.

This dissertation characterizes the fate of urban contaminants through the groundwater-soil interface, improving our ability to predict spatial patterns of urban soil contamination.

## Table of Contents

Preface.....	xvii
<b>1.0 Introduction.....</b>	<b>1</b>
<b>1.1 Bibliography.....</b>	<b>7</b>
<b>2.0 Seasonal Drivers of Chemical Flux from Roadside Infiltration-Based Green Infrastructure .....</b>	<b>13</b>
<b>2.1 Introduction .....</b>	<b>13</b>
<b>2.2 Materials and Methods .....</b>	<b>15</b>
<b>2.2.1 Study Site .....</b>	<b>15</b>
<b>2.2.2 Sample Collection and Analysis.....</b>	<b>18</b>
<b>2.2.3 Infiltration Rate Calculation and Chemical Flux Estimation.....</b>	<b>19</b>
<b>2.3 Results and Discussion .....</b>	<b>21</b>
<b>2.3.1 Water Infiltration from Trenches.....</b>	<b>21</b>
<b>2.3.2 Seasonal Patterns in Infiltration Rate.....</b>	<b>22</b>
<b>2.3.3 Dissolved Metal and Nutrient Concentration Patterns in Infiltration Trenches .....</b>	<b>24</b>
<b>2.3.4 Sodium Pulse and Sodium Driven Patterns in Dissolved Metal Concentration .....</b>	<b>28</b>
<b>2.3.5 Oxidation/Reduction Dynamics Observed in Metal and Nutrient Concentrations .....</b>	<b>30</b>
<b>2.3.6 Unexplained Patterns Observed in Zinc and Chromium.....</b>	<b>33</b>
<b>2.4 Conclusions .....</b>	<b>35</b>

2.5 Bibliography.....	36
<b>3.0 Groundwater Flow and Geochemistry in Urban Aquifers of the Appalachian Plateau.....</b>	<b>42</b>
<b>3.1 Introduction .....</b>	<b>42</b>
<b>3.2 Materials and Methods .....</b>	<b>46</b>
3.2.1 Study Site .....	46
3.2.2 Sample Collection and Analysis.....	47
3.2.3 Antecedent Precipitation .....	48
<b>3.3 Results.....</b>	<b>48</b>
3.3.1 Ca/Sr Ratios in Discharging Spring Water and Aquifer Source.....	48
3.3.2 Silicon Concentrations and Water Residence Time.....	52
3.3.3 Nitrogen and Oxygen Isotopes of Nitrate .....	54
<b>3.4 Discussion .....</b>	<b>55</b>
3.4.1 Short-term Dynamics in Groundwater Spring Chemistry.....	55
3.4.2 Dissolved metal Concentrations in Spring Water Discharge.....	57
3.4.3 Nitrate in Urban Springwater .....	60
<b>3.5 Conclusions .....</b>	<b>62</b>
<b>3.6 Bibliography.....</b>	<b>64</b>
<b>4.0 Spring Water Discharge as a Mechanism for Legacy Metal Enrichment in Urban Soils.....</b>	<b>68</b>
<b>4.1 Introduction .....</b>	<b>68</b>
<b>4.2 Methods .....</b>	<b>71</b>
4.2.1 Sample Collection and Analysis.....	71

4.2.2 Metal Concentration Measurements .....	73
4.2.3 Metal Phase Concentration Interpretation.....	74
4.3 Results.....	76
4.3.1 Upslope/Downslope Differences.....	76
4.3.2 Lithium Concentrations and Spring Water Enrichment .....	77
4.3.3 Steel Alloy Metal Patterns .....	80
4.3.3.1 Cobalt.....	80
4.3.3.2 Chromium .....	83
4.3.3.3 Nickel .....	86
4.3.3.4 Vanadium .....	89
4.4 Discussion .....	91
4.4.1 Lithium Concentrations .....	91
4.4.2 Metal Concentrations in Soils Surrounding Groundwater Springs.....	92
4.4.3 Confounding Effects of Urban Soil Redistribution.....	95
4.4.4 Total Metal Concentrations .....	96
4.5 Conclusions .....	97
4.6 Bibliography.....	98
Appendix A Chapter 2 Supporting Information .....	102
Appendix A.1 Bibliography .....	108

**List of Tables**

**Table 3-1. Average nitrate isotopic values, slope, and R<sup>2</sup> from all samples collected divided by sampling location. .... 55**

**Table 4-1. P-values resulting from student’s t-tests comparing concentrations of pore water, exchangeable, and Fe-normalized total Li, Co, Cr, Ni, and V collected upslope and downslope of spring discharge. Samples were divided by sampling location. The “\*” indicates a statistically significant difference between populations. .... 76**

**Table 4-2. P-values resulting from student’s t-tests comparing concentrations of pore water, exchangeable, and Fe-normalized total Li, Co, Cr, Ni, and V collected upslope and downslope of spring discharge. The “\*” indicates a statistically significant difference between populations..... 77**

**Table 4-3. Maximum, minimum, average, and coefficient of variation of pore water, Fe-normalized total, and exchangeable concentrations of Co, Cr, Ni, and V measured in soil cores across all transects..... 80**

**Table 4-4. Range of average total soil metal concentrations of Co, Cr, Ni, and V measured upslope and downslope of discharging springs divided by transect. Average total metal concentrations in other urban soil surveys. Maximum total concentrations measured in this study and maximum concentrations for ecological health..... 94**

**Appendix Table A-1. Maximum, minimum, average, and standard deviation of concentrations of dissolved cations and anions in two infiltration trenches over the entire time of collection (January 2016 – January 2018). (BDL = Below Detectable Limit)..... 106**

**Appendix Table A-2. Comparison of total range of dissolved metal and nutrient concentrations measured in the upper infiltration trench (UT) and lower infiltration trench (LT) water between January 2016 – December 2017 and June 22, 2018 – June 28, 2018..... 107**

**Appendix Table A-3. Average bulk metal soil concentrations collected in Pittsburgh, PA compared to concentrations measured in previous studies of urban soil contamination..... 107**

**List of Figures**

**Figure 2-1. Location of infiltration trenches and groundwater spring in Schenley Park, Pittsburgh (Allegheny County Imagery 2017). The blue circle indicates the location of a groundwater spring and the gray boxes outline the infiltration trenches. .... 16**

**Figure 2-2. Stormwater capture and diversion to infiltration trench conceptual design. Gray dotted line indicates design flaw where pipe to sewer is a lower elevation than pipe to level spreader..... 17**

**Figure 2-3. Continuous record of A) precipitation and water elevation in the B) Lower Trench and C) Upper Trench from January 2016 to December 2017. 0 indicates the bottom of each trench. .... 20**

**Figure 2-4. Observed infiltration rates (red triangles & blue circles) compares with proportional predicted changes in water infiltration (black boxes) using the water temperature at the beginning of the storm event. Gray areas indicate periods of low evapotranspiration activity determined by observed patterns in the local water table. .... 21**

**Figure 2-5. Dissolved concentrations of chemicals influenced by road de-icer application in the upper trench (red triangles) and lower trench (blue circles) between January 2016 and December 2017. Blue boxes indicate approximate times during the year in which road de-icers were applied. .... 25**

**Figure 2-6. Dissolved concentrations of chemicals influenced by inferred reduced conditions in the upper trench (red triangles) and lower trench (blue circles) between January**

2016 and December 2017. Black arrows indicate timing of chemical responses to the formation of a reducing environment. .... 27

**Figure 2-7. Conceptual model showing seasonal changes in water table and contaminants introduced to roadside infiltration trenches..... 31**

**Figure 2-8. Dissolved concentrations of A) Cr and B) Zn measured in the upper trench (red triangles) and lower trench (blue circles) between January 2016 and December 2017 ..... 33**

**Figure 3-1. Conceptual model demonstrating multiple possible recharge sources to perched water tables in study area..... 45**

**Figure 3-2. A) Aerial imagery of the study area in Schenley Park (Pittsburgh, PA) (Allegheny County Imagery 2017) B) elevation transect extracted from LiDAR DEMs (PA Map Program 2008) showing the relative elevations of groundwater spring collection sites. And C) aerial imagery of the study area with groundwater well and precipitation gauge. Confining layers are hypothetical and connectivity between springs may be greater than illustrated..... 46**

**Figure 3-3. Molar ratio of dissolved Ca and Sr measured in four groundwater springs between August 30, 2017 and April 10, 2019. Dotted lines indicate periods where samples were not collected due to frozen or dry conditions..... 49**

**Figure 3-4. Concentrations of dissolved A) P, B) Pb, C) Cr, D) Cd, and E) Fe measured in four groundwater springs between August 30, 2017 and April 10, 2019. Dotted lines indicate times during which sampling were not collected due to frozen or dry conditions. .... 51**

**Figure 3-5. Concentrations of dissolved Si measured in four groundwater springs between August 30, 2017 and April 10, 2019. Dotted lines indicate times during which sampling were not collected due to frozen or dry conditions. .... 52**

**Figure 3-6. Concentrations of dissolved Si measured in four groundwater springs between August 30, 2017 and April 10, 2019 plotted against the time between the most recent storm and sample collection. Orange dotted line indicates average groundwater Si concentration (based on 15 samples) measured in local groundwater wells. Orange box indicates range of Si concentrations in these groundwater samples. Blue dotted line indicates average precipitation Si concentration measured in samples collected within the watershed (15sample) The solid black line is LOESS fit. .... 53**

**Figure 3-7. A) Concentrations of  $\text{NO}_3^-$  measured in four groundwater springs between August 30, 2017 and April 10, 2019. Dotted lines indicate times during which samples were not collected due to frozen or dry conditions. B) Results from dual isotope analysis of nitrate in groundwater spring samples. C) data cluster in “human-animal waste” section of plot. X indicates average isotope compositions measured in groundwater collected from local groundwater wells. (Figure modified from (Kendall et al. 2007) ..... 54**

**Figure 3-8. A) Cr, B) P, and C) Pb concentrations measured in four groundwater springs between August 30, 2017 and April 10, 2019 compared to hours between last storm event and time of sample collection. Orange dotted lines indicate average groundwater concentrations. Blue dotted lines indicate average precipitation concentrations. Orange box indicates range of concentrations measured in groundwater samples..... 58**

**Figure 3-9. NO<sub>3</sub><sup>-</sup> concentrations measured in four groundwater springs between August 30, 2017 and April 10, 2019 compared to hours between last storm event and time of sample collection. .... 62**

**Figure 4-1. Conceptual profiles of soil metal concentrations surrounding a groundwater spring discharge location. Soil metal concentrations are expected to spike at the point of discharge, then decrease as distance from the spring increases downslope..... 70**

**Figure 4-2. Study area in Schenley Park (Pittsburgh, PA) with transect locations (hillshade of LiDAR DEM (PAMAP Program, PA Department of Conservation and Natural Resources 2006-2008)) ..... 71**

**Figure 4-3. LiDAR extracted elevation transects of elevations at the four sampling locations. Blue circles indicate locations of soil cores. Yellow star indicates approximate location of groundwater springs within the transect. (PAMAP Program, PA Department of Conservation and Natural Resources 2006-2008). Y-axes are adjusted to all span 3.5 meters of elevation. .... 73**

**Figure 4-4. Total, Fe-normalized, exchangeable, and pore water Li measured in soil cores collected along four transects intersecting groundwater springs. Black dotted lines indicate location of groundwater discharge along transect. .... 79**

**Figure 4-5. Total, Fe-normalized, exchangeable, and pore water Co measured in soil cores collected along four transects intersecting groundwater springs. Black dotted lines indicate the location of groundwater discharge ..... 82**

**Figure 4-6. Total, Fe-normalized total, exchangeable, and pore water Cr measured in soil cores collected along four transects intersecting groundwater springs. Black dotted lines indicate the location of groundwater discharge ..... 85**

**Figure 4-7. Total, Fe-normalized total, exchangeable, and pore water Ni measured in soil cores collected along four transects intersecting groundwater springs. Black dotted lines indicate the location of groundwater discharge. .... 88**

**Figure 4-8. Total, Fe-normalized total, exchangeable, and pore water V measured in soil cores collected along four transects intersecting groundwater springs. Black dotted lines indicate the location of groundwater discharge. .... 90**

**Figure 4-9. Total Fe measured in soil cores collected along four transects intersecting groundwater springs. Black dotted lines indicated location of groundwater discharge. .... 95**

**Appendix Figure A-1. Design of fix installed in the upper infiltration trench..... 102**

**Appendix Figure A- 2. Map of soil metal collection points for metal analyses surrounding infiltration trenches in Schenley Park, Pittsburgh, PA (Allegheny County Division of Computer Services Geographic Information Systems Group Allegheny County Imagery 2017)..... 103**

**Appendix Figure A-3. Example infiltration event measured to calculate infiltration rate from the lower trench..... 103**

**Appendix Figure A-4. Groundwater table fluctuations showing the onset of evapotranspiration diurn diurnal patterns starting on April 12, 2016. .... 104**

**Appendix Figure A-5. Box plots showing seasonal distributions of infiltration rates for both infiltration trenches ..... 105**

**Appendix Figure A-6. Comparison of change in infiltration rate compared to changes in temperature. Black line indicates highest possible infiltration rate calculated using**

**temperature driven viscosity changes. The observed changes in infiltration rate are much higher than those expected of viscosity driven changes..... 105**

**Appendix Figure A-7. Dissolved concentrations of sodium in infiltration trenches and nearby groundwater spring between January 2016 and October 2017..... 106**

**Appendix Figure A-8. Dissolved concentrations of sulfate in infiltration trenches and nearby groundwater spring between October 2016 and October 2017..... 106**

## Preface

Funding for this research was provided by The Pittsburgh Parks Conservancy, The Heinz Foundation, the Richard King Mellon Foundation and the University of Pittsburgh. Several collaborators made this research possible, including Erin Pfeil-McCullough, Kristina Hopkins, Sarah Lavin (all former students at the University of Pittsburgh), and Erin Copeland with the Pittsburgh Parks. I am grateful for their support in both collaboration and the production of data necessary to complete my work.

I would also like to acknowledge everyone who helped with sample collection and analysis. This includes Erin Pfeil-McCullough, Memphis Hill, Becky Tisherman, Marja Copeland, Becky Forgrave, Ian Flynn, Angela Chung, Kayla Maurer, Troy Ferland, Wes Scott, Elliott Arnold, Wyatt Wilson, Juan Castaneda, Blake McCourt, Mary Mullins, and David Mullins. Special thanks go to the alumni and members of the Bain Lab Group who provided valuable feedback throughout the writing process.

I would like to thank my committee members for their expertise and guidance. In particular, I thank my advisor Dan Bain for his patience, understanding, support, advice, and for pushing me to become a better scientist and a better person. Without your encouragement, this thesis would not have happened.

Finally, I would like to thank my family for their love and support. Thank you for encouraging a young girl to explore her interest in science. I also thank my partner, Wyatt Wilson, who has provided constant support and kept me grounded over the past years. To all of you, I will be forever grateful.

## 1.0 Introduction

Between 1950 and 2000, urban land cover in the United States has increased 500% and by 2030, global urban area is projected to increase another 180% (Seto and Kaufmann 2003). This rapid urbanization changes hydrology in unpredictable ways, making it challenging to counteract or prevent its effects. Urban hydrology is heavily influenced by the replacement of natural land surfaces with impervious cover. Increased impervious cover lowers infiltration of precipitation, causing flashier storm responses, increased stormwater runoff volumes, and slope instability from channel incision (Harbor 1994; Walsh et al. 2005; Bhaskar et al. 2015). Decreased infiltration also has the potential to reduce groundwater recharge or change points of recharge and discharge (Paul and Meyer 2001). Groundwater recharge and base flow are lower in some regions of urban development while groundwater elevation and base flow can also increase in urban areas due to water supply pipe leakage, reduced evapotranspiration, or discharge of wastewater from imported or confined water (Walsh et al. 2005; Bhaskar et al. 2015).

Urban stormwater is rich in contaminants such as nutrients, suspended sediments, and heavy metals and these pollutants often accumulate in roadside environments (Hogan and Walbridge 2007). Metal contamination sources for urban runoff include the abrasion of car breaks and tires and weathering of paints and metals from buildings (Ni, Cr, Pb, Cu, and Zn). Cities with histories of intense industrial activity, like Pittsburgh, also have abundant legacy metal contamination from atmospheric deposition of industrial emissions (Davis et al. 2009). Further, widespread use of leaded gasolines prior to 1986 led to substantial legacy heavy metal contamination in roadside soils (Mielke and Reagan 1998). Trace metals found in urban soils can be toxic when biota including vegetation, animals, and humans are exposed at high enough

concentrations (Hammond and Aronson 1964; Foy et al. 1978; Alexander and Delves 1981; Mielke et al. 1999). Therefore, ecosystem health is likely negatively impacted by the concentration or mobilization of trace metal contamination in urban environments.

While many studies focus on soil contamination or surface water hydrologic change, few have connected soil contamination and groundwater contamination to subsurface transport (e.g. Foos 2003; Bardsley et al. 2015; Gabor et al. 2017). There is a critical need to understand how urban groundwater transports metal contamination, especially from roadside environments, through subsurface groundwater flow. It is also important to characterize the metal contaminant chemistry at the interface between groundwater and soil and points of surface discharge like springs and seeps. This dissertation clarifies subsurface contamination transport, identifies potential locations of novel exposure to humans and ecosystems, and improves our ability to manage these exposures. In particular, this dissertation characterizes urban trace metal contamination with a focus on interactions between infiltration-based green infrastructure, groundwater, springs, and the soils surrounding spring discharge points. This research addresses 1) biogeochemical regimes in infiltration-based green infrastructure installed in a roadside environment, 2) urban spring water chemistry in the context of complicated urban subsurface flow, and 3) the interaction between soil and contaminated groundwater at springs and seeps.

Chapter 2 explores the geochemical consequences of human interventions to reduce rapid runoff and associated impacts to the hydrologic cycle, namely green infrastructure. Low impact development (LID) and green infrastructure (GI) have become popular means of mitigating the negative impacts of urbanization and restoring natural hydrological function (Dietz 2007; Ahiablame et al. 2012). LID is a set of practices that manage runoff as close to the source as possible and green infrastructure, a subset of LID, consists of engineered systems that rely on using

soil and vegetation to capture runoff and reduce flows to drainage collection systems (USEPA). Specifically, infiltration-based GI designs are intended to store stormwater runoff and reroute it to slower soil and ground water flowpaths (Campisano et al. 2011).

GI and LID can reduce surface runoff (Selbig and Bannerman 2007; Davis 2008), however, these structures may also negatively affect the chemical regimes of near road subsurface environments. As previously noted, urban stormwater runoff contains contaminants from a variety of sources (Davis et al. 2009) and roadside soils also contain elevated concentrations of legacy metals (Mielke and Reagan 1998). Road salts increase the mobility of trace metals in soils through cation exchange and chloride complexation (Amrhein et al. 1992; Norrström and Bergstedt 2001; Bäckström et al. 2004). Further, additional saturation of roadside soils resulting from the concentration and introduction of high volumes of road runoff may create anaerobic conditions (Machusick et al. 2011). Therefore, efforts to reduce negative hydrological impacts of urbanization through GI use may create negative impacts in roadside chemical environments. That is, GI may increase subsurface contamination both through the introduction of runoff contamination and the remobilization of legacy contamination.

Although extensive research focuses on road runoff chemistry and hydrological effects of recent GI installation in the United States, the long-term effects of such projects on roadside heavy metal chemistry are not well characterized (Hunt et al. 2006; Hogan and Walbridge 2007; Emerson and Traver 2008). Therefore, the direct consequences of infiltration-based GI on the chemistry of roadside shallow groundwater chemistry remains unclear. The multi-year study on geochemical regimes of infiltration-based GI described in Chapter 2 documents chemical variability arising from seasonal changes in road salt and redox conditions and clarifies how GI systems evolve over time.

Chapter 3 examines transport of contaminants through urban groundwater using discharging springs, an underutilized access point to groundwater in areas where access is difficult. Current characterization of contaminant transport in urban groundwater is limited because groundwater wells are rare in urban areas (Manga 2001). Groundwater springs can be used as an alternative for the characterization of groundwater chemistry as the discharging water reflects the materials through which it moved (Garrels and Mackenzie 1967). Further, multiple measurements taken from groundwater springs over time can clarify sources of water to the spring (Mazor et al. 1985). Therefore, the use of multiple groundwater springs in an urban area can offer insight into the origin of groundwater contamination.

Despite the valuable insight into groundwater processes offered by springs, particularly in regions altered by urbanization, most current groundwater spring studies have focused on regions of karst geology (Vesper 2001; Vesper and White 2003; Heinz et al. 2009). While limited, studies on urban groundwater springs have shown a connection between urbanization and groundwater chemistry. A study measuring road salt contamination found that the volume of surface application and distance from the contaminant source (e.g. roads) controlled concentrations of dissolved Na and Cl in discharging groundwater springs (Foos 2003). Similarly, Gabor et al. (2017) observed that groundwater springs sourced by aquifers recharged in urban areas had higher concentrations of contamination. Therefore, surface contamination created by urbanization can negatively impact groundwater chemistry. Cities located in the Appalachian Plateau are built on a distinct bedrock geology of horizontal, redundant shale or siltstone beds that control flow of groundwater and results in a shallow regional water table and numerous groundwater springs (Sheets and Kozar 2000). This abundance of springs in Pittsburgh makes it an ideal location to study multiple springs as a comparative set across multiple aquifers.

Previous work has identified a connection between surface contamination and groundwater spring chemistry (Foos 2003; Bardsley et al. 2015; Gabor et al. 2017). However, the exact sources of contamination to urban springs remains ambiguous given the complex nature of urban groundwater flow. Chapter 3 characterizes changes in groundwater chemistry in discharging springs, identifying two sources contributing to spring discharge. Separating the precipitation-like, short residence time water source from the groundwater-like, long residence time water source demonstrates a complicated mix of sources contributing contamination to spring discharge.

Finally, the interaction between contaminated groundwater and soils at point of discharge was examined in Chapter 4. Urbanization creates complex patterns of soil contamination through the displacement of native soils and introduction of non-native soils in construction and excavation activities (Ajmone-Marsan and Biasioli 2010). Although soil metal contamination has been mapped in a number of urban settings, the specific mechanisms driving contamination patterns have not been thoroughly examined (e.g. Madrid et al. 2006; Pouyat et al. 2007; Cannon and Horton 2009; Luo et al. 2012; da Silva et al. 2020). Urban aquifers may gather legacy contaminants over their broad recharge zones as water infiltrates through contaminated soils. If this groundwater discharges at distinct points (e.g., springs) then these metals may concentrate at points of discharge. Thus, the subsurface movement of urban contaminants through ground and soil water flow paths and subsequent chemical discharge at springs and seeps can result in points of elevated soil contamination.

Due to the interconnected nature of groundwater and surface water, the impacts of contaminated groundwater discharge on surface water quality have been extensively researched (e.g. Reay et al. 1992; Gallagher et al. 1996; Rivett et al. 2011). This research has found a clear connection between contaminated groundwater springs and reaches with elevated contaminant

loads in streams. In particular, shallow aquifers tend to introduce greater loads of contaminants to surface waters (Kornelsen and Coulibaly 2014). Therefore, urban groundwater has the potential to introduce contamination where it discharges into soils rather than into a body of water. This may result in greater contaminant heterogeneity or elevated concentrations of metal contamination that may pose an environmental risk in surface soils at points of groundwater discharge. Pittsburgh's intense industrial history has resulted in elevated concentrations of heavy metal contamination from atmospheric deposition of industrial emissions (Tarr 2004; Maxim 2019). This makes the city a good location to study the effects of contaminated groundwater discharge on the redistribution of legacy contamination.

Despite extensive research on the contribution of contaminated groundwater to receiving surface waters, the effects of contaminated groundwater on soil receptors have not been well characterized, particularly in urban environments. The comparison of metal concentrations in soils upslope and downslope of groundwater springs described in Chapter 4 evaluates the role of contaminated groundwater discharge on urban soil metal dynamics and demonstrates the potential generation of hot-spots of hazardous soil contamination.

Although it is a vital part of the urban hydrologic cycle, groundwater remains an understudied aspect of urban environments. Knowledge gaps remain in how surface contamination interacts with groundwater and how contaminated groundwater affects soil chemistry. Further, the potential of concentration and transport of these contaminants through the groundwater needs to be clarified. Subsurface transportation of urban contamination may lead to hazardous levels of heavy metals in urban soils in areas where groundwater discharges to the surface. This dissertation characterizes the fate of urban contaminants through the groundwater-soil interface, following

contaminants from stormwater runoff infiltration, through subsurface groundwater conveyance, and finally to contaminated groundwater discharge into surface soils.

## 1.1 Bibliography

- Ahiablame LM, Engel BA, Chaubey I. Effectiveness of low impact development practices: literature review and suggestions for future research. *Water Air Soil Pollut.* 2012 Sep;223(7):4253–4273.
- Ajmone-Marsan F, Biasioli M. Trace elements in soils of urban areas. *Water Air Soil Pollut.* 2010 Nov;213(1-4):121–143.
- Alexander FW, Delves HT. Blood lead levels during pregnancy. *Int Arch Occup Environ Health.* 1981 Feb;48(1):35–39.
- Amrhein C, Strong JE, Mosher PA. Effect of deicing salts on metal and organic matter mobilization in roadside soils. *Environ Sci Technol.* 1992 Apr;26(4):703–709.
- Bäckström M, Karlsson S, Bäckman L, Folkesson L, Lind B. Mobilisation of heavy metals by deicing salts in a roadside environment. *Water Res.* 2004 Feb;38(3):720–732.
- Bardsley AI, Hammond DE, von Bitner T, Buenning NH, Townsend-Small A. Shallow groundwater conveyance of geologically derived contaminants to urban creeks in southern California. *Environ Sci Technol.* 2015 Aug 18;49(16):9610–9619.
- Bhaskar AS, Welty C, Maxwell RM, Miller AJ. Untangling the effects of urban development on subsurface storage in Baltimore. *Water Resour Res.* 2015 Feb;51(2):1158–1181.
- Campisano A, Creaco E, Modica C. A simplified approach for the design of infiltration trenches. *Water Science & Technology.* 2011 Sep;64(6):1362.

- Cannon WF, Horton JD. Soil geochemical signature of urbanization and industrialization – Chicago, Illinois, USA. *Applied Geochemistry*. 2009 Aug;24(8):1590–1601.
- Davis AP. Field performance of bioretention: hydrology impacts. *J Hydrol Eng*. 2008 Feb;13(2):90–95.
- Davis AP, Hunt WF, Traver RG, Clar M. Bioretention technology: overview of current practice and future needs. *J Environ Eng*. 2009 Mar;135(3):109–117.
- Dietz ME. Low Impact Development Practices: A Review of Current Research and Recommendations for Future Directions. *Water Air Soil Pollut*. 2007 Oct 6;186(1-4):351–363.
- Emerson CH, Traver RG. Multiyear and Seasonal Variation of Infiltration from Storm-Water Best Management Practices. *J Irrig Drain Eng*. 2008 Oct;134(5):598–605.
- Foos A. Spatial distribution of road salt contamination of natural springs and seeps, Cuyahoga Falls, Ohio, USA. *Environmental Geology*. 2003 May;44(1):14–19.
- Foy CD, Chaney RL, White MC. The physiology of metal toxicity in plants. *Annu Rev Plant Physiol*. 1978 Jun;29(1):511–566.
- Gabor RS, Hall SJ, Eiriksson DP, Jameel Y, Millington M, Stout T, et al. Persistent urban influence on surface water quality via impacted groundwater. *Environ Sci Technol*. 2017 Sep 5;51(17):9477–9487.
- Gallagher DL, Dietrich AM, Reay WG, Hayes MC, Simmons GM. Ground water discharge of agricultural pesticides and nutrients to estuarine surface water. *Groundwater Monit R*. 1996 Feb;16(1):118–129.

- Garrels RM, Mackenzie FT. Origin of the chemical compositions of some springs and lakes. In: Stumm W, editor. Equilibrium concepts in natural water systems. WASHINGTON, D.C.: AMERICAN CHEMICAL SOCIETY; 1967. p. 222–242.
- Hammond PB, Aronson AL. Lead poisoning in cattle and horses in the vicinity of a ' smelter. Ann N Y Acad Sci. 1964 Apr 24;111:595–611.
- Harbor JM. A Practical Method for Estimating the Impact of Land-Use Change on Surface Runoff, Groundwater Recharge and Wetland Hydrology. Journal of the American Planning Association. 1994 Mar 31;60(1):95–108.
- Heinz B, Birk S, Liedl R, Geyer T, Straub KL, Andresen J, et al. Water quality deterioration at a karst spring (Gallusquelle, Germany) due to combined sewer overflow: evidence of bacterial and micro-pollutant contamination. Environmental Geology. 2009 Apr;57(4):797–808.
- Hogan DM, Walbridge MR. Best management practices for nutrient and sediment retention in urban stormwater runoff. J Environ Qual. 2007 Apr;36(2):386–395.
- Hunt WF, Jarrett AR, Smith JT, Sharkey LJ. Evaluating bioretention hydrology and nutrient removal at three field sites in north carolina. J Irrig Drain Eng. 2006 Dec;132(6):600–608.
- Kornelsen KC, Coulibaly P. Synthesis review on groundwater discharge to surface water in the Great Lakes Basin. J Great Lakes Res. 2014 Jun;40(2):247–256.
- Luo X, Yu S, Zhu Y, Li X. Trace metal contamination in urban soils of China. Sci Total Environ. 2012 Apr 1;421-422:17–30.
- Machusick M, Welker A, Traver R. Groundwater Mounding at a Storm-Water Infiltration BMP. J Irrig Drain Eng. 2011 Mar;137(3):154–160.

- Madrid L, Diaz-Barrientos E, Ruiz-Cortés E, Reinoso R, Biasioli M, Davidson CM, et al. Variability in concentrations of potentially toxic elements in urban parks from six European cities. *J Environ Monit.* 2006 Nov;8(11):1158–1165.
- Manga M. Using springs to study groundwater flow and active geologic processes. *Annu Rev Earth Planet Sci.* 2001 May;29(1):201–228.
- Maxim A. Urban Soils in a Historically Industrial City: Concentration and Biogeochemical Speciation of Trace Metals in Pittsburgh, Pennsylvania. Univeristy of Pittsburgh. 2019;
- Mazor E, Vuataz FD, Jaffé FC. Tracing groundwater components by chemical, isotopic and physical parameters — Example: Schinznach, Switzerland. *J Hydrol (Amst).* 1985 Feb;76(3-4):233–246.
- Mielke HW, Gonzales CR, Smith MK, Mielke PW. The urban environment and children’s health: soils as an integrator of lead, zinc, and cadmium in new orleans, louisiana, U.S.A. *Environ Res.* 1999 Aug;81(2):117–129.
- Mielke HW, Reagan PL. Soil is an important pathway of human lead exposure. *Environ Health Perspect.* 1998 Feb;106 Suppl 1:217–229.
- Norrström AC, Bergstedt E. The Impact of Road De-Icing Salts (NaCl) on Colloid Dispersion and Base Cation Pools in Roadside Soils. *Water, Air, and Soil Pollution.* 2001 Apr 1;127(1-4):281–299.
- Paul MJ, Meyer JL. Streams in the Urban Landscape. *Annu Rev Ecol Syst.* 2001 Nov;32(1):333–365.
- Pouyat RV, Yesilonis ID, Russell-Anelli J, Neerchal NK. Soil Chemical and Physical Properties That Differentiate Urban Land-Use and Cover Types. *Soil Sci Soc Am J.* 2007;71(3):1010.

Reay WG, Gallagher DL, Simmons GM. Groundwater discharge and its impact on surface water quality in a Chesapeake Bay inlet. *J Am Water Resources Assoc.* 1992 Dec;28(6):1121–1134.

Rivett MO, Ellis PA, Mackay R. Urban groundwater baseflow influence upon inorganic river-water quality: The River Tame headwaters catchment in the City of Birmingham, UK. *J Hydrol (Amst).* 2011 Mar;400(1-2):206–222.

Selbig WR, Bannerman RT. Evaluation of Street Sweeping as a Stormwater- Quality-Management Tool in Three Residential Basins in Madison, Wisconsin. US Geological Survey. 2007;

Seto KC, Kaufmann RK. Modeling the Drivers of Urban Land Use Change in the Pearl River Delta, China: Integrating Remote Sensing with Socioeconomic Data. *Land Econ.* 2003 Feb;79(1):106–121.

Sheets CJ, Kozar MD. Ground-Water Quality in the Appalachian Plateaus, Kanawha River Basin, West Virginia.pdf. *Water-Resources Investigations Report.* 2000;99(4269).

Da Silva EB, Gao P, Xu M, Guan D, Tang X, Ma LQ. Background concentrations of trace metals As, Ba, Cd, Co, Cu, Ni, Pb, Se, and Zn in 214 Florida urban soils: Different cities and land uses. *Environ Pollut.* 2020 May;114737.

Tarr JA, editor. *Devastation and renewal: an environmental history of Pittsburgh and its region.* University of Pittsburgh Press; 2004.

Urban Runoff: Low Impact Development | Polluted Runoff: Nonpoint Source (NPS) Pollution | US EPA [Internet]. [cited 2020 Sep 22]. Available from: <https://www.epa.gov/nps/urban-runoff-low-impact-development>

Vesper D. Contaminant transport in karst aquifers. *Theoretical and Applied ....* 2001;

Vesper DJ, White WB. Metal transport to karst springs during storm flow: an example from Fort Campbell, Kentucky/Tennessee, USA. *J Hydrol (Amst)*. 2003 May;276(1-4):20–36.

Walsh CJ, Roy AH, Feminella JW, Cottingham PD, Groffman PM, Morgan RP. The urban stream syndrome: current knowledge and the search for a cure. *Journal of the North American Benthological Society*. 2005 Sep;24(3):706–723.

## **2.0 Seasonal Drivers of Chemical Flux from Roadside Infiltration-Based Green Infrastructure**

### **2.1 Introduction**

Urbanization affects hydrology, causing flashier storm responses, increased stormwater runoff volumes, and slope instability from channel incision (Harbor 1994; Walsh et al. 2005; Bhaskar et al. 2015). Low impact development (LID) and green infrastructure (GI) have become popular means of mitigating urbanization impacts and restoring hydrologic function (Dietz 2007; Ahiablame et al. 2012). Previous studies demonstrate that LID reduces surface runoff and diminishes storm response (Selbig and Bannerman 2007; Davis 2008). Infiltration-based GI designs are intended to store stormwater runoff and slowly release it to surrounding roadside soil (Campisano et al. 2011). Although infiltration-based GI (e.g., infiltration trenches) capture and reduce stormwater runoff, they may also introduce contaminated road runoff directly into surrounding hydrologic systems, bypassing the organic-rich top layer of soil that frequently stabilizes mobile metal contaminants (Couture et al. 2015; Khan et al. 2017).

Urbanization introduces soil water contamination through increased road runoff which then accumulates in soils in environments close to roads (Medley et al. 1995; Hatt et al. 2004). Urban stormwater runoff carries contaminants such as nutrients, suspended sediments, and heavy metals (Hogan and Walbridge 2007). Contamination sources in urban runoff include the abrasion of car breaks and tires, paints and metals from buildings, and atmospheric deposition of industrial emissions, and road salt application in cities that receive snowfall (Davis et al. 2009). Further,

widespread use of leaded gasolines prior to 1986 and heavy industrial activity have led to substantial amounts of legacy heavy metal contamination in roadside soils (Mielke and Reagan 1998).

Efforts to minimize urban hydrologic impacts with roadside GI systems, like infiltration trenches, that directly receive road runoff, can transport street generated pollution to subsurface roadside environments. Several factors can change established roadside chemistry, in particular the application of road salt in cold environments. Amrhein et al. (1992), Bäckström et al. (2004), and Norrström & Bergstedt (2001) all documented chemical changes in roadside environments resulting from cation exchange and chloride complexation, and found that dissolved heavy metal concentrations (cadmium [Cd], copper [Cu], lead [Pb], and zinc [Zn]) increase in response to road salt application. However, much of the road salt literature focuses on the salt pulse and does not necessarily consider other potential mobilization processes, particularly chemical reduction (Lagerwerff and Specht 1970; Li et al. 2001; Snodgrass et al. 2017).

The addition of road runoff to roadside subsurface point sources such as infiltration trenches can raise the water table leading to increased soil saturation (Machusick et al. 2011). Anaerobic zones in roadside soils can form as soils become saturated and heterotrophic bacteria quickly consume the restricted amounts of oxygen available. The formation of these anaerobic zones in roadside soils leads to the mobilization of metals and metalloids such as iron [Fe], manganese [Mn], and arsenic [As] through reduction of metal oxides. For reduction to occur in roadside environments, three conditions must be met. First, dissolved oxygen concentrations must become depleted, second there must be a microbial population capable of reduction processes such as denitrification, and finally there must be a source of carbon to serve as an electron donor for the reduction reactions. Reduction is more likely to occur during the summer when biological activity

is at its peak (Couture et al. 2015). Reducing processes can be observed in changes in water chemistry in a predictable pattern that follows the order of redox succession (Puckett et al. 2002).

The long-term interactions between GI function and geochemistry have yet to be characterized, despite extensive research on road runoff chemistry and recent implementation of GI in the United States (Brown and Peake 2006; Mell 2017). Thus, accurate prediction of contaminant transport from roads into surrounding soils through infiltration-based GI is currently not possible. This paper clarifies the connection between infiltration trench function (i.e., infiltration rate) and transport of dissolved heavy metals to urban soils and groundwater based on observations of two infiltration trenches during 2016 and 2017. Changes in dissolved metal concentrations in the trench water, combined with stormwater infiltration rates from the trenches, are used to evaluate trench function and measure dissolved metal transport from the trench systems.

## **2.2 Materials and Methods**

### **2.2.1 Study Site**

Two infiltration trenches were installed in Schenley Park (Pittsburgh, PA) the summer of 2014 (Figure 2-1). Water was collected in roadside catch basins then transported directly to an inline drain that brings water to the infiltration trench through a distribution pipe located at least sixty cm below the ground surface. A perforated pipe surrounded by at least 44 cm of geotextile contained limestone gravel fill then distributes the water horizontally throughout the trench and a solid distribution pipe at a higher elevation moves water to a level spreader to release excess water

as overland flow. Water at elevations below the perforated distribution pipe remain in the infiltration trench, resulting in constant standing water (Figure 2-2).

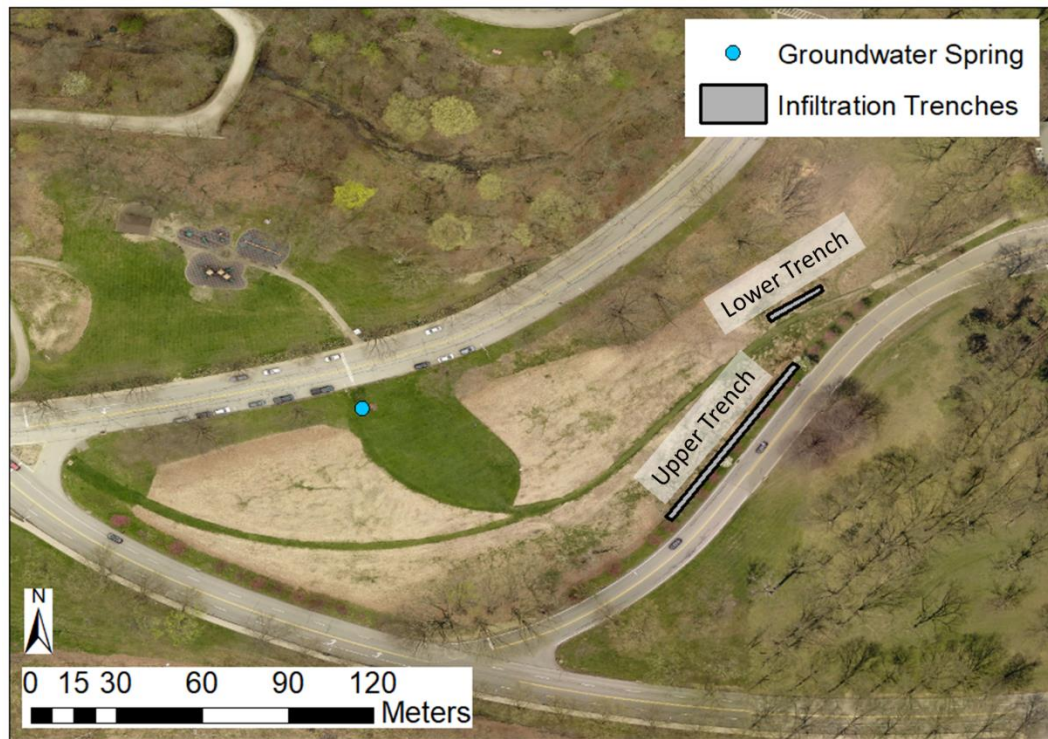


**Figure 2-1. Location of infiltration trenches and groundwater spring in Schenley Park, Pittsburgh (Allegheny County Imagery 2017). The blue circle indicates the location of a groundwater spring and the gray boxes outline the infiltration trenches.**

The trenches are located on a grassy hillside within a moderately urbanized residential neighborhood (population density: 2100 people/km<sup>2</sup>) (Census 2010) and forested parkland. The “upper trench” was installed higher on the slope and closer to the road and is approximately 55 m long, 1 m wide, and has a level spreader at 0.6 m depth. The “lower trench” is shorter than the upper trench and is not as deep (18 m x 1 m x 0.45 m). While the upper trench is located at a higher elevation than the lower trench, it is not directly upslope. Therefore, interactions between trench waters are unlikely. The vegetation on the hillside was converted from turf grass to a “meadow” cover as part of the infiltration trench project to increase surface infiltration and evapotranspiration

(ET) rates. A groundwater spring that pools water on the soil surface is located at the bottom of the hillslope, though not directly downslope of either infiltration trench.

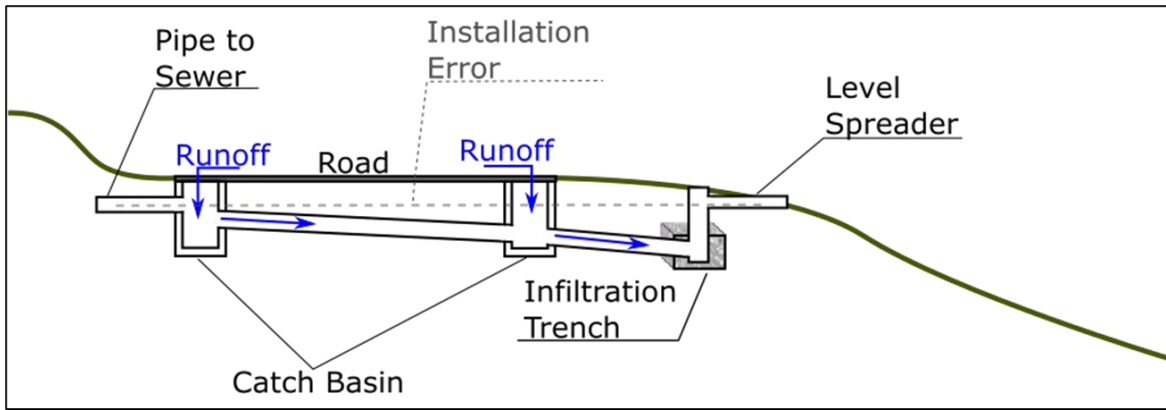


**Figure 2-2. Stormwater capture and diversion to infiltration trench conceptual design. Gray dotted line indicates design flaw where pipe to sewer is a lower elevation than pipe to level spreader.**

In summer 2016, it was determined that the upper trench was not installed properly and was diverting less water than the lower trench. This observation resulted in a reassessment of the installation that revealed the upper trench overflow back to the combined sewer system was erroneously installed lower than the overflow to the level spreader (Figure 2-2). Therefore, stormwater was diverted back into the combined sewer before the trench was filled to design capacity for much of the record discussed here. A fix was applied in July 2017, raising the level at which water begins to flow back to the sewer to a higher level than necessary to flow to the level spreader (Figure A-1). This error affected both infiltration rates measured from the trench as water levels were consistently lower and dissolved chemical concentrations as less stormwater was introduced to the system, resulting in less dilution and higher concentrations.

### 2.2.2 Sample Collection and Analysis

Water samples were collected from the trench sumps in both infiltration trenches approximately bi-weekly from January 2016 to January 2018. Water discharged from the spring was also sampled bi-weekly, from May 2016 to January 2018. From July to October 2016 and from September to December 2017, there was no surface water discharging from the spring during sampling events, therefore no samples were collected. Unfiltered water samples were collected in high-density polyethylene (HDPE) containers triple rinsed with sampled water and refrigerated at 4°C for no more than 24 hours before they were filtered (0.2-micron polyethersulfone) in the laboratory and split for metal and nutrient analysis. Water samples used for dissolved metal measurement were acidified using sub-boil distilled, concentrated nitric acid and stored at -20°C. Subsamples were then diluted with 2% nitric acid and spiked with an internal standard containing beryllium [Be], germanium [Ge], and titanium [Ti]. Diluted and spiked samples were analyzed on a PerkinElmerNexion 300x inductively coupled plasma-mass spectrometer (ICP-MS) for the following metals: sodium [Na], Mn, Fe, Cu, Zn, Cd, chromium [Cr], and Pb. Unacidified samples were measured for anions (sulfate [SO<sub>4</sub><sup>2-</sup>], and nitrate [NO<sub>3</sub><sup>-</sup>]) on a Dionex ICS2000 Ion Chromatograph. Standards and blanks were included regularly throughout sample batches. Regular duplicates showed a precision of within 10% of the measured values. Iron concentrations were measured using the kinetic energy discrimination (KED) method on the ICP-MS to reduce polyatomic interferences.

Soil samples were collected in June 2018 from 10 locations surrounding the infiltration trenches (Figure A-2). The samples were collected to a depth of approximately 10 cm. The soil materials were then dried and metal analysis subsamples were powdered in a ball mill (tungsten

carbide bomb). Total metal concentrations in powdered samples were measured by ALS Chemex (ME-MS61).

### **2.2.3 Infiltration Rate Calculation and Chemical Flux Estimation**

Trench water elevations and temperature were measured in 5-minute intervals using pressure transducers (Onset U20) deployed in the trench inline drains and corrected for atmospheric pressure with a nearby logger deployed at the ground surface. Trench water elevation was plotted alongside precipitation to identify infiltration events (Figure 2-3). Water infiltration rates from the trenches were calculated by dividing the change in water elevation by the time between the start of a storm response and the return of the water level to a baseline (i.e., when elevation no longer continued to decrease or when the next storm response began) (Figure A-3). To account for overflow from the trenches, the rate was not calculated until water elevations within the trench were decreasing at a steady rate (spikes at the beginning of a storm that reached elevations above the level spreader were disregarded). Precipitation intensity data (15-minute intervals) were based on the University of Pittsburgh gauge (Station 9) in the Three Rivers Wet Weather Calibrated Radar Rainfall Network located roughly 1 km from the study area

(3riverswetweather). Groundwater table fluctuations were monitored in a well located roughly 300 m from the study area. The well was approximately three meters deep and downslope of the trenches, though too far from the trenches to observe any influence. Diurnal groundwater fluctuations were used to identify periods of ET (Figure A-4).

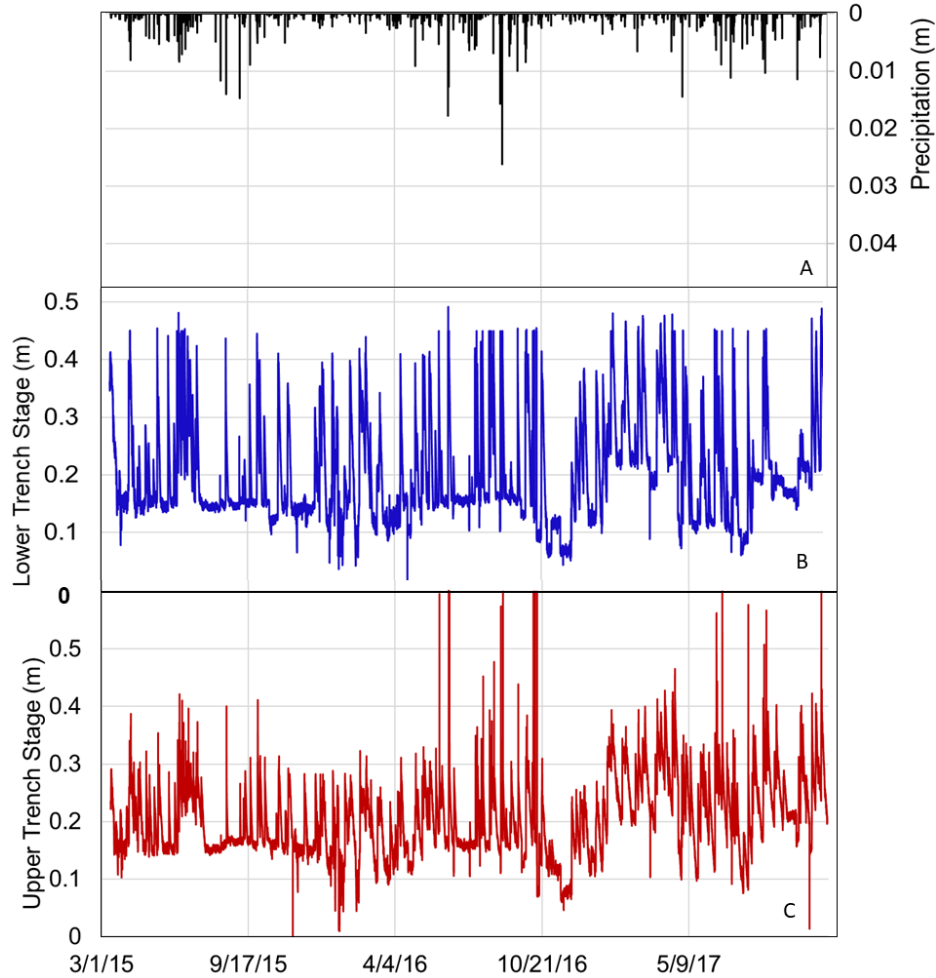


**Figure 2-3. Continuous record of A) precipitation and water elevation in the B) Lower Trench and C) Upper Trench from January 2016 to December 2017. 0 indicates the bottom of each trench.**

Predicted infiltration rates based on changes in water viscosity were calculated using water viscosity and density values calculated with the temperature data collected by the pressure transducers. The ratio of density divided by viscosity during each infiltration event was used to estimate infiltration rate (Emerson and Traver 2008). This estimated rate was then normalized to what the rate would be at 0°C to evaluate percentage change over time. The changes in infiltration rate using this method were then compared to actual measured infiltration rates in Figure 2-4.

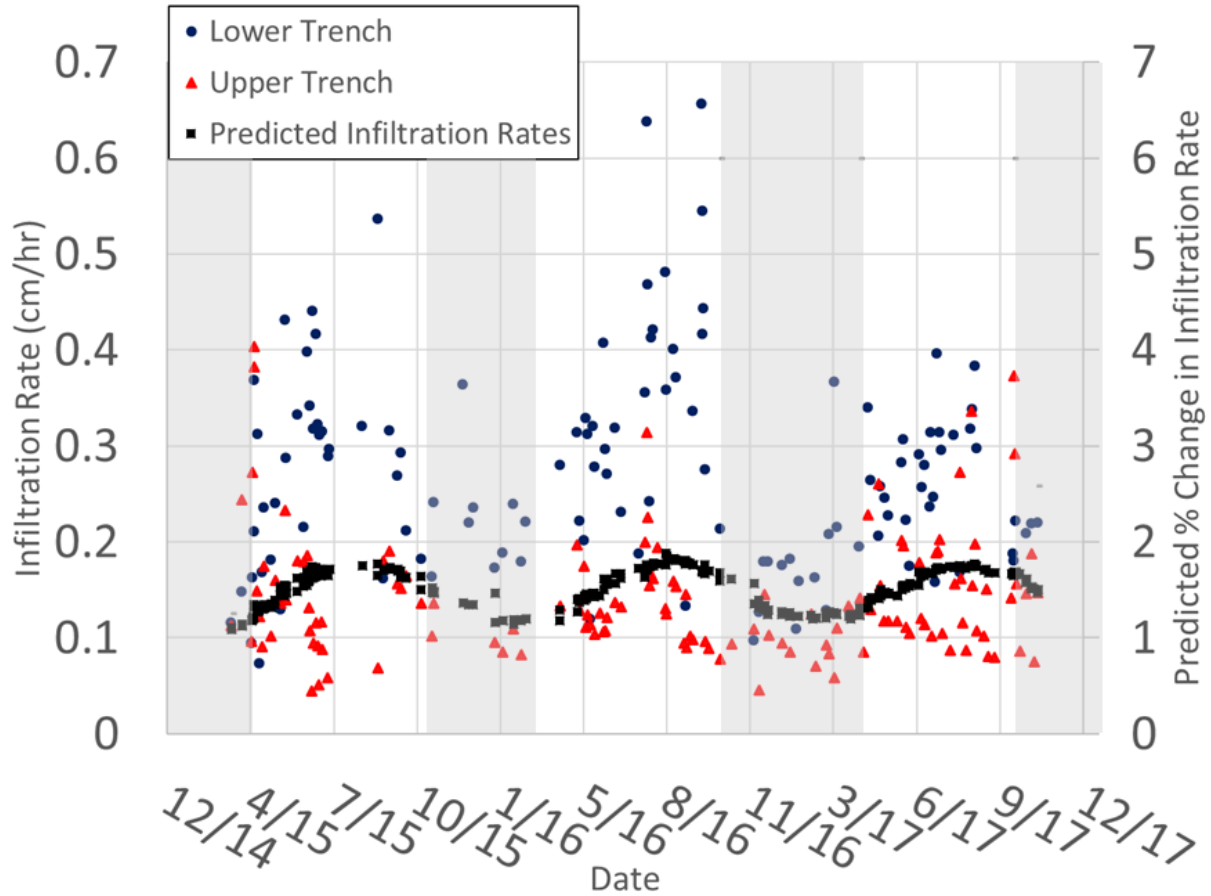


**Figure 2-4. Observed infiltration rates (red triangles & blue circles) compares with proportional predicted changes in water infiltration (black boxes) using the water temperature at the beginning of the storm event. Gray areas indicate periods of low evapotranspiration activity determined by observed patterns in the local water table.**

## 2.3 Results and Discussion

### 2.3.1 Water Infiltration from Trenches

Over the course of the study, 126 separate infiltration events were recorded in the lower trench and 133 in the upper trench. The median infiltration rate measured in the lower trench was

0.26 cm/hr (range 0.07- 0.66 cm/hr). The upper trench had a median infiltration rate of 0.13 cm/hr (range 0.04 - 0.40 cm/hr) (Figure 2-4). Over the course of the study period, the site received 218 cm of precipitation – 104 cm in 2016 and 114 cm in 2017. The median infiltration rate from the lower trench was 0.18 cm/hr in the spring and summer and 0.32 cm/hr in the fall and winter. The upper trench had a spring/summer median infiltration rate of 0.13 cm/hr and a fall/winter infiltration rate of 0.10 cm/hr. Following the fix in July of 2017, higher infiltration rates from the upper trench were more common with a marginally higher average infiltration rate of 0.16 cm/hr. However, there is not enough data to draw any conclusions about the efficacy of the fix (Figure 2-4).

Periods of high evapotranspiration (ET) were inferred from the occurrence of diurnal water table patterns (i.e., ET drawdown) in a nearby observation well (Figure A-4) (White 1932). Detectable ET (evidenced by the diurnal water table pattern) began approximately on April 14 in 2016 and April 12 in 2017 and ended on October 6 in 2016 and October 2 in 2017. Periods where ET was not the primary driver of groundwater elevation changes are depicted with gray boxes in Figure 2-4.

### **2.3.2 Seasonal Patterns in Infiltration Rate**

Annual infiltration rate patterns were similar in the trenches: higher infiltration rates occurred in the spring and summer (March 20-September 22) and decreased in the fall and winter (September 23-March 21) (Figure 2-4). The mean infiltration rate was significantly higher during the spring and summer than the mean infiltration rate during the fall and winter (Student's T-test,  $p < 0.005$  [lower trench],  $p < 0.01$  [upper trench]) (Figure A-5). The seasonal change in infiltration observed in the upper trench was less variable due to the installation error shown in Figure 2-2.

This seasonal pattern in infiltration rates has been observed in other infiltration-based green infrastructure (Hunt et al. 2006). Emerson & Traver (2008) attribute seasonal infiltration rate patterns in Philadelphia, PA, to temperature-driven changes in water viscosity. We evaluated the temperature influence on the infiltration rates by comparing the observed infiltration rates and temperatures with relative changes in water infiltration rates estimated from the average water temperature during infiltration (Figure A-6). Based on the observed temperature range, the infiltration rate should increase during the summer roughly by a factor of two. However, observed infiltration rates increased by roughly an order of magnitude (0.7 mm/hr to 6.6 mm/hr) over this same range of temperatures. Temperature influence on viscosity cannot explain the observed range of infiltration rates. (Figure A-6). In addition, the upper trench infiltration rate varied minimally with season (Figure A-6); however, this behavior was a result of the design flaw and the shallower water depths in the upper trench.

In addition to the temperature estimate evidence of flow, the temporal patterns in measured infiltration rate were distinct from seasonal patterns. In particular, the predicted infiltration rates were essentially sinusoidal, matching seasonal variation in temperature (Figure 2-4). A strong temperature control on infiltration should create a sinusoidal variation in infiltration rates. However, the measured infiltration rates dropped abruptly in October, decreasing about 0.20 cm/hr (Figure 2-4). The gradual increase begins with the increase of ET activity and the abrupt decline with the decrease of ET intensity. Therefore, the observed changes in infiltration rate appear to be more sensitive to changes in ET than temperature. The increase of ET lowers the local water table, increasing the hydraulic gradient surrounding the trenches and leading to greater infiltration rates. Groundwater affects this moisture content of the soil above the water table as well, lowering the

capillary force of the soil surrounding the infiltration trenches and reducing infiltration rates (Mangangka 2008).

Finally, observations of an ephemeral groundwater spring at the bottom of the study hillslope (Figure 2-1) also indicate decreases in the local water table during increased evapotranspiration. From the July 14, 2016 sampling date to the October 28, 2016 sampling date, the spring was not observed discharging, indicating decreases in the local water table during the growing season (Figure 2-8). In 2017, a relatively wetter year, the spring was not observed to be dry until the September 15 sampling date. Most importantly, the spring flow ceased over a time period similar to when infiltration rates increased, supporting the hypothesis that infiltration rate is driven by the lowering of the water table.

### **2.3.3 Dissolved Metal and Nutrient Concentration Patterns in Infiltration Trenches**

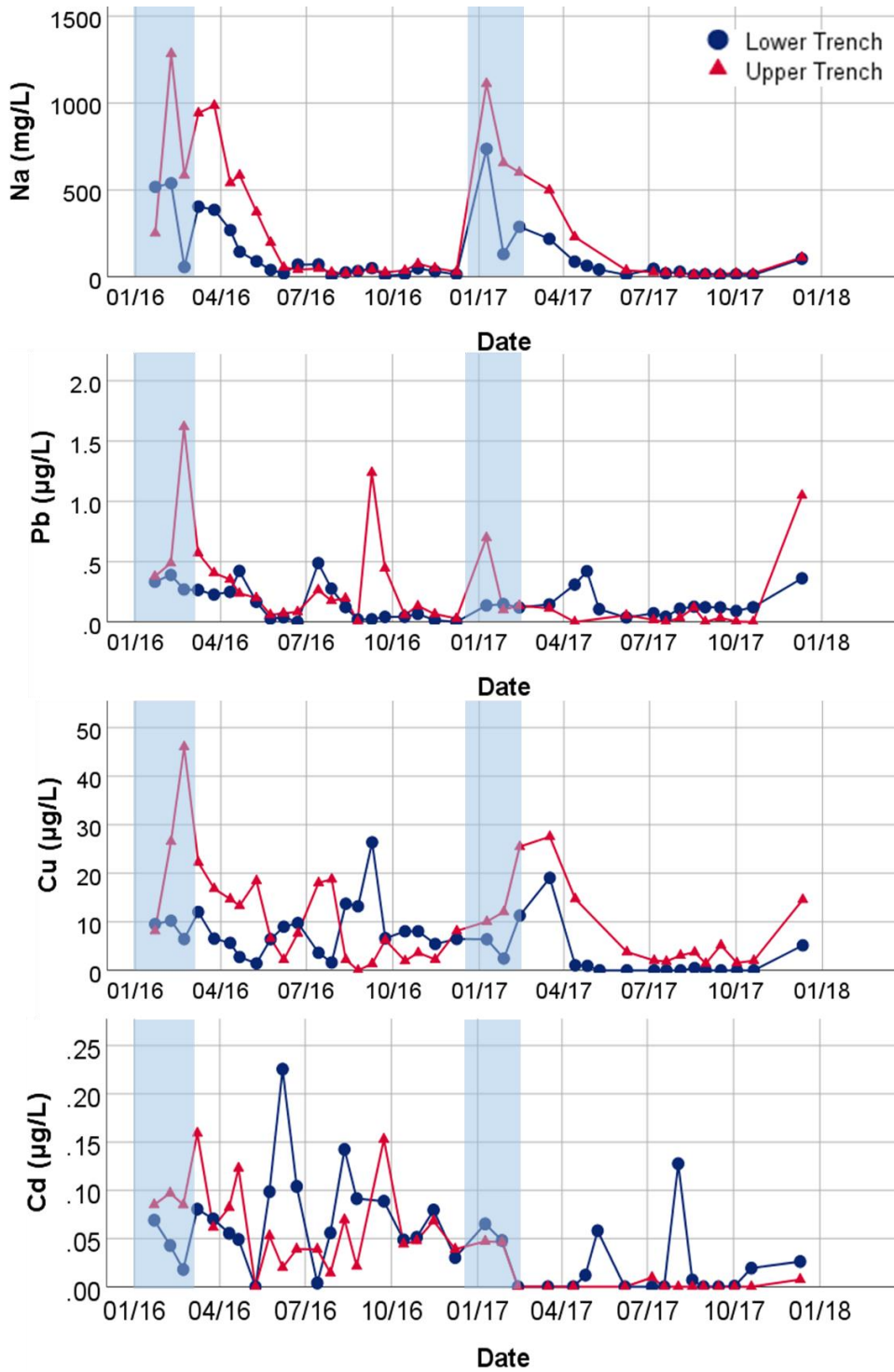


Figure 2-5. Dissolved concentrations of chemicals influenced by road de-icer application in the upper trench (red triangles) and lower trench (blue circles) between January 2016 and December 2017. Blue boxes indicate approximate times during the year in which road de-icers were applied.

Between January 22, 2016 and January 11, 2018, 78 water samples were collected from the infiltration trenches (Table A-1) and analyzed for seasonal patterns in dissolved chemical concentrations. Na concentrations in both trenches were highest in the winter due to the application of road de-icers (Figure 2-5). Concentrations of dissolved metal contamination increased in the trench water during the spring and summer months, particularly Mn and Fe, with the highest Mn concentrations observed on May 9, 2016 (1.04 mg/L) and the highest Fe concentrations on July 14, 2016 (0.76 mg/L) (Figure 2-6). Dissolved Pb concentrations increased during the winter months and during July and August (Figure 2-5). The increase in Pb concentrations coincided with increased iron concentrations during the summer, e.g., 0.49 µg/L on July 14, 2016. However, the highest Pb concentration measured was on February 22, 2016 (1.6 µg/L), in a sample with a high Na concentration (Figure 2-5). Conversely, nutrient concentrations decreased in the spring and summer. NO<sub>3</sub><sup>-</sup> concentrations decreased in the spring from over 10 mg/L in February to less than 0.1 mg/L in April of 2016. Likewise, SO<sub>4</sub><sup>2-</sup> concentrations decreased from 7.6 mg/L on March 25, 2016 to 2.8 on April 11, 2016 (Figure 2-6).

Samples were collected from the trenches daily the week of June 22, 2018 to characterize variation in trench chemistry and support the validity of bi-weekly sampling. A storm event occurred during that week on June 24, 2018. The difference between the highest and lowest metals and nutrient concentrations collected over a week were an order of magnitude lower than the difference between the highest and lowest concentrations measured over the course of a year in all studied metals except for Pb concentrations in the lower trench. Therefore, bi-weekly sampling appears to be an acceptable approximation of variation in the infiltration trenches (Table A-2).

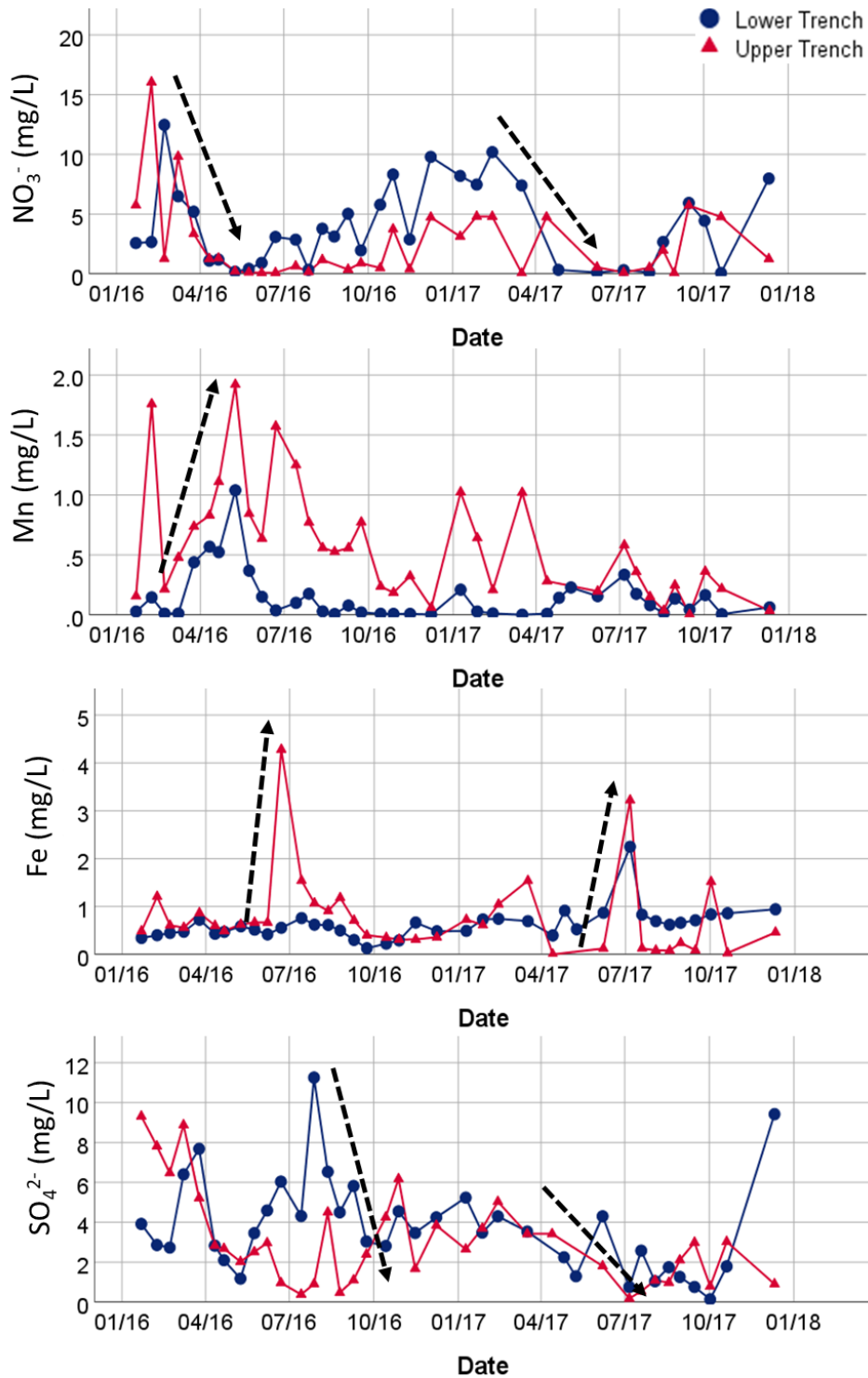


Figure 2-6. Dissolved concentrations of chemicals influenced by inferred reduced conditions in the upper trench (red triangles) and lower trench (blue circles) between January 2016 and December 2017. Black arrows indicate timing of chemical responses to the formation of a reducing environment.

### **2.3.4 Sodium Pulse and Sodium Driven Patterns in Dissolved Metal Concentration**

Road deicer application dramatically increased concentrations of dissolved Na in the trenches during the winter (Figure 2-5; Figure 2-8). The City of Pittsburgh almost exclusively uses NaCl rock salt for de-icing public roads (Rossi et al. 2017). Therefore, changes in Na concentrations in the infiltration trenches are directly correlated to the amount of road salt introduced to the system. Dissolved Na in the trenches reached concentrations of over 1000 mg/L in January and dropped below 100 mg/L in May (Figure 2-5). The cessation of road salt application coincided with decreasing Na concentrations, as road runoff from subsequent storms flushed the excess Na from the trenches. In contrast, observations in groundwater chemistry from the spring indicated Na input from the soil remained constant throughout the year (Figure A-7). Therefore, groundwater concentrations were lower than measured trench concentrations in the winter and higher in the summer (Figure A-7). The persistence of Na loading from soil and groundwater following the cessation of road deicer application was congruous with the accumulation of Na in roadside soils (Cunningham et al. 2008; Cooper et al. 2014; Ledford et al. 2016; Rossi et al. 2017). Although there was little Na output from the trenches in the summer, Na introduced from the trenches in the winter will likely accumulate in the surrounding soil and affect soil water year-round (Robinson et al. 2017).

The application of NaCl to roads can mobilize soil-bound metals from roadside soils through cation exchange (Amrhein et al. 1992; Bäckström et al. 2004). Observed patterns of dissolved Pb concentrations in the trenches measured in the winter were accordant with road salt mobilization of legacy heavy metals in roadside soils. Increased concentrations were observed during the winter with increased Na concentrations (Figure 2-5). Amrhein et al. (1992) and Norrström, (2005) found evidence of cation exchange in response to road salt application. These

studies observed the release of Pb ions in column experiments where soils were exposed to de-ionized water following Na leaching.

The soils surrounding the infiltration trenches are rich in clays; especially in the B horizon (27-40%), indicating ample exchange sites to bind Pb (USDA, 1981). While the trenches are filled with gravel, there is ample opportunity for interactions with contaminated soils at the edges, but more important is the potential for the trenches to capture local groundwater, a flowpath that passes through soil. Soil samples collected from the site showed elevated concentrations of Pb compared to other urban soils (an average of 195 ppm, Table A-3), likely from the use of leaded gasolines from the 1960s to 1995 throughout North America (Datko-Williams et al. 2014; Rossi et al. 2017). Thus, the elevated Pb concentrations observed in the trenches could result from mobilized legacy contamination from surrounding soils (Harrison et al. 1981; Calvillo et al. 2015).

Other heavy metal contaminants were also sensitive to road deicer application. Dissolved Cu concentrations increased in the trenches during the salting season (Figure 2-5). Legacy Pb, Cu, Cr, and Zn are all associated with vehicle-derived wastes, such as gasoline exhaust, lubricant leaks, or wear of car components (Li et al. 2001). Increases in dissolved Cu and Zn have been observed in urban stream water and roadside soil water in response to road salt application (Löfgren; Warren and Zimmerman 1994; Bäckström et al. 2004; Merrikhpour and Jalali 2013). Therefore, dissolved chemical patterns of infiltration trench water in winter were likely driven by the interaction of road-salt with both road runoff and legacy metal contamination in soils. Any such mobilization of legacy metal contamination increases downslope transport and mobilizes contamination to soils further from the source of contamination.

Dissolved Cd has been observed following NaCl application due to cation exchange and the formation of Cl complexes (Nelson et al. 2009). However, in this study, increased Cd

concentrations were observed outside the salting season. Local soil Cd concentrations were similar to other urban soil Cd measurements (Table A-3), so if road cation exchange or chloride complexation are the primary control on Cd, it should be mobilized from these soils. Many studies that identify Cd as an element that is particularly sensitive to chloride complexation rely on equilibrium models or laboratory systems (Amrhein et al. 1992; Bauske and Goetz 1993; Bäckström et al. 2004). Observations suggest biogeochemical controls in these trenches that interfere with expected Cd/NaCl interactions.

### **2.3.5 Oxidation/Reduction Dynamics Observed in Metal and Nutrient Concentrations**

Observed dissolved nutrient and metal concentrations throughout the late spring and early summer suggest the trenches become reducing environments. Dissolved Mn and Fe concentrations in the infiltration trenches spiked in May and June respectively, as expected with the dissolution of their respective oxyhydroxides through reduction (Alloway 2013). Conversely,  $\text{NO}_3^-$  almost completely disappeared, likely due to microbial assimilation and denitrification (Korom 1992) (Figure 2-6). Although the decrease in  $\text{NO}_3^-$  concentrations coincided with the onset of the growing season and may result in part from assimilation, denitrification through reduction is likely a contributing factor as  $\text{NO}_3^-$  concentrations decrease immediately before increases in dissolved Mn and Fe.

The unexpected reduction of  $\text{SO}_4^{2-}$  before Fe in May and June of 2017 highlights the complex and unpredictable nature of trench water chemistry. One explanation for the unexpected timing of Fe and  $\text{SO}_4^{2-}$  reduction is that a groundwater source may be contributing  $\text{SO}_4^{2-}$  to the system.  $\text{SO}_4^{2-}$  concentrations in the nearby groundwater spring were elevated relative to the trenches (average 1.4 mg/L in lower trench, 9.4 in groundwater) (Figure A-8). Therefore, the

elevated  $\text{SO}_4^{2-}$  concentrations in the trenches in August 2016 could be from a groundwater pulse (Figure 2-6). During storm events, the high  $\text{SO}_4^{2-}$  concentrations driven by groundwater are flushed from the system. Dissolved Pb and Cu concentrations increased in July, correlating with elevated dissolved Fe (Figure 2-6). Fe oxide dissolution would mobilize legacy metals bound to hydroxides in the surrounding soil and trench sediments (Figure 2-7). Thus, the establishment of reducing conditions in the summer and spring leads to increased dissolved metal concentrations.

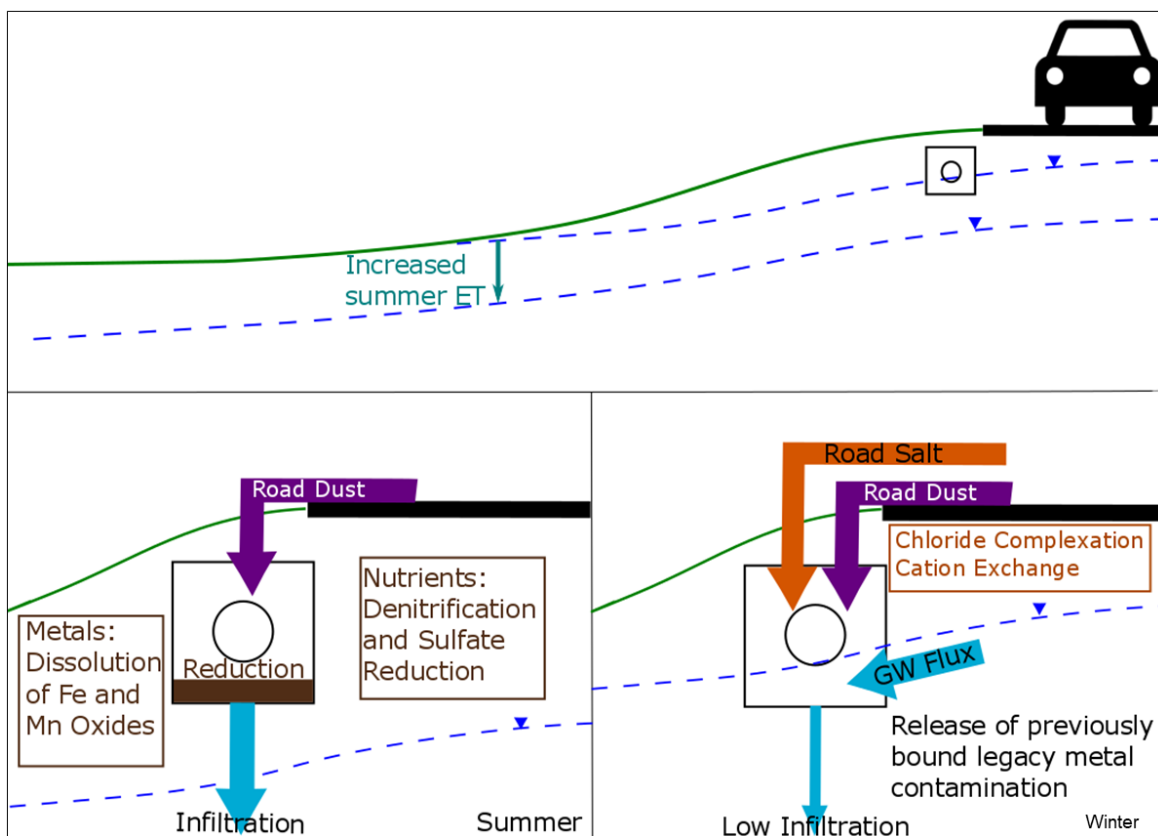


**Figure 2-7. Conceptual model showing seasonal changes in water table and contaminants introduced to roadside infiltration trenches.**

Stormwater runoff likely oxidizes trench waters throughout the summer as large storm events are more frequent (Figure 2-3). The resulting reactions, including precipitation of Fe oxides, occur before reducing conditions begin to re-establish. Danfoura and Gurdak (2016) noted that the regular inflow of oxic runoff will lower reduction rates temporarily following large storm events.

The runoff in the two trenches also likely contains higher levels of organic matter and nutrients that may accelerate oxygen depletion, resulting in short time periods (2-3 days) between storm events and a return to  $\text{NO}_3^-$  reduction. Frequent summer re-oxygenation of trench waters followed by re-establishment of reducing conditions is further supported by the  $\text{SO}_4^{2-}$  patterns measured in the trenches in 2017. The decrease in  $\text{SO}_4^{2-}$  concentrations in 2016 was much faster than that measured in 2017. The spring and summer seasons of 2017 were wetter than 2016 (70 cm precipitation in 2017, compared to 59 cm in 2016), thus, storm flow to the trenches occurred more frequently, flushing and re-oxygenating the trenches (64 infiltration events in 2017, 55 events in 2016). Sustained  $\text{SO}_4^{2-}$  reduction was observed only in the upper trench as concentrations of  $\text{SO}_4^{2-}$  remain low throughout the entire summer while lower trench concentrations increase in May (Figure 6). This trend may be the result of more stagnant conditions in the upper trench caused by the design flaw. Higher water throughput in the lower trench likely flushed and re-oxygenated the trench waters, resulting in a relatively less reducing environment.

Finally, field observations of Mn deposits and sulfurous odors inside the trenches in the spring and summer suggest that reducing conditions exist in the trenches. Examination of metal and nutrient dynamics in reduction-sensitive species suggest the importance of reduction/oxidation dynamics in trench water chemistry. The timing of  $\text{NO}_3^-$ , Fe, Mn, and  $\text{SO}_4^{2-}$  dynamics reveal temporal trends consistent with the expected biological succession of terminal electron accepting processes ( $\text{NO}_3^- > \text{Mn(IV)} > \text{Fe(III)} > \text{SO}_4^{2-}$ ) as  $\text{NO}_3^-$  concentrations began decreasing on April 11, followed by a spike in Mn on May 9, then Fe on June 22, and finally  $\text{SO}_4^{2-}$  become depleted on July 14 in 2016 (as indicated by the black arrows on Figure 2-6). (Drever 1988; McMahon and Chapelle 2008).

While the GI benefits of nutrient mitigation are often cited (Bettez and Groffman 2012; Pennino et al. 2016), these benefits have to be weighed against increased metal mobility. The heavy metal concentrations observed in these trenches never exceeded USEPA safe drinking water standards (USEPA 2001). Regardless, roadside system’s potential for metal mobilization should be evaluated before stormwater management practices are installed (Kondo et al. 2016).

### 2.3.6 Unexplained Patterns Observed in Zinc and Chromium

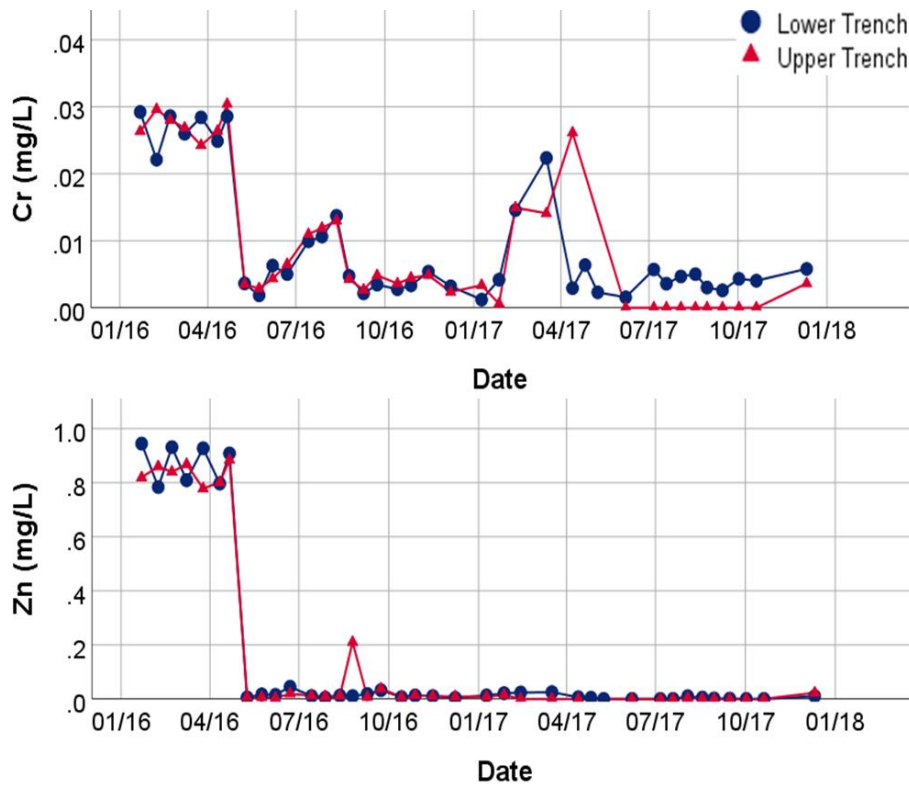


**Figure 2-8. Dissolved concentrations of A) Cr and B) Zn measured in the upper trench (red triangles) and lower trench (blue circles) between January 2016 and December 2017**

Previous studies show that Zn and Cr can be susceptible to either cation exchange or reduction of metal oxides (Figure 2-8) (Harrison et al. 1981; Warren and Zimmerman 1994; Norrström and Jacks 1998; Bäckström et al. 2004). However, Zn and Cr concentrations in the

trenches had no discernable trend due to unexpected patterns in concentration observed during the study period. These patterns may be caused by an unknown source of contamination. Between January 22, 2016 and April 21, 2016, the dissolved Zn and Cr concentrations remained relatively and consistently high (0.77-0.94 mg/L for Zn, 0.022-0.030 mg/L for Cr). Beginning in May, the concentrations in both trenches dropped by at least an order of magnitude and remained low for the rest of the year (Figure 2-7). Cr and Zn concentrations did not repeat these elevated and sustained concentrations throughout the duration of the study.

This observation was carefully evaluated for laboratory contamination, particularly given the use of Zn as a common plasticizer. Samples collected before and after the dramatic shift were remeasured in the initial dilution and in subsequent dilutions of archived samples and contamination issues were ruled out. In addition, the blanks that were run as part of normal quality assurance did not indicate Zn or Cr contamination. The source of these metals was probably temporary, as these sustained and elevated concentrations only occurred during this short time period. This contamination may result from construction activity and a mix of galvanized Fe materials coated in Zn and dust from stainless steel hardened with Cr. The abrupt drop in April 2016 is coincident with the onset of street sweeping in the area, which does not occur between November and April, and this activity may have removed the source (Fergusson et al. 1986). This source appears temporary, as these sustained, elevated concentrations of Zn and Cr were not observed after April 2016.

## 2.4 Conclusions

Both infiltration trench function and geochemical variability show distinct seasonal patterns. First, the function of infiltration trenches is highly dependent on the local water table, which fluctuated with the onset of the growing season and transpiration. Trench infiltration rates are significantly lower during the winter when local water tables are elevated. Local groundwater activity dramatically changes the efficacy of infiltration-based green infrastructure and likely needs to be more carefully addressed during design of GI. Therefore, local hydrology should be taken into account before widespread implementation of infiltration based green infrastructure.

In addition, seasonal variability in trench water chemistry can mobilize legacy contamination in both winter and summer. Pb and other legacy metal concentrations in the trenches are elevated in the winter during periods of elevated Na concentrations that result from road salt application. The formation of biologically driven reducing conditions in the summer elevates legacy heavy metals concentrations in July. Although this study does not have sufficient data to demonstrate detailed metal transport patterns, the increased dissolved concentrations of metals in infiltration infrastructure is assumed to transport contamination downgradient. The remobilization of previously soil-bound legacy contaminants and transport could lead to unexpected exposure downslope from infiltration-based green infrastructure.

## 2.5 Bibliography

- Ahiablame LM, Engel BA, Chaubey I. Effectiveness of low impact development practices: literature review and suggestions for future research. *Water Air Soil Pollut.* 2012 Sep;223(7):4253–4273.
- Alloway BJ. Sources of heavy metals and metalloids in soils. In: Alloway BJ, editor. *Heavy metals in soils*. Dordrecht: Springer Netherlands; 2013. p. 11–50.
- Amrhein C, Strong JE, Mosher PA. Effect of deicing salts on metal and organic matter mobilization in roadside soils. *Environ Sci Technol.* 1992 Apr;26(4):703–709.
- Bäckström M, Karlsson S, Bäckman L, Folkesson L, Lind B. Mobilisation of heavy metals by deicing salts in a roadside environment. *Water Res.* 2004 Feb;38(3):720–732.
- Bauske B, Goetz D. Effects of Deicing-Salts on Heavy Metal Mobility Zum Einfluß von Streusalzen auf die Beweglichkeit von Schwermetallen. *Acta hydrochim hydrobiol.* 1993 Apr;21(1):38–42.
- Bettez ND, Groffman PM. Denitrification potential in stormwater control structures and natural riparian zones in an urban landscape. *Environ Sci Technol.* 2012 Oct 16;46(20):10909–10917.
- Bhaskar AS, Welty C, Maxwell RM, Miller AJ. Untangling the effects of urban development on subsurface storage in Baltimore. *Water Resour Res.* 2015 Feb;51(2):1158–1181.
- Brown JN, Peake BM. Sources of heavy metals and polycyclic aromatic hydrocarbons in urban stormwater runoff. *Sci Total Environ.* 2006 Apr 15;359(1-3):145–155.
- Calvillo SJ, Williams ES, Brooks BW. Street dust: implications for stormwater and air quality, and environmental through street sweeping. *Rev Environ Contam Toxicol.* 2015;233:71–128.

- Campisano A, Creaco E, Modica C. A simplified approach for the design of infiltration trenches. *Water Science & Technology*. 2011 Sep;64(6):1362.
- City of Pittsburgh Neighborhood Profiles, 2010 Census Summary File 1 (SF1) Data. Retrieved from [www.ucsur.pitt.edu](http://www.ucsur.pitt.edu)
- Cooper CA, Mayer PM, Faulkner BR. Effects of road salts on groundwater and surface water dynamics of sodium and chloride in an urban restored stream. *Biogeochemistry*. 2014 Oct;121(1):149–166.
- Couture R-M, Charlet L, Markelova E, Madé B, Parsons CT. On-off mobilization of contaminants in soils during redox oscillations. *Environ Sci Technol*. 2015 Mar 3;49(5):3015–3023.
- Cunningham MA, Snyder E, Yonkin D, Ross M, Elsen T. Accumulation of deicing salts in soils in an urban environment. *Urban Ecosyst*. 2008 Mar;11(1):17–31.
- Danfoura M, Gurdak J. Redox Dynamics and Oxygen Reduction Rates of Infiltrating Urban Stormwater beneath Low Impact Development (LID). *Water (Basel)*. 2016 Oct 4;8(10):435.
- Datko-Williams L, Wilkie A, Richmond-Bryant J. Analysis of U.S. soil lead (Pb) studies from 1970 to 2012. *Sci Total Environ*. 2014 Jan 15;468-469:854–863.
- Davis AP. Field performance of bioretention: hydrology impacts. *J Hydrol Eng*. 2008 Feb;13(2):90–95.
- Davis AP, Hunt WF, Traver RG, Clar M. Bioretention technology: overview of current practice and future needs. *J Environ Eng*. 2009 Mar;135(3):109–117.
- Dietz ME. Low Impact Development Practices: A Review of Current Research and Recommendations for Future Directions. *Water Air Soil Pollut*. 2007 Oct 6;186(1-4):351–363.

Drever JI. The geochemistry of natural waters. [hwbdocuments.env.nm.gov](http://hwbdocuments.env.nm.gov); 1988.

Emerson CH, Traver RG. Multiyear and Seasonal Variation of Infiltration from Storm-Water Best Management Practices. *J Irrig Drain Eng*. 2008 Oct;134(5):598–605.

Fergusson JE, Forbes EA, Schroeder RJ, Ryan DE. The elemental composition and sources of house dust and street dust. *Science of The Total Environment*. 1986 Apr;50:217–221.

Harbor JM. A Practical Method for Estimating the Impact of Land-Use Change on Surface Runoff, Groundwater Recharge and Wetland Hydrology. *Journal of the American Planning Association*. 1994 Mar 31;60(1):95–108.

Harrison RM, Laxen DPH, Wilson SJ. Chemical associations of lead, cadmium, copper, and zinc in street dusts and roadside soils. *Environ Sci Technol*. 1981 Nov;15(11):1378–1383.

Hatt BE, Fletcher TD, Walsh CJ, Taylor SL. The influence of urban density and drainage infrastructure on the concentrations and loads of pollutants in small streams. *Environ Manage*. 2004 Jul;34(1):112–124.

Hogan DM, Walbridge MR. Best management practices for nutrient and sediment retention in urban stormwater runoff. *J Environ Qual*. 2007 Apr;36(2):386–395.

Hunt WF, Jarrett AR, Smith JT, Sharkey LJ. Evaluating bioretention hydrology and nutrient removal at three field sites in north carolina. *J Irrig Drain Eng*. 2006 Dec;132(6):600–608.

Khan MA, Khan S, Khan A, Alam M. Soil contamination with cadmium, consequences and remediation using organic amendments. *Sci Total Environ*. 2017 Dec 1;601-602:1591–1605.

Kondo MC, Sharma R, Plante AF, Yang Y, Burstyn I. Elemental concentrations in urban green stormwater infrastructure soils. *J Environ Qual*. 2016 Jan;45(1):107–118.

- Korom SF. Natural denitrification in the saturated zone: A review. *Water Resour Res.* 1992 Jun;28(6):1657–1668.
- Lagerwerff JV, Specht AW. Contamination of roadside soil and vegetation with cadmium, nickel, lead, and zinc. *Environ Sci Technol.* 1970 Jul;4(7):583–586.
- Ledford SH, Lautz LK, Stella JC. Hydrogeologic Processes Impacting Storage, Fate, and Transport of Chloride from Road Salt in Urban Riparian Aquifers. *Environ Sci Technol.* 2016 May 17;50(10):4979–4988.
- Li X, Poon C, Liu PS. Heavy metal contamination of urban soils and street dusts in Hong Kong. *Applied Geochemistry.* 2001 Aug;16(11-12):1361–1368.
- Löfgren S. The Chemical Effects of Deicing Salt on Soil and Stream Water of Five Catchments in Southeast Sweden. *Water, Air, and Soil Pollution.*
- Machusick M, Welker A, Traver R. Groundwater Mounding at a Storm-Water Infiltration BMP. *J Irrig Drain Eng.* 2011 Mar;137(3):154–160.
- Mangangka IR. The Decline of Soil Infiltration Capacity Due To High Elevation Groundwater. *Civil Engineering Dimension.* 2008 May 30;
- McMahon PB, Chapelle FH. Redox processes and water quality of selected principal aquifer systems. *Ground Water.* 2008 Apr;46(2):259–271.
- Medley KE, McDonnell MJ, Pickett STA. Forest-Landscape Structure along an Urban-To-Rural Gradient\*. *The Professional Geographer.* 1995 May;47(2):159–168.
- Mell IC. Green infrastructure: reflections on past, present and future praxis. *Landsc Res.* 2017 Feb 17;42(2):135–145.
- Merrikhpour H, Jalali M. The effects of road salt application on the accumulation and speciation of cations and anions in an urban environment. *Water Environ J.* 2013 Dec;27(4):524–534.

- Mielke HW, Reagan PL. Soil is an important pathway of human lead exposure. *Environ Health Perspect.* 1998 Feb;106 Suppl 1:217–229.
- Nelson SS, Yonge DR, Barber ME. Effects of road salts on heavy metal mobility in two eastern washington soils. *J Environ Eng.* 2009 Jul;135(7):505–510.
- Norrström AC. Metal mobility by de-icing salt from an infiltration trench for highway runoff. *Applied Geochemistry.* 2005 Oct;20(10):1907–1919.
- Norrström AC, Bergstedt E. The Impact of Road De-Icing Salts (NaCl) on Colloid Dispersion and Base Cation Pools in Roadside Soils. *Water, Air, and Soil Pollution.* 2001 Apr 1;127(1-4):281–299.
- Norrström AC, Jacks G. Concentration and fractionation of heavy metals in roadside soils receiving de-icing salts. *Science of The Total Environment.* 1998 Jul;218(2-3):161–174.
- Pennino MJ, McDonald RI, Jaffe PR. Watershed-scale impacts of stormwater green infrastructure on hydrology, nutrient fluxes, and combined sewer overflows in the mid-Atlantic region. *Sci Total Environ.* 2016 Sep 15;565:1044–1053.
- Puckett LJ, Cowdery TK, McMahon PB, Tornes LH, Stoner JD. Using chemical, hydrologic, and age dating analysis to delineate redox processes and flow paths in the riparian zone of a glacial outwash aquifer-stream system. *Water Resour Res.* 2002 Aug;38(8):-.
- Rossi RJ, Bain DJ, Elliott EM, Divers M, O’Neill B. Hillslope soil water flowpaths and the dynamics of roadside soil cation pools influenced by road deicers. *Hydrol Process.* 2017 Jan 1;31(1):177–190.
- Selbig WR, Bannerman RT. Evaluation of Street Sweeping as a Stormwater- Quality-Management Tool in Three Residential Basins in Madison, Wisconsin. US Geological Survey. 2007;

Three Rivers Wet Weather, d. Calibrated Radar Rainfall data. Retrieved from <http://3riverswetweather.org>

USEPA, 2001. National primary drinking water regulations; arsenic and clarifications to compliance and new source contaminants monitoring; final rule. Fed Reg. 2001;66(14).

USDA, 1981. Soil Survey of Allegheny County, Pennsylvania. Washington D.C.

Walsh CJ, Roy AH, Feminella JW, Cottingham PD, Groffman PM, Morgan RP. The urban stream syndrome: current knowledge and the search for a cure. Journal of the North American Benthological Society. 2005 Sep;24(3):706–723.

Warren LA, Zimmerman AP. The influence of temperature and NaCl on cadmium, copper and zinc partitioning among suspended particulate and dissolved phases in an urban river. Water Res. 1994 Sep;28(9):1921–1931.

### **3.0 Groundwater Flow and Geochemistry in Urban Aquifers of the Appalachian Plateau**

#### **3.1 Introduction**

Urbanization disrupts natural groundwater flowpaths and contaminates groundwater, yet groundwater remains an under studied component of the urban hydrologic cycle. Characterization of contamination patterns in urban groundwater and clarification of subsurface flowpaths can clarify contaminant transport through urban hydrologic systems. However, urban groundwater is challenging to study due to limited access in urban areas (there are relatively fewer wells relative to more rural areas) (Manga 2001). To gain access, groundwater discharge points (including springs) offer opportunities in areas where wells are scarce.

Groundwater springs provide relatively cheap access for characterization of groundwater chemistry where wells are limited. For example, montane systems where aquifers can be thin and population is sparse, springs are commonly used to probe groundwater chemistry. Spring water chemistry provides a window into water-rock interactions. Garrels and Mackenzie (1967) demonstrated that groundwater spring chemistry reflects the weathering of aquifer materials as the water moves through. Similarly, Mazar et al. (1985) found that repeated measurements of groundwater springs in a spa in Schinznach, Switzerland could clarify groundwater sources. Therefore, characterizing springwater discharge chemistry is a useful tool in clarifying sources and flowpaths. Mountain studies commonly use springs to identify and characterize the influence of groundwater on the hydrologic system (Clow et al. 2003; Roy and Hayashi 2009). This study aims to adopt a similar strategy in another access limited area and use urban groundwater springs to clarify complex urban groundwater systems.

Research on urban groundwater springs, while limited, reveals the impact of urbanization on groundwater chemistry. Foos (2003) used springs to analyze road salt application impacts on groundwater quality, identifying a direct relationship between the amount of road salt applied and the magnitude of road salt contamination in the groundwater in Cuyahoga Falls (OH, USA). Bardsley et al. (2015) documented a mixture between local meteoric sources and imported municipal water in spring discharge. These springs discharged high loads of sulfate and trace metal contamination to urban creeks, often exceeding regulatory standards. Similarly Gabor et al. (2017) found increased contaminant loads to a Salt Lake City (UT) stream in the lower reaches of the stream. The increase in stream contamination resulted from the increased relative contribution of urban impacted spring waters to these reaches as upstream water was diverted for irrigation. Therefore, urbanization can negatively impact groundwater chemistry which can then be observed in discharging urban springs and seeps.

Urbanization introduces new contaminants to hydrologic systems. Urban contaminant sources include car emissions and abrasion, industrial emissions, and leaking sewer pipes. Trace metal contamination, including that in car exhaust and road dust can be transported through urban runoff and then transported to shallow groundwater systems (Turer et al. 2001; Davis et al. 2009; Mullins et al. 2020). The widespread use of leaded gasolines prior to 1986 and heavy industrial activity have imparted substantial legacy metal contamination to urban soils and this contamination can be remobilized by ground and surface water (Mielke and Reagan 1998; Datko-Williams et al. 2014). In addition, leakage from sewer pipes introduces nutrient contaminants like nitrate to urban groundwater systems (Lerner 2002; Divers et al. 2014).

To characterize the impact of urbanization on groundwater systems, the unique geology of the Appalachian Plateau offers an opportunity to study multiple springs across an urban landscape.

Bedrock geology in the Appalachian Plateau controls groundwater flow in specific ways, resulting in multiple perched aquifers that crop out as numerous groundwater springs along valley hillslopes. While groundwater flow in the Appalachian Plateau is not fully understood, two conceptual models are used to clarify the movement and age of regional groundwater. Sheets and Kozar (2000) focus on the redundant, horizontal layers of sandstone, siltstone, shale, and coal characteristic of the Appalachian Plateau and suggest groundwater flows horizontally over low conductivity strata, resulting in numerous springs and seeps in hillsides and valleys where these layers intersect the valley wall. This conceptualization builds on the Wyrick and Borchers (1981) model that proposed connectivity among these strata aquifers occurs through vertical fracture networks forming as overburden stresses are released during landscape denudation.

Dissolved Si concentrations can provide relative estimates of residence times and clarify hydrologic pathways in these complicated systems (Rodgers et al. 2005). Dissolved Si concentrations increase with increased water-rock interactions (Asano et al. 2002; Marçais et al. 2018). Therefore, Si can serve as a proxy for groundwater residence time. This leads to a contrast in dissolved Si concentrations between precipitation and groundwater sources. Precipitation has much lower concentrations of dissolved Si relative to groundwater. The contrast between these two endmembers can be used to clarify contributions to spring discharge and potentially contaminant sources to the springs.

Based on the conceptual models, spring discharges at lower elevations was expected to have longer residence times. They are expected to be recharged through increasingly thicker bedrock layers and therefore take longer to travel from the point of recharge (elevation highs) than relatively higher strata aquifers (Figure 3-1). However, infiltration along the hillslope also has the potential to influence spring water chemistry. Ultimately, spring discharge chemistry reflects a

dynamic a mixture of short-residence time waters from hillslope infiltration and longer-residence time waters sourced from the strata aquifers. Using a transect of groundwater springs along an elevation gradient, this study seeks to elucidate the influence that hillslope recharge has on the hydrologic system and identify potential mixing patterns between the two groundwater sources.

This study measured water chemistry in four groundwater springs along an elevation transect in Pittsburgh, PA to clarify subsurface chemical transport and characterize sources of contamination influencing these waters. Dissolved metal and nutrient concentrations were measured bi-weekly between August 2017 and March 2019. This study documents the chemistry of spring water in the context of complicated urban subsurface flow, emphasizing the influence of multiple source mixing on contaminant discharge from the springs.

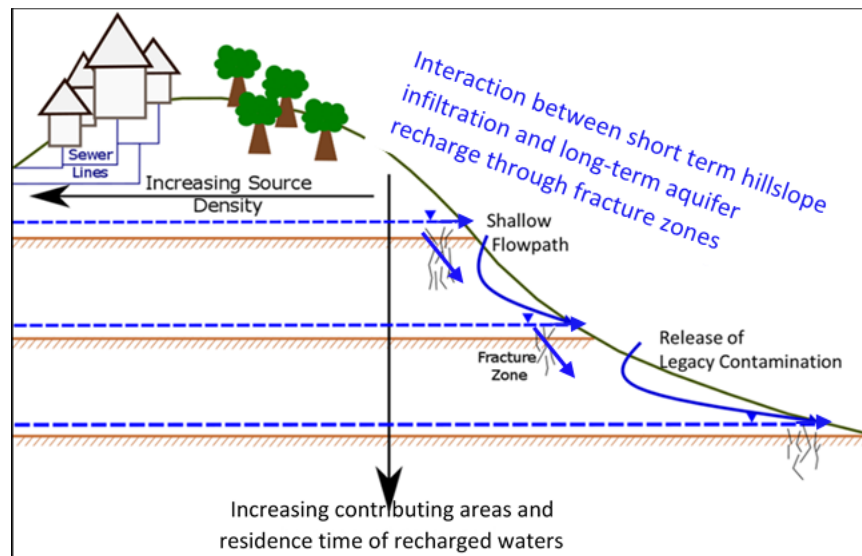


**Figure 3-1. Conceptual model demonstrating multiple possible recharge sources to perched water tables in study area.**

## 3.2 Materials and Methods

### 3.2.1 Study Site

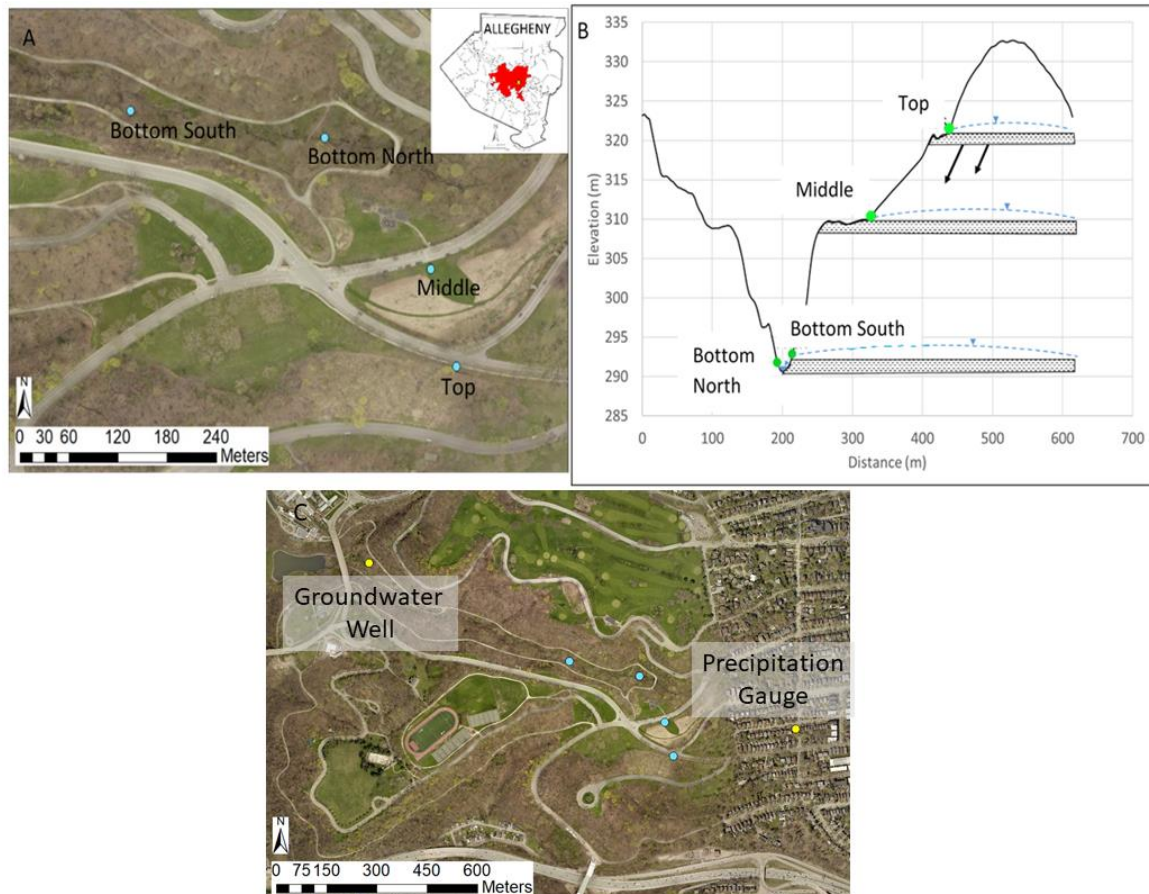


**Figure 3-2. A) Aerial imagery of the study area in Schenley Park (Pittsburgh, PA) (Allegheny County Imagery 2017) B) elevation transect extracted from LiDAR DEMs (PA Map Program 2008) showing the relative elevations of groundwater spring collection sites. And C) aerial imagery of the study area with groundwater well and precipitation gauge. Confining layers are hypothetical and connectivity between springs may be greater than illustrated**

Four ephemeral groundwater springs were identified in Schenley Park (Pittsburgh, PA) along an elevation transect (Figure 3-2B). The two springs at higher elevation (Top and Middle) discharge on grassy hillsides upslope of moderately trafficked roads (>5000 annual average daily

vehicle traffic) (PennDOT, 2020). Bottom South and Bottom North springs are in the base of a valley and discharge near Panther Hollow Run (a small stream where upstream reaches have been buried and piped (Hopkins, Bain & Copeland 2014)) (Figure 3-2A).

### **3.2.2 Sample Collection and Analysis**

Water samples were collected bi-weekly from each spring between August 2017 and March 2019. On some sampling dates, samples were not collected due to iced conditions in the winter or lack of discharge in the summer. Groundwater samples were also collected monthly from a groundwater well approximately 350 m down valley from Top spring. Precipitation samples were collected at a rain gauge ~700 m from the furthest groundwater spring (Figure 3-2C). The well water samples were screened in the riparian aquifer rather than the strata aquifers supplying spring discharge. However, the well samples are the only available reference for comparison of local groundwater chemistry that we know of.

During sample collection at the springs, a hole was dug near the point of discharge and allowed to fill, then samples were collected from the hole. Dissolved metal samples were collected in HDPE containers triple rinsed with spring water. The water samples for metal analysis were refrigerated at 4°C within 30 minutes of collection and for no more than 24 hours before they were filtered in the lab (0.2 micron PES filters). The lab-filtered samples used for metal analysis were then acidified using sub-boil distilled concentrated nitric acid and stored at -20°C. Sub samples of these acidified samples were diluted with 2% nitric acid and spiked with an internal standard containing Be, Ge, and Ti and concentrations of Ca, Sr, P, Pb, Cr, Cd, Fe, and Si measured on a Perkin/Elmer Nexion 300x inductively coupled plasma-mass spectrometer (ICP-MS) . Standards and blanks were included regularly throughout sample batches. Regular duplicates showed a

precision of within 10% of the measured values. Iron concentrations were measured using the kinetic energy discrimination (KED) method on the ICP-MS to reduce polyatomic interferences.

Finally, nitrate isotope samples were filtered in the field (0.2 micron, PES), collected in HDPE containers triple rinsed with filtered spring water, and stored at -20°C within 30 minutes of collection. Nitrate concentrations were measured using the Lachat Quickchem 8500 Flow Injection Analyzer. These concentrations were then used to determine nitrate isotope compositions on an Isoprime Continuous Flow Mass Spectrometer using the denitrifier method (Sigman et al. 2001).

### **3.2.3 Antecedent Precipitation**

The most recent storm preceding each collection time was identified using precipitation intensity data in 15-minute intervals from the University of Pittsburgh gauge in the Three Rivers Wet Weather Calibrated Radar Rainfall network (3riversewtweather.org). Here storm events were defined as precipitation lasting for at least 30 minutes or accumulating greater than 0.5 mm in a 15-minute interval. Time since precipitation was compared with spring discharge chemistry.

## **3.3 Results**

### **3.3.1 Ca/Sr Ratios in Discharging Spring Water and Aquifer Source**

Seventy-five samples were collected from the springs between August 30, 2017 and March 10, 2019, fifteen samples were collected from a groundwater well between February 8, 2016 and November 30, 2018, and one precipitation sample collected on June 10, 2019. Ca/Sr ratios (molar)

were examined to evaluate water sources to the discharging springs. Ca/Sr ratios in spring discharges from higher elevations (Top and Middle) and lower elevations (Bottom North and Bottom South) are relatively distinct, suggesting separate sources of water or variation in the mixture of water fed each spring (Figure 3-3). While the conceptual model (Figure 3-1) assumes that all four springs are distinct systems, the Ca/Sr ratios suggest the Top and Middle springs are similar or connected.

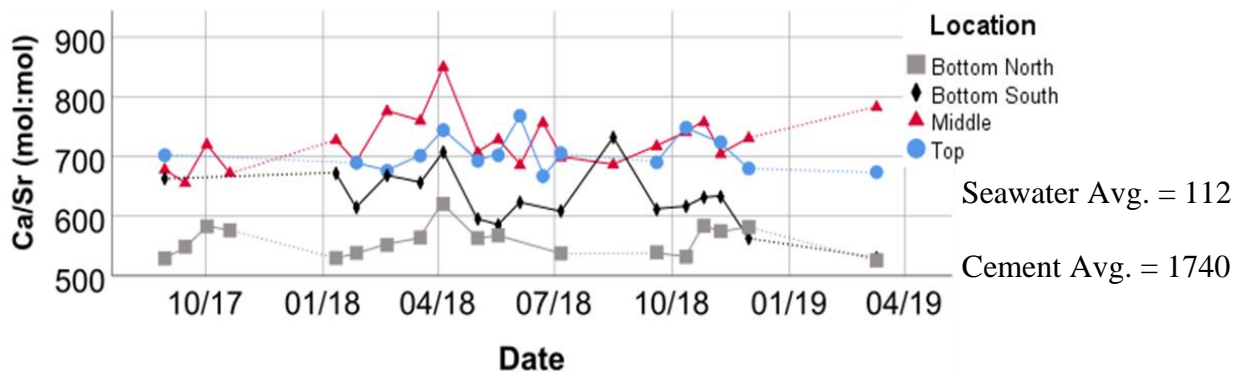


**Figure 3-3. Molar ratio of dissolved Ca and Sr measured in four groundwater springs between August 30, 2017 and April 10, 2019. Dotted lines indicate periods where samples were not collected due to frozen or dry conditions.**

Cr, Pb, and P concentrations are remarkably similar on individual sampling dates across the springs (Figures 3-4A-C). To quantify this similarity, the coefficient of variation (CV) was measured for every sampling date where more than two samples were collected. The average daily coefficient of variations was compared to the total coefficient of variation across all samples. This comparison was used as an estimate of how variable discharge chemistry was among springs. For Cr, Pb, and P the daily variations were 14%, 32%, and 25% respectively compared to total CVs of 67%, 95%, and 79% . When the Pb excursions measured on September 19 and October 12, 2018 were excluded (Figure 3-4B) , the daily variation was only 23% with a total CV of 83%.

Not all dissolved metals were as consistent across aquifer sources. While iron concentrations from all four springs increase and decrease on the same sampling dates, the individual concentrations are not similar among aquifer sources. Other metals, like cadmium, are not similar among springs (Figure 3-4D). There is no consistency in Cd contamination across separate spring sources as individual springs increase and decrease independently of the behavior of other spring chemistries. While Cr, Pb, and P have relatively tight daily variation, Cd concentrations are more variable with an average daily CV of 53% with a total CV of 79%.

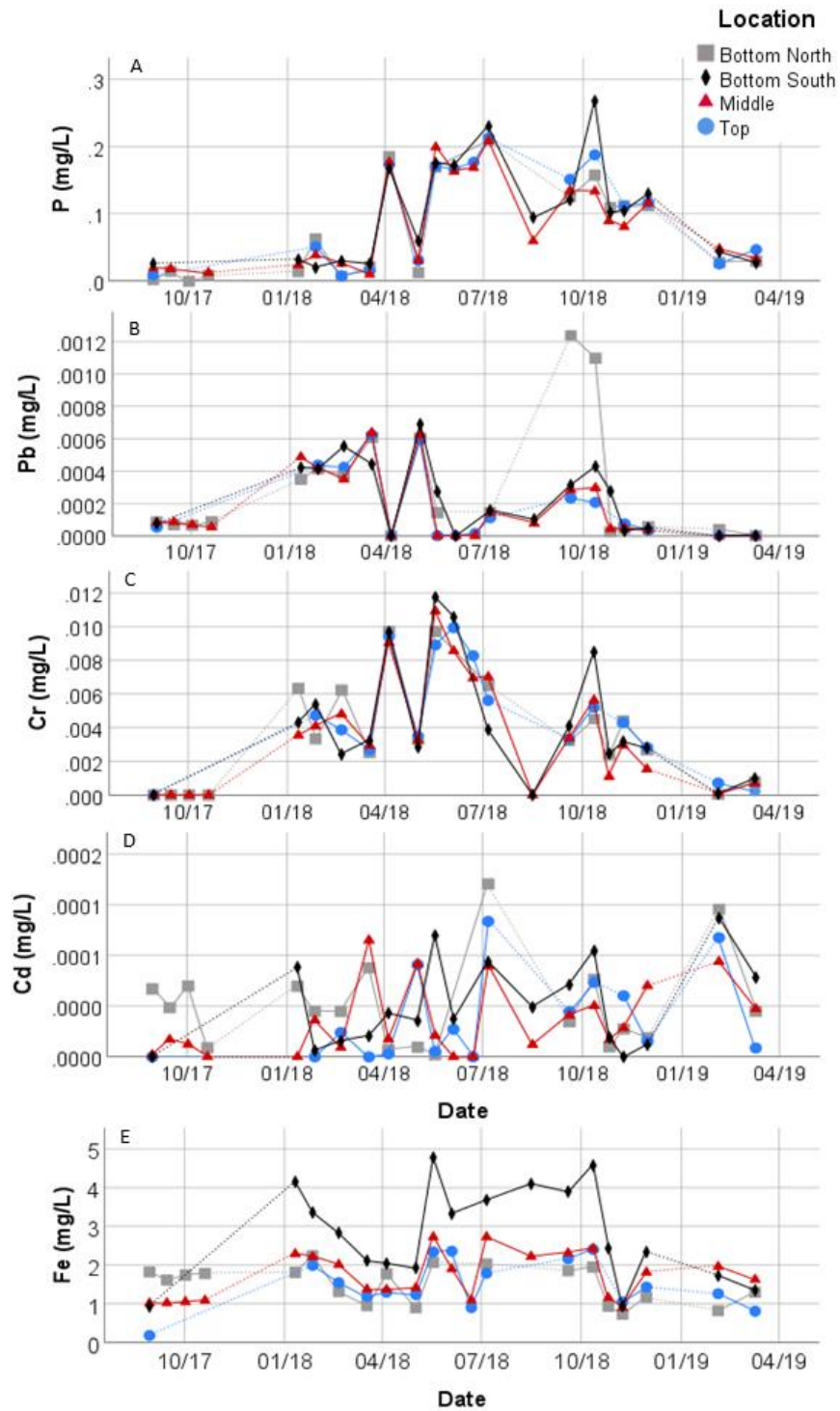
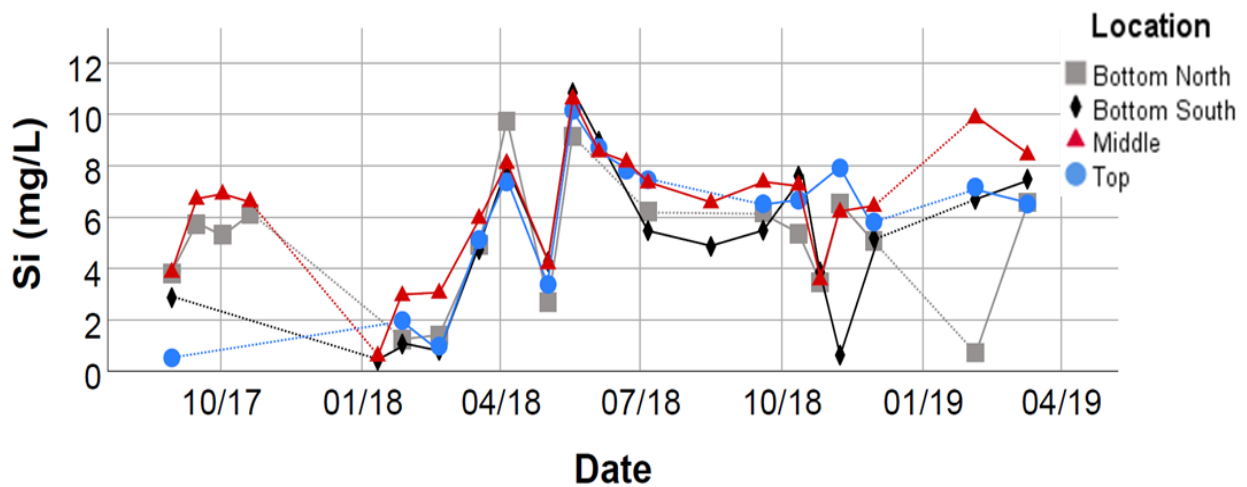


Figure 3-4. Concentrations of dissolved A) P, B) Pb, C) Cr, D) Cd, and E) Fe measured in four groundwater springs between August 30, 2017 and April 10, 2019. Dotted lines indicate times during which sampling were not collected due to frozen or dry conditions.

### 3.3.2 Silicon Concentrations and Water Residence Time

There is no obvious relationship between spring elevation and observed silicon concentration patterns. Lower elevation springs were expected to have longer flow paths, and therefore relatively longer residence times and higher Si concentrations. However, the Top Spring (highest in elevation/closest to recharge) has the highest Si concentration on more sampling dates than either Bottom North or Bottom South (i.e., the lowest springs (Figure 3-5).



**Figure 3-5. Concentrations of dissolved Si measured in four groundwater springs between August 30, 2017 and April 10, 2019. Dotted lines indicate times during which sampling were not collected due to frozen or dry conditions.**

Dissolved silicon concentrations in the spring water were highest when they were collected within ~ 2 days (50 hours) of a storm event (Figure 3-6). However, as the time between collection and the most recent storm event grew longer than 50 hours, dissolved Si in spring water dropped rapidly, suggesting increased contributions from more precipitation influenced waters (i.e., shorter residence time waters). As the hours since a storm continue to increase past this 50-hour point, Si concentrations increased steadily over hundreds of hours to concentrations more consistent with those measured in the groundwater. This suggests longer residence time water is discharged from

these springs during periods following precipitation. Water samples collected from groundwater well within the watershed had an average dissolved Si concentration of 6.3 mg/L and a range of 2.3 to 11.5 mg/L. This wide range of concentrations were the result of seasonal variations in evapotranspiration activity within the watershed, in contrast to patterns observed in the springs which showed no seasonal variation. This concentration is similar to spring discharge collected within 50 hours of precipitation (average 7.1 mg/L). Precipitation (the shortest residence time water) had dissolved Si concentrations of 0.35 mg/L, much lower than groundwater (Figure 3-6).

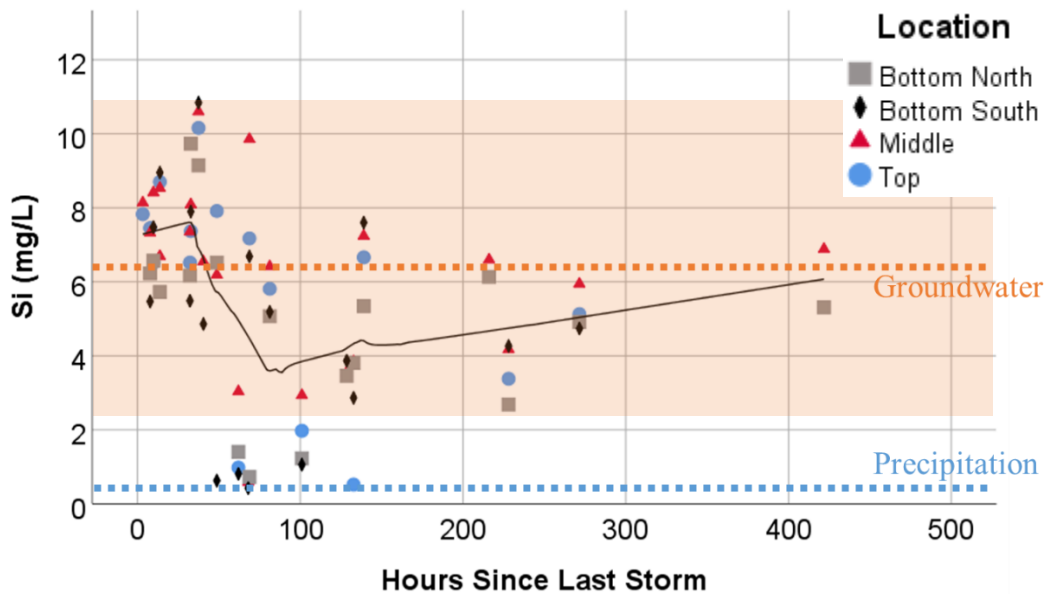


**Figure 3-6. Concentrations of dissolved Si measured in four groundwater springs between August 30, 2017 and April 10, 2019 plotted against the time between the most recent storm and sample collection. Orange dotted line indicates average groundwater Si concentration (based on 15 samples) measured in local groundwater wells. Orange box indicates range of Si concentrations in these groundwater samples. Blue dotted line indicates average precipitation Si concentration measured in samples collected within the watershed (15sample) The solid black line is LOESS fit.**

### 3.3.3 Nitrogen and Oxygen Isotopes of Nitrate

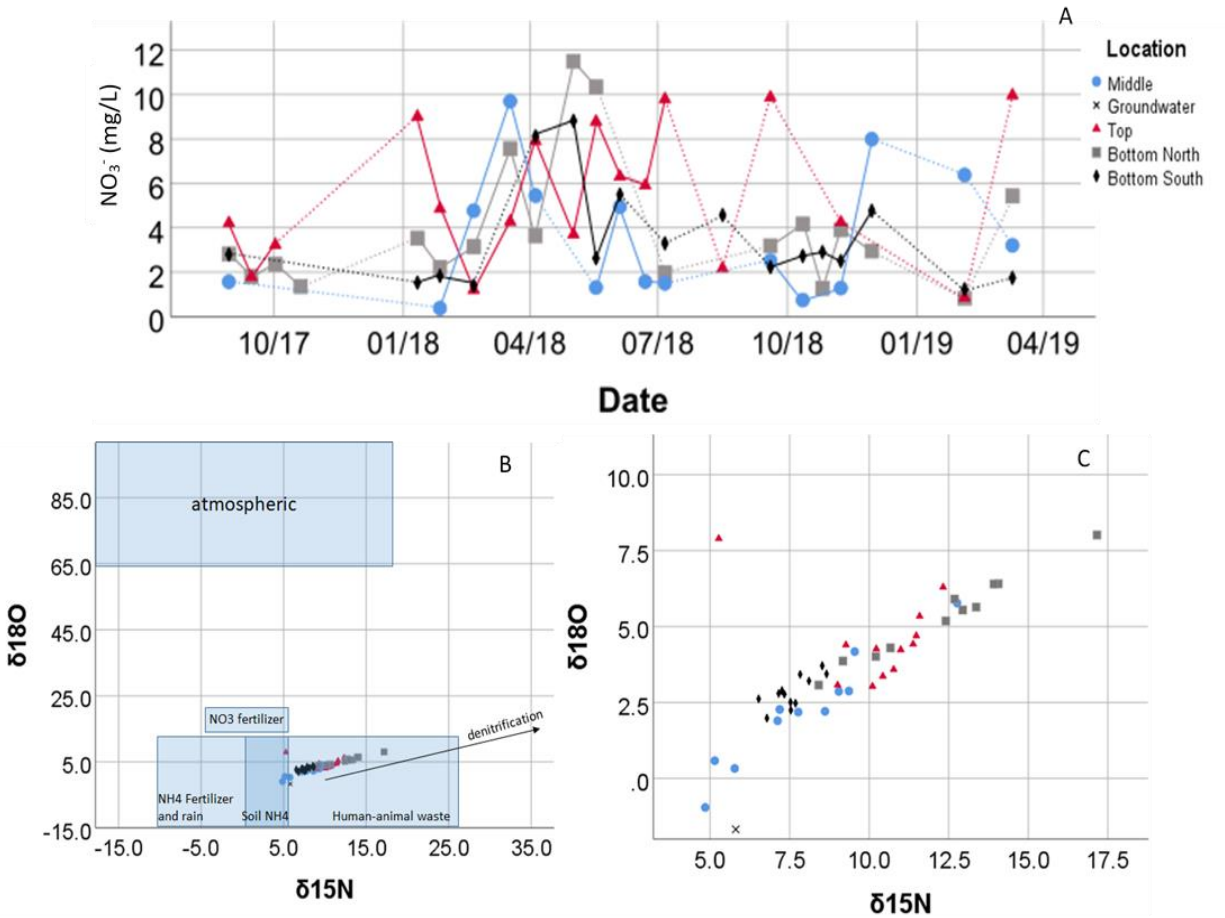


**Figure 3-7. A) Concentrations of  $\text{NO}_3^-$  measured in four groundwater springs between August 30, 2017 and April 10, 2019. Dotted lines indicate times during which samples were not collected due to frozen or dry conditions. B) Results from dual isotope analysis of nitrate in groundwater spring samples. C) data cluster in “human-animal waste” section of plot. X indicates average isotope compositions measured in groundwater collected from local groundwater wells. (Figure modified from (Kendall et al. 2007)**

All nitrate isotope compositions measured suggest a minimal atmospheric deposition source to spring water nitrate (Figure 3-7B). The low end of measured isotope ratios fall within the ranges typical of 1) human and animal waste and 2) nitrate derived from soil  $\text{NH}_4^+$  while the majority of samples fall solely in the human and animal waste range (Figure 3-8B). When all

samples are plotted on the Kendall plot, the isotope compositions fall along a line with a slope of 0.62 (Figure 3-8C). Nitrate  $\delta^{15}\text{N}_{\text{NO}_3^-}$  vs  $\delta^{18}\text{O}_{\text{NO}_3^-}$  slopes vary for individual groundwater springs, but all four springs have slopes typically observed in samples influenced by denitrification (Table 3-1). Bottom North spring has the strongest relationship between  $\delta^{15}\text{N}_{\text{NO}_3^-}$  and  $\delta^{18}\text{O}_{\text{NO}_3^-}$  and the lowest slope, likely a result of its smaller range compared to the other springs.

**Table 3-1. Average nitrate isotopic values, slope, and R<sup>2</sup> from all samples collected divided by sampling location.**

<b>Spring Name</b>	<b><math>\delta^{15}\text{N}_{\text{NO}_3^-}</math> Average</b>	<b><math>\delta^{18}\text{O}_{\text{NO}_3^-}</math> Average</b>	<b>Slope</b>	<b>R<sup>2</sup></b>	<b><math>\delta^{15}\text{N}_{\text{NO}_3^-}</math> Range</b>	<b><math>\delta^{18}\text{O}_{\text{NO}_3^-}</math> Range</b>
Top	+10.16‰	+4.46‰	0.73	0.56	7.05	4.87
Middle	+7.92‰	+2.20‰	0.77	0.93	7.92	6.73
Bottom North	+12.27‰	+5.31‰	0.56	0.98	8.75	4.95
Bottom South	+7.58‰	+2.84‰	0.61	0.56	1.50	1.73

### 3.4 Discussion

#### 3.4.1 Short-term Dynamics in Groundwater Spring Chemistry

Antecedent moisture (inferred from time since precipitation) seems to influence patterns in dissolved Si concentrations in spring discharge. Dissolved Si was generally more concentrated, and both water isotopes had heavier values when samples were collected within 50 hours of the most recent precipitation event. This pattern suggests discharge has a larger proportion of long residence time water in the first 50 hours following a storm event (Figure 3-6). When the time between a storm event and sample collection reaches 50 hours, the Si concentrations rapidly decrease. The low concentrations of Si suggest an increased contribution of shorter residence time

water to spring discharge. Following the drop at 50 hours, Si concentrations slowly increase and level off near the average concentration in the riparian aquifer.

We expected lower elevation groundwater springs (Bottom North and Bottom South springs) would have longer residence times as recharge must travel through increasingly thicker bedrock layers (Figure 3-1B). However, there was no consistent increase in dissolved Si concentrations measured across springs (Figure 3-5) suggesting groundwater contributions to the springs are unexpectedly similar mixtures. As the local water table varies seasonally (evidenced by the drying of the springs in the summer), Si concentrations in spring discharge could potentially be driven by concentration and dilution effects rather than aquifer depth. However, no seasonally driven patterns were observed in the Si concentrations (Figure 3-5), despite annual changes in the local water table.

The relationships among antecedent moisture, dissolved Si concentrations, suggests a two-endmember mix of water sources to spring discharge. Spring discharge is dominated by a relatively longer residence time source (groundwater signal) within 50 hours of a precipitation event. These spring water chemistry patterns are consistent with precipitation driven pressure waves observed in runoff generation (Jung et al. 2004; Vidon 2012). As infiltrating precipitation dominated waters reach the spring through shallow flow paths, low Si concentrations cause spring water to reflect increased contributions from a precipitation-like source. As time between precipitation and collection grows following the dynamics in the first couple days (i.e., >100 h), the influence of short residence time waters (precipitation) on the chemistry of discharging water wanes and the influence of the groundwater-like source increases, resulting in Si concentrations that reflect the groundwater endmember (Figure 3-6).

### 3.4.2 Dissolved metal Concentrations in Spring Water Discharge

Contrary to our conceptualization (Figure 3-1) there seems to be a limited influence of aquifer elevation on dissolved trace metal concentrations. Sheets and Kozar (2000) suggest aquifers in the Appalachian Plateau are recharged primarily at topographic highs, although they recognize some recharge likely occurs along hillsides. The recharge from topographic highs flows laterally across horizontal shale bedrock layers and downward through fractures to other aquifers (Sheets and Kozar 2000). As a result, the highest urban contamination concentration should seemingly be in the topographically highest aquifer (Top Spring). Lower aquifers should have relatively less contamination due to sorption of contaminants during flow through the aquifer and dilution in the larger (deeper) aquifers. Therefore, water collected from Bottom North and Bottom South were expected to have relatively less anthropogenic contamination. However, dissolved Cr, P, and Pb concentrations are remarkably similar across springs, suggesting that recharge from high elevations is not the mechanism driving contamination levels in spring water discharge. Although greater historical contamination in deeper aquifers could offset any dilution effect, there is no evidence that legacy contamination increases with depth in the study area.

While metal concentrations and aquifer elevation do not appear to be related, comparing dissolved metal concentrations to time since precipitation does reveal differences in patterns from those observed in [Si] and water isotopes. Silicon concentrations increase during the first 50 hours following a storm (i.e., long residence time groundwater) and then sharply change to concentrations reflecting short residence, precipitation-like water after 50 hours (Figure 3-6). P and Cr concentrations both have similar periods of elevated concentrations within 50 hours of a storm (Figure 3-8A). However, in both Cr and P there are later periods (~140 hours) of increased [P] and [Cr]. These elevated concentrations occur during a period when [Si] data seem to indicate

dominance of short-residence time water. This second increase may result from mobilization of soil bound metals during storm water infiltration and transport to the springs as precipitation concentrations are low (unpublished data).

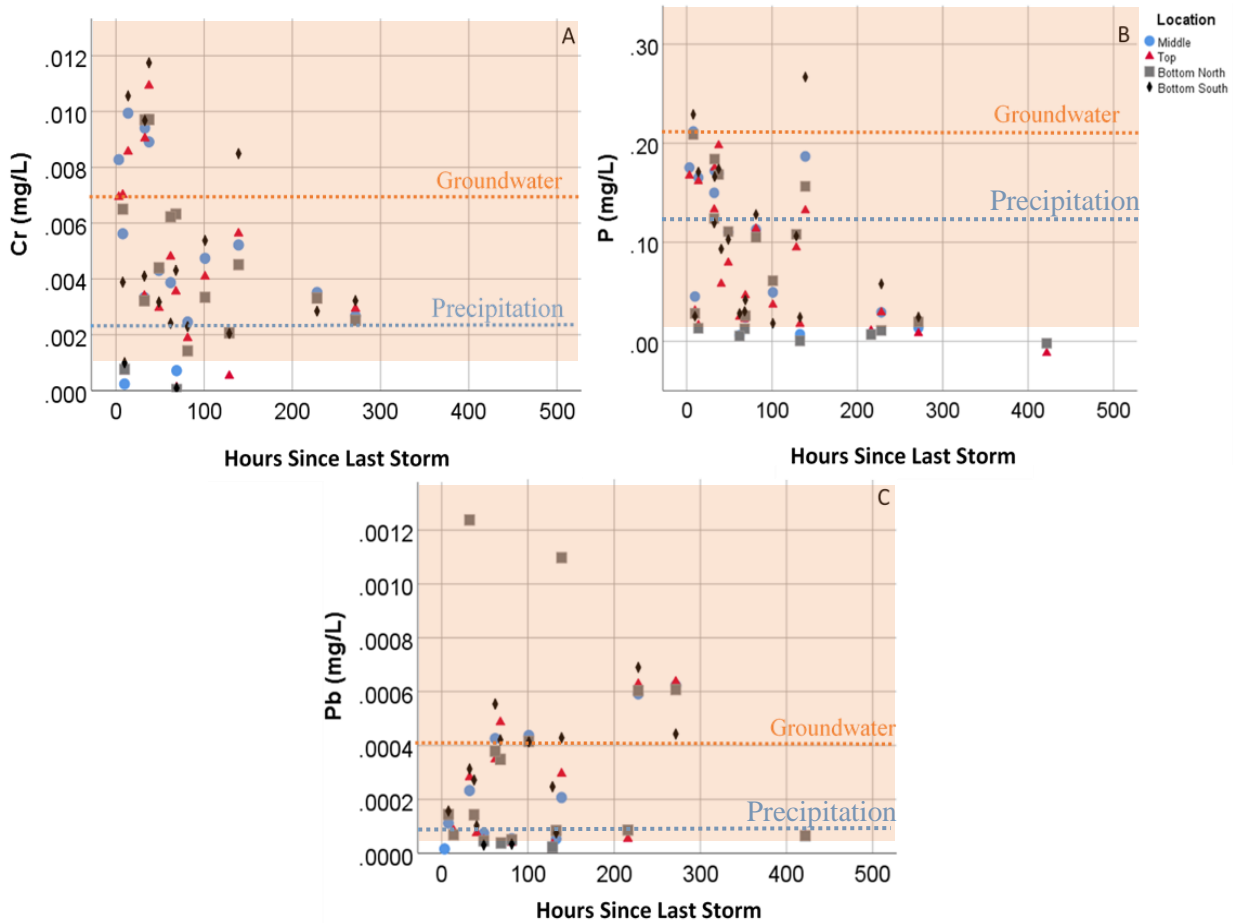


**Figure 3-8. A) Cr, B) P, and C) Pb concentrations measured in four groundwater springs between August 30, 2017 and April 10, 2019 compared to hours between last storm event and time of sample collection. Orange dotted lines indicate average groundwater concentrations. Blue dotted lines indicate average precipitation concentrations. Orange box indicates range of concentrations measured in groundwater samples.**

As another example, Pb concentration dynamics seem to be strongly influenced by short residence time sources. Within 50 hours of a storm, [Pb] remains low. In fact, the lowest detectable concentration of Pb (~0.00002) was measured in a sample collected only three hours after a storm (Figure 3-8C). After 50 hours, the period when Si concentrations are rapidly changing to more

precipitation-like concentrations, Pb concentrations grow. This suggests shorter residence time waters (i.e., precipitation moving through shallow flowpaths) dominate observed Pb dynamics. These waters may remobilize Pb from soils/shallow flow paths during movement and deliver it to spring discharge (Figure 3-2). The Pb patterns also suggest multiple shallow flow paths as [Pb] also increases at around 230 hours since precipitation in all springs (Figure 9C). We do not have the data to delineate these flow paths, but the consistency among springs merits additional future scrutiny. The flip side of this observation is that groundwater (i.e., long-term residence time water) has relatively low [Pb].

While we do not have sufficient data to clarify flow path, urban soils are generally lead contaminated (Pouyat and McDonnell 1991). Urban soils can also be enriched in Cr through coal and oil combustion (Cheng et al. 2014) or the production of steel alloys (Testa et al 2004). The application of fertilizers and leaking sewer pipes can elevate P concentrations in urban soils (Carpenter et al. 1998). However, to get consistent metal concentrations, soil contamination patterns in the study would have to be similar and travel through these shallow paths consistently from spring to spring. We know urban metal contamination is not homogenous (Pouyat and McDonnell 1991), making the consistency in water chemistry hard to explain solely from shallow interactions with contamination. Currently, we do not have sufficient data to clarify mechanisms driving consistent spring P, Cr, or Pb concentrations.

There are antecedant moisture driven geochemical sinks on the hillsides that could explain some of the consistency. For example, the reduction of iron and manganese oxyhydroxides would mobilize any bound metals. However, spring water chemistry patterns do not appear to indicate consistent reduction processes. Between May 18, 2018 and October 12, 2018 Fe concentrations remain elevated relative to concentrations measured in the winter (Figure 3-4E) yet, during the

same period, P concentrations are much more variable (Figure 3-4C). If dissolved metals resulted from oxyhydroxide dissolution, P concentrations should be elevated during periods where Fe is reduced. The lack of correlation between Fe and P concentrations ( $R^2 = 0.08$ ) during periods when soils may be reducing suggests a minimal role for reduction in the observed patterns. While the discrepancy between Fe and P may result from biological uptake of dissolved P, there is also no relationship ( $R^2 = 0.04$ ) between Fe and Pb or Cr concentrations during this time ( $R^2 = 0.04$  and  $0.13$  respectively). If Pb and Cr concentrations were driven by the reduction of Fe complexes, the increase in Fe should be mirrored in Pb and Cr (Figure 3-4B). Therefore, the seasonal variations of soil metal mobility do not seem to control spring water chemistry.

### 3.4.3 Nitrate in Urban Springwater

Spring elevation was expected to influence nitrate concentration in discharge. Sewer pipes are laid near the surface, distant from the deeper aquifers. Therefore, the Bottom North and Bottom South springs were expected to have lower nitrate concentrations when compared to the Top and Middle springs. However, concentrations are not consistently higher in the Top and Middle springs (Figure 3-8A)

To clarify nitrate sources,  $\delta^{15}\text{N}_{\text{NO}_3^-}$  and  $\delta^{18}\text{O}_{\text{NO}_3^-}$  were compared to each other.  $\delta^{15}\text{N}_{\text{NO}_3^-}$  and  $\delta^{18}\text{O}_{\text{NO}_3^-}$  are strongly related ( $R^2 = 0.891$ , slope = 0.62) (Figure 3-8B). Most of the nitrate isotope values measured fall in the human and animal waste region of the Kendall plot, likely from leaking sewers and potentially soil  $\text{NO}_3^-$  (Figure 3-8C). To evaluate the influence of source mixing and/or denitrification in each spring,  $\delta^{15}\text{N}_{\text{NO}_3^-}$  values were compared to  $1/\text{NO}_3^-$  and  $\ln\text{NO}_3^-$  for each individual spring respectively (Table 1) (Kendall et al. 2007). If mixing is the dominant process controlling nitrate concentrations in the system, plotting  $\delta^{15}\text{N}_{\text{NO}_3^-}$  against  $1/\text{NO}_3^-$  will yield a

straight line, while  $\delta^{15}\text{N}_{\text{NO}_3^-}$  vs.  $\ln\text{NO}_3^-$  will be a straight line if denitrification dominates the system. As there are no strong linear relationships between  $\delta^{15}\text{N}_{\text{NO}_3^-}$  and either  $1/\text{NO}_3^-$  or  $\ln\text{NO}_3^-$ , a combination of both mixing and denitrification likely creates the observed relationships between  $\delta^{15}\text{N}_{\text{NO}_3^-}$  and  $\delta^{18}\text{O}_{\text{NO}_3^-}$  (Figure 3-8A).

The influence of denitrification was further evaluated by comparing  $\delta^{18}\text{O}_{\text{NO}_3^-}$  values to  $\text{NO}_3^-$  concentrations. A strong inverse relationship between  $\delta^{18}\text{O}_{\text{NO}_3^-}$  and  $\text{NO}_3^-$  suggests that denitrification occurs in the spring water and results in heavier  $\delta^{18}\text{O}_{\text{NO}_3^-}$  and  $\delta^{15}\text{N}_{\text{NO}_3^-}$  values. The top, middle, and bottom north springs all have inverse linear relationships while the bottom south spring has no relationship between  $\delta^{18}\text{O}_{\text{NO}_3^-}$  and  $\text{NO}_3^-$ , indicating that denitrification is likely influencing the nitrate isotopic compositions in all but the Bottom South spring (Table 3-1). The range of isotopic compositions in the Bottom South Spring is very small (Table 3-1) compared to other springs. This consistency suggests a single source of nitrate to the Bottom South spring while the other springs that show evidence of mixing between at least two nitrate sources.

When compared to antecedent moisture,  $\text{NO}_3^-$  concentrations suggest that  $\text{NO}_3^-$  chemistry is influenced by both short and long-term residence time sources. Within 50 hours of a storm, there are elevated  $\text{NO}_3^-$  concentrations, which originates from a longer residence time source given patterns in [Si]. As time between precipitation and collection increases past 50 hours  $\text{NO}_3^-$  concentrations decrease. However, there is also a peak in concentration measured after 200 hours between precipitation and sampling (Figure 3-9). These elevated  $\text{NO}_3^-$  concentrations coincide an increase in dissolved Pb discharging from the spring (Figure 3-8C). As historical Pb and ongoing  $\text{NO}_x$  emissions from car exhaust create elevated concentrations of these contaminants in roadside soils (Al-Chalabi and Hawker 2000; Redling et al. 2013), this secondary spike may be the result of shallow flow paths that travel through roadside soils.

### 3.5 Conclusions

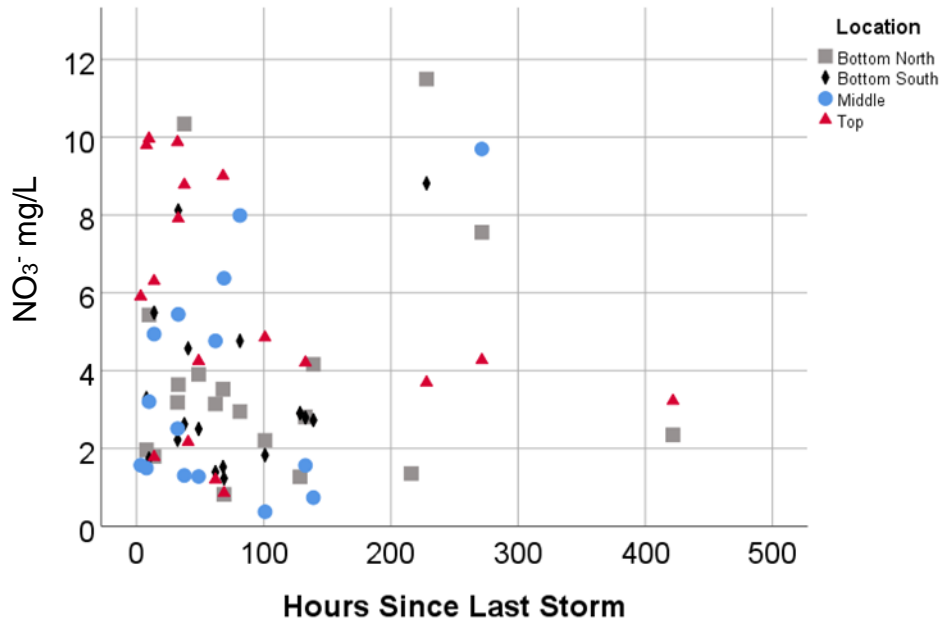


Figure 3-9.  $\text{NO}_3^-$  concentrations measured in four groundwater springs between August 30, 2017 and April 10, 2019 compared to hours between last storm event and time of sample collection.

The spatial variability in four urban groundwater springs along an elevation transect was assessed to evaluate the patterns of contamination in discharging spring water. We observed an unexpected consistency in water chemistry (P, Pb, Cr) across space and through time. It is a challenge to evaluate this similarity as there are few if any studies that have used elevation transects of groundwater springs. This consistency in water chemistry among spring chemistry suggests an unexpected homogeneity in urban groundwater chemistry. This work expands on previous studies of urban springs (Foos 2003; Bardlsey et al. 2015; Gabor et al. 2017), revealing unexpected patterns and raising fundamental questions about how multiple subsurface flowpaths influence spring water chemistry in cities overlying the Appalachian Plateau.

The observed consistency of water chemistry is particularly interesting given the apparent mix of fast and slow flowpath waters in spring water discharge. Dissolved [Si] suggests a

groundwater-like, longer residence time water dominates in the first 50 hours following a precipitation event. After 50 hours, spring discharge chemistry rapidly shifts to more precipitation like waters. As time between precipitation and sample collection continues to increase, Si concentrations settle into values that reflect the groundwater endmember. The metal concentrations, when examined in the fast-slow flow context, seem to indicate short term residence waters are a source of metal contamination to spring discharge. High concentrations of soil mobilized Pb, P, and Cr at different time scales suggest multiple shallow flowpaths contributing to spring discharge. Shorter residence time waters, an important source of metal content in these stream waters, seem to mobilize metals from near surface zones. However, this consistency in mobilization would require relatively uniform contamination across the urban landscape. We cannot evaluate the uniformity of contamination, but these interactions between shallow flowpaths and spring discharge warrant further examination.

Nitrate chemistry in the spring water also seemed to be influenced by the dynamics of fast and slow waters. Observed  $\text{NO}_3^-$  concentrations suggest a longer residence time, groundwater like source, potentially from leaking urban infrastructure. A secondary source of  $\text{NO}_3^-$  from short residence time water that travels through  $\text{NO}_x$  contaminated soils also contributes to spring discharge. The source of  $\text{NO}_3^-$  is therefore consistent with observations made in soil metal concentrations.

Fundamentally, springs are important windows for characterization of urban groundwater, particularly in the Appalachian Plateau. Unexpected patterns in water chemistry suggest that mixing of distinct water sources drives spring discharge chemistry. Further, this mixing dictates the timing of high contaminant fluxes from discharging springs, complicating source identification.

### 3.6 Bibliography

- Al-Chalabi AS, Hawker D. Distribution of vehicular lead in roadside soils of major roads of Brisbane, Australia. *Water Air Soil Pollut.* 2000;188(3-4):299–310.
- Asano Y, Uchida T, Ohte N. Residence times and flow paths of water in steep unchannelled catchments, Tanakami, Japan. *J Hydrol (Amst).* 2002 Apr;261(1-4):173–192.
- Bardsley AI, Hammond DE, von Bitner T, Buehning NH, Townsend-Small A. Shallow groundwater conveyance of geologically derived contaminants to urban creeks in southern California. *Environ Sci Technol.* 2015 Aug 18;49(16):9610–9619.
- Carpenter SR, Caraco NF, Correll DL, Howarth RW, Sharpley AN, Smith VH. Nonpoint pollution of surface waters with phosphorus and nitrogen. *Ecol Appl.* 1998 Aug;8(3):559–568.
- Cheng H, Zhou T, Li Q, Lu L, Lin C. Anthropogenic chromium emissions in China from 1990 to 2009. *PLoS ONE.* 2014 Feb 5;9(2):e87753.
- Clow DW, Schrott L, Webb R, Campbell DH, Torizzo A, Dornblaser M. Ground water occurrence and contributions to streamflow in an alpine catchment, Colorado Front Range. *Ground Water.* 2003 Dec;41(7):937–950.
- Datko-Williams L, Wilkie A, Richmond-Bryant J. Analysis of U.S. soil lead (Pb) studies from 1970 to 2012. *Sci Total Environ.* 2014 Jan 15;468-469:854–863.
- Davis AP, Hunt WF, Traver RG, Clar M. Bioretention technology: overview of current practice and future needs. *J Environ Eng.* 2009 Mar;135(3):109–117.
- Divers MT, Elliott EM, Bain DJ. Quantification of nitrate sources to an urban stream using dual nitrate isotopes. *Environ Sci Technol.* 2014 Sep 16;48(18):10580–10587.
- Foos A. Spatial distribution of road salt contamination of natural springs and seeps, Cuyahoga Falls, Ohio, USA. *Environmental Geology.* 2003 May;44(1):14–19.

- Gabor RS, Hall SJ, Eiriksson DP, Jameel Y, Millington M, Stout T, et al. Persistent urban influence on surface water quality via impacted groundwater. *Environ Sci Technol*. 2017 Sep 5;51(17):9477–9487.
- Garrels RM, Mackenzie FT. Origin of the chemical compositions of some springs and lakes. In: Stumm W, editor. *Equilibrium concepts in natural water systems*. WASHINGTON, D.C.: AMERICAN CHEMICAL SOCIETY; 1967. p. 222–242.
- Hopkins KG, Bain DJ, Copeland EM. Reconstruction of a century of landscape modification and hydrologic change in a small urban watershed in Pittsburgh, PA. *Landscape Ecol*. 2014 Mar;29(3): 413-24.
- Jung M, Burt TP, Bates PD. Toward a conceptual model of floodplain water table response. *Water Resour Res*. 2004 Dec;40(12).
- Kendall C, Elliott EM, Wankel SD. Tracing anthropogenic inputs of nitrogen to ecosystems. In: Michener R, Lajtha K, editors. *Stable isotopes in ecology and environmental science*. Oxford, UK: Blackwell Publishing Ltd; 2007. p. 375–449.
- Lerner DN. Identifying and quantifying urban recharge: a review. *Hydrogeol J*. 2002 Feb;10(1):143–152.
- Manga M. Using springs to study groundwater flow and active geologic processes. *Annu Rev Earth Planet Sci*. 2001 May;29(1):201–228.
- Marçais J, Gauvain A, Labasque T, Abbott BW, Pinay G, Aquilina L, et al. Dating groundwater with dissolved silica and CFC concentrations in crystalline aquifers. *Sci Total Environ*. 2018 Sep 15;636:260–272.

- Mazor E, Vuataz FD, Jaffé FC. Tracing groundwater components by chemical, isotopic and physical parameters — Example: Schinznach, Switzerland. *J Hydrol (Amst)*. 1985 Feb;76(3-4):233–246.
- Mielke HW, Reagan PL. Soil is an important pathway of human lead exposure. *Environ Health Perspect*. 1998 Feb;106 Suppl 1:217–229.
- Mullins AR, Bain DJ, Pfeil-McCullough E, Hopkins KG, Lavin S, Copeland E. Seasonal drivers of chemical and hydrological patterns in roadside infiltration-based green infrastructure. *Sci Total Environ*. 2020 Apr 20;714:136503.
- Pouyat RV, McDonnell MJ. Heavy metal accumulations in forest soils along an urban- rural gradient in Southeastern New York, USA. *Water Air Soil Pollut*. 1991 Aug;57-58(1):797–807.
- Rodgers P, Soulsby C, Waldron S. Stable isotope tracers as diagnostic tools in upscaling flow path understanding and residence time estimates in a mountainous mesoscale catchment. *Hydrol Process*. 2005 Jul;19(11):2291–2307.
- Redling K, Elliott E, Bain D, Sherwell J. Highway contributions to reactive nitrogen deposition: tracing the fate of vehicular NO<sub>x</sub> using stable isotopes and plant biomonitors. *Biogeochemistry*. 2013 Dec;116(1-3):261–274.
- Roy JW, Hayashi M. Multiple, distinct groundwater flow systems of a single moraine–talus feature in an alpine watershed. *J Hydrol (Amst)*. 2009 Jun;373(1-2):139–150.
- Sheets CJ, Kozar MD. Ground-Water Quality in the Appalachian Plateaus, Kanawha River Basin, West Virginia.pdf. *Water-Resources Investigations Report*. 2000;99(4269).

- Sigman DM, Casciotti KL, Andreani M, Barford C, Galanter M, Böhlke JK. A bacterial method for the nitrogen isotopic analysis of nitrate in seawater and freshwater. *Anal Chem*. 2001 Sep 1;73(17):4145–4153.
- Turer D, Maynard JB, Sansalone JJ. Heavy Metal Contamination in Soils of Urban Highways: Comparison Between Runoff and Soil Concentrations at Cincinnati, Ohio. Springer Science and Business Media LLC. 2001;
- Vidon P. Towards a better understanding of riparian zone water table response to precipitation: surface water infiltration, hillslope contribution or pressure wave processes? *Hydrological Processes*. 2012 Oct 15;26(21):3207–3215.
- Wyrick GG, Borchers JW. Hydrologic effects of stress-relief fracturing in an Appalachian Valley. 1981.

## **4.0 Spring Water Discharge as a Mechanism for Legacy Metal Enrichment in Urban Soils**

### **4.1 Introduction**

Soil is vital to urban ecosystems, driving biogeochemical cycling, providing nutrients and substrate for plant growth, and filtering and storing water (Effland and Pouyat 1997; Luo et al. 2012). The distribution of metals in soils in both urban and non-urban environments depends on a variety of interacting factors. In non-urban environments, natural soil heterogeneity is controlled by several factors: underlying bedrock, climate, vegetation, topography, and age of the soil (Essington 2015). Urbanization however, creates much more complex patterns of soil metals. Spatial heterogeneity of urban soils has increased due to construction and excavation which mix soils and import non-native soils (Ajmone-Marsan and Biasioli 2010). Further, urbanization concentrates point sources of contamination like sewage outflows and non-point sources like car or industrial exhaust (Cobelo-García and Prego 2004). Few studies have focused on specific “natural” mechanisms driving distribution of metals in urban soils. In general, metals are associated with land use (i.e. roads, smokestacks, etc.) (Pouyat 2015). However, the transportation of metals through groundwater systems and subsequent discharge of contaminated groundwater at springs or seeps far from the source may redistribute metal contaminants in unexpected ways.

Pittsburgh’s industrial history has degraded the city’s soil chemistry, particularly by adding metals throughout the city. Historically, industrial activities generated large quantities of metal contamination like Pb and Zn through atmospheric deposition that is still present in urban soils (Vermillion et al. 2005; Mattielli et al. 2009). Pittsburgh’s historical economic base provides the opportunity to study dynamics of metals associated with steel metallurgy. Between 1880 and 1920,

Pittsburgh was one of the pre-eminent industrial centers in America, earning the name “The Steel City” (Tarr 2004; Dieterich-Ward 2016). Due to Pittsburgh’s history of steel production, elevated levels of metals used as steel hardening agents (Co, Cr, Ni, and V) are likely found in shallow soil throughout the city.

Groundwater chemistry has frequently been linked to surface water chemistry as most surface water flow arises from groundwater sources (Reay et al. 1992; Rozemeijer and Broars 2007; Brooks et al. 2015). Therefore, contaminated groundwater has been associated with degraded water quality in urban hydrologic systems. Rivett et al. (2011) found elevated concentrations of major and minor ions in waters deeper in the water column that occasionally exceeded surface concentrations in an urban river. These concentration increases resulted from groundwater contaminant plumes discharging to the river system below the water surface. Further, Gabor et al. (2017) attributed elevated Cl and  $\text{NO}_3^-$  in an urban stream to contributions from groundwater springs impacted by urbanization. Chapter 3 documented the chemistry of discharging groundwater springs in Pittsburgh and revealed contaminant transport through the groundwater system. Given that groundwater springs often discharge to relatively small spatial zones, urban contamination transported through the subsurface may be focused at these springs and therefore disproportionately impact soils far from the original source .

Groundwater flow can mobilize metals during recharge and transport these metals to soils downgradient of groundwater discharge points. These focused areas of contamination likely increase soil metal heterogeneity in shallow soils across urban landscapes and may result in hot spots of hazardous metal contamination. This contamination likely is greatest near the spring discharge source. Further downgradient, contamination is expected to decrease as the contamination diffuses. This may create hot spots of soil metal contamination near and below

springs discharging contaminated groundwater (Figure 4-1). This study evaluates the impact of contaminated groundwater discharge on urban soils by examining multiple soil sampling transects stretching from upslope to downslope of groundwater springs. Contamination hotspots in urban soils can negatively impact ecological health, affecting plant communities and organisms feeding near these springs. For example, Ni uptake from contaminated soils interferes with uptake of other essential metals, reducing photosynthesis and plant growth (Yusuf et al. 2011). Similarly, ingested heavy metal contamination can accumulate and degrade wildlife and human health (Wu et al. 2018). Therefore, the identification of elevated soil metal concentrations across an urban landscape is vital for effective ecosystem management.

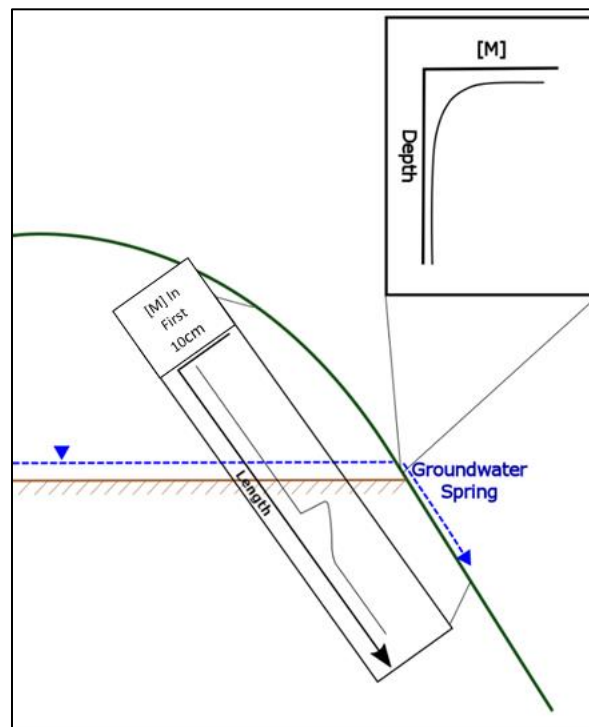


**Figure 4-1. Conceptual profiles of soil metal concentrations surrounding a groundwater spring discharge location. Soil metal concentrations are expected to spike at the point of discharge, then decrease as distance from the spring increases downslope.**

Cobalt, Cr, Ni and V concentrations were measured in soil cores collected along four transects to evaluate the influence of groundwater contaminant transport on soil concentrations in

near spring areas. Soil metals were measured in three different phases, allowing inference of metal dynamics at multiple time scales: total metals, exchangeable metals, and pore water concentrations. This sampling identifies locations of high contamination potential at the interface between groundwater and soil and evaluates a poorly characterized mechanism of potential soil metal contamination.

## 4.2 Methods

### 4.2.1 Sample Collection and Analysis

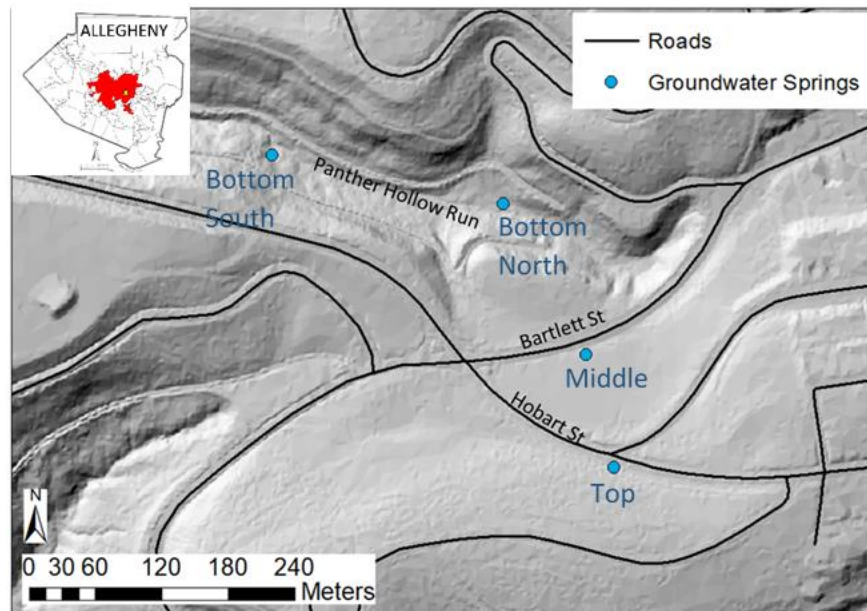


**Figure 4-2. Study area in Schenley Park (Pittsburgh, PA) with transect locations (hillshade of LiDAR DEM (PAMAP Program, PA Department of Conservation and Natural Resources 2006-2008))**

Soil-trace metal interactions are examined at seeps and springs to evaluate groundwater contamination influences on urban soil contamination patterns. To characterize this interaction,

soil cores were collected along four transects centered on a groundwater spring or seep in Pittsburgh, PA (Figure 4-3). Soil cores were collected at three-meter intervals upslope and downslope of groundwater springs to characterize impacts of spring water discharge on soil trace metal concentrations. Soil metal concentrations downslope of spring water discharges were directly compared to upslope concentrations to evaluate soil metal enrichment. The transects were labeled Top, Middle, Bottom North, and Bottom South based on the elevation of the spring within the study area (Figure 4-2). Top and Middle springs discharge on grassy hillsides upslope of moderately trafficked roads. The other springs (Bottom South and Bottom North) are in the base of a valley and discharge upslope of Panther Hollow Run (Figure 4-3).

Soil cores were collected in September of 2019 from twenty-six locations. A tape was laid across each spring, centered on the point of groundwater discharge. Soil cores were collected every three meters along these soil transects to a depth of fifteen cm or until refusal. The core transects started nine meters upslope from any saturated area at each spring and ended nine meters downslope of the spring. Cores were only collected to six meters below the spring in the Bottom North transect as the transect intersected Panther Hollow Run (Figure 4-3).

Each soil core was separated into three depth intervals: 0-5 cm, 5-10 cm, and 10-15 cm and stored in 25 mL centrifugal 0.22  $\mu\text{m}$  filters. Prior to field sampling the centrifugal filters and tubes were soaked in at 10% hydrochloric acid bath for 24 hours and rinsed three times with 18M $\Omega$  water before sample collection. Metal concentrations in core increments were measured in three different geochemical phases: total digestion of sediments, exchangeable metals, and dissolved (pore water) metals (methods detailed below). In addition, total concentrations were also normalized using the total iron concentration, (referred to as “Fe-normalized total concentrations”).

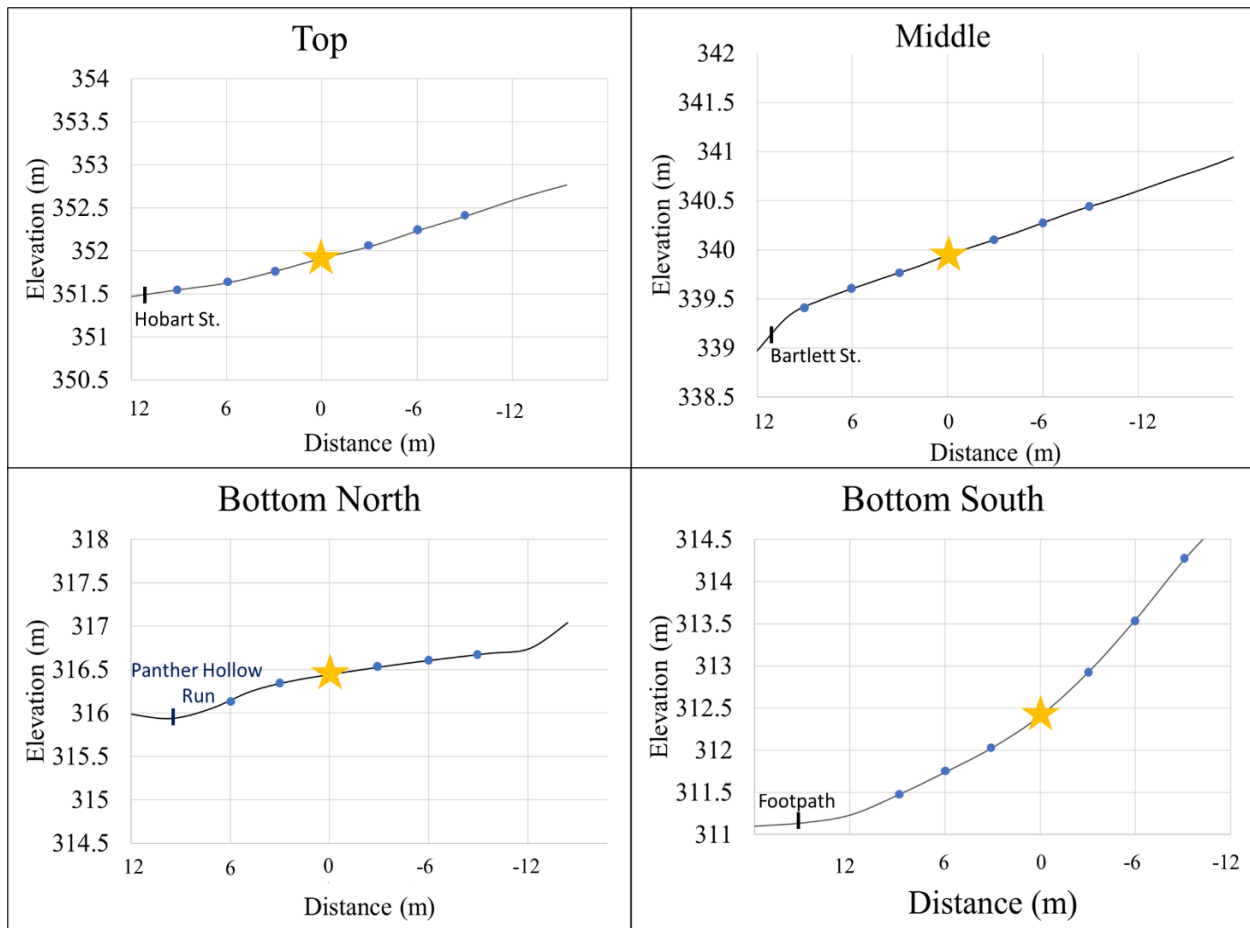


**Figure 4-3. LiDAR extracted elevation transects of elevations at the four sampling locations. Blue circles indicate locations of soil cores. Yellow star indicates approximate location of groundwater springs within the transect. (PAMAP Program, PA Department of Conservation and Natural Resources 2006-2008). Y-axes are adjusted to all span 3.5 meters of elevation.**

#### 4.2.2 Metal Concentration Measurements

**Pore Water Concentrations:** Samples (collected in centrifuge filter tubes) were centrifuged at 4000 rpm for 1 hour forcing porewater through the acid washed 0.22  $\mu\text{m}$  filters. Subsamples of the pore water were diluted with 2% nitric acid and spiked with an internal standard containing beryllium [Be], germanium [Ge], and tellurium [Tl]. Metal concentrations (Fe, Si, Li,

Co, Cr, Ni, V) were measured on a PerkinElmer Nexion 300x inductively coupled plasma-mass spectrometer (ICP-MS). Fe concentrations were measured using the kinetic energy discrimination (KED) method on the ICP-MS to reduce polyatomic interferences. Duplicates and blanks were included every ten samples throughout sample batches. Comparison of sample duplicates indicate measurements were generally within 5% of each other, with the exception of Cr, which were consistently within 10%.

**Exchangeable Metal Concentrations:** After pore water was extracted, the solid soil samples were removed from the centrifuge tubes, dried for 48 hours at 50°C, and powdered in a ball mill (tungsten carbide bomb). Exchangeable metals were extracted from the powdered soil (0.125g of soil was extracted with 5 mL of 0.11 M acetic acid, shaken for 16 hours at room temperature) (Mossop and Davidson 2003). Extractants were separated by centrifuging the extract solution for 20 minutes at 3000 rpm and decanted to a clean centrifuge tube. Subsamples of the exchangeable extract were diluted and measured using the same method as pore water samples.

**Total Metal Concentrations:** Total metal concentrations in powdered soils were measured by ALS Chemex (ME-MS61).

#### **4.2.3 Metal Phase Concentration Interpretation**

**Pore Water Concentrations:** Dissolved metal concentrations in pore water collected from cores downslope are interpreted as recent contributions from springs that are equilibrating with the local soil environment while upslope pore water is interpreted as infiltrated precipitation and overland runoff. Metals introduced to the soil from discharging spring water are transported

through pore spaces on a scale of days to months. Therefore, pore water chemistry should reflect relatively recent spring water chemistry.

**Exchangeable Metal Concentrations:** Exchangeable metal concentrations are interpreted to reflect the contribution of metals from spring discharge over longer time periods than the pore water. Exchangeable metal concentrations reflect the dynamic equilibrium between dissolved metals and exchange sites. Exchangeable metals offer insight into transect chemistry on a time scale ranging from months to years. This allows for detection of occasional or seasonal pulses of dissolved metals from the springs that would not be apparent in the pore water samples. However, due to the ambiguous equilibrium state of exchangeable and pore water metals, exchangeable metals may contribute to pore water concentrations when exchangeable metals remobilize. Therefore, it is possible that exchangeable metals enrich the pore water concentration.

**Total and Normalized Concentrations:** Total concentrations are interpreted to reflect metal accumulation downslope of spring discharge over periods stretching from years to decades. That is, total metal concentrations downslope of springs should reflect the influence of consistent inputs of discharging groundwater on downslope soils as ambient metals are incorporated into longer-forming geochemical phases. To normalize the influence of variability in iron oxyhydroxides and the impact on sorbed metals, bulk concentrations were normalized by iron concentrations (iron concentration is treated as a proxy for oxyhydroxide content). The more iron oxyhydroxide binding sites there are in a soil, the more potential for trace metals to bind to these geochemically favorable sites. Therefore, an increase in Fe concentration downslope could result in higher concentrations of other metals disproportionate to the concentrations of the trace metals in the discharge. The normalization by Fe concentrations allows comparison of these long-term trace metal enrichment across samples where oxyhydroxide content can vary widely.

## 4.3 Results

### 4.3.1 Upslope/Downslope Differences

Student’s t-tests were run for each trace metal at each sampling location, comparing means of metal concentrations collected upslope of spring discharge and those collected at or downslope of spring discharge. This resulted in 60 total p-value results when evaluating whether the populations were statistically different (Table 4-1). Of the 60 p-values, 29 were significantly different ( $< 0.05$ ). Due to the small sample size of each transect, p-values  $\leq 0.1$  were considered to be “trending toward significance”. There were 11 more p-values trending toward significance, resulting in two-thirds of the t-tests significant or nearing significant differences between upslope and downslope metal contents. However, repeated tests are needed to conclusively determine the p-value for these transects.

To evaluate the broader influence of springs on soil chemistry, all transect values of each metal species above/below the spring were combined into two sets and compared (Table 4-2). When combined across transects, all of the pore water and Fe-normalized total concentrations were significantly higher in the downslope portion. Li concentrations were the only metal species to be significantly different in the exchangeable phase.

**Table 4-1. P-values resulting from student’s t-tests comparing concentrations of pore water, exchangeable, and Fe-normalized total Li, Co, Cr, Ni, and V collected upslope and downslope of spring discharge. Samples were divided by sampling location. The “\*” indicates a statistically significant difference between populations.**

<b>P-values for single transect analysis</b>	<b>Top Transect</b>	<b>Middle Transect</b>	<b>Bottom North Transect</b>	<b>Bottom South Transect</b>
<b>Pore Water Li</b>	0.01*	0.112	0.67	0.41
<b>Exchangeable Li</b>	0.018*	0.004*	0.001*	0.002*

<b>Fe-Normalized Li</b>	0.07	0.01*	0.002*	0.243
<b>Pore Water Co</b>	0.064	0.228	0.022*	0.326
<b>Exchangeable Co</b>	0.22	0.836	0.007*	0.177
<b>Fe-Normalized Co</b>	0.707	0.031*	0.024*	0.01*
<b>Pore Water Cr</b>	0.17	0.004*	0.027*	0.028*
<b>Exchangeable Cr</b>	0.113	0.471	0.043*	0.517
<b>Fe-Normalized Cr</b>	0.023*	0.046*	0.081	0.893
<b>Pore Water Ni</b>	0.009*	0.016*	0.104	0.774
<b>Exchangeable Ni</b>	0.199	0.096	0.124	0.099
<b>Fe-Normalized Ni</b>	0.05*	0.029*	0.066	0.008*
<b>Pore Water V</b>	0.064	0.136	0.184	0.176
<b>Exchangeable V</b>	0.005*	0.007*	0.719	0.816
<b>Fe-Normalized V</b>	0.019*	0.001*	0.005*	0.01*

**Table 4-2. P-values resulting from student's t-tests comparing concentrations of pore water, exchangeable, and Fe-normalized total Li, Co, Cr, Ni, and V collected upslope and downslope of spring discharge. The “\*” indicates a statistically significant difference between populations.**

<b>P-values for cross-transect comparison</b>	<b>Li</b>	<b>Cr</b>	<b>Co</b>	<b>Ni</b>	<b>V</b>
<b>Pore Water</b>	0.0001*	0.001*	0.007*	0.037*	0.011*
<b>Exchangeable</b>	0.044*	0.816	0.106	0.178	0.355
<b>Fe-Normalized</b>	0.039*	0.001*	0.004*	0.007*	0.001*

### **4.3.2 Lithium Concentrations and Spring Water Enrichment**

**Pore Water Li:** In general, Li pore water concentrations increase at the point of groundwater discharge and remain elevated compared to concentrations measured upslope (Figure 4-4). Although the Bottom North transect has elevated concentrations of dissolved Li upslope of discharge, there is still an increase in concentration between the core collected three meters upslope of the spring and the core collected at the spring. When all values of Li up and downslope of spring discharge were compared, downslope values were higher (t-test results in Table 4-1).

**Exchangeable Li:** Exchangeable Li concentrations also tend to increase at or downslope of spring discharge (Figure 4-4). Lithium exchangeable concentrations at all four transects were significantly higher in the downslope portion (Table 4-2). One important exception is that the highest exchangeable concentration of Li in the Bottom South transect was measured upslope of the spring.

**Fe-Normalized Total Li:** Although Fe-normalized total Li concentrations are not as consistently higher in downslope soil when compared to upslope soils, downslope totals still tend to be higher (Figure 4). The Middle and Bottom North transects significantly increase downslope while the Top transect is trending toward significance ( $p$ -value = 0.07, Table 4-1). However, just as with the exchangeable Li concentration, the highest Fe-normalized total Li concentration in the Bottom South transect was upslope of discharge (Figure 4-4).

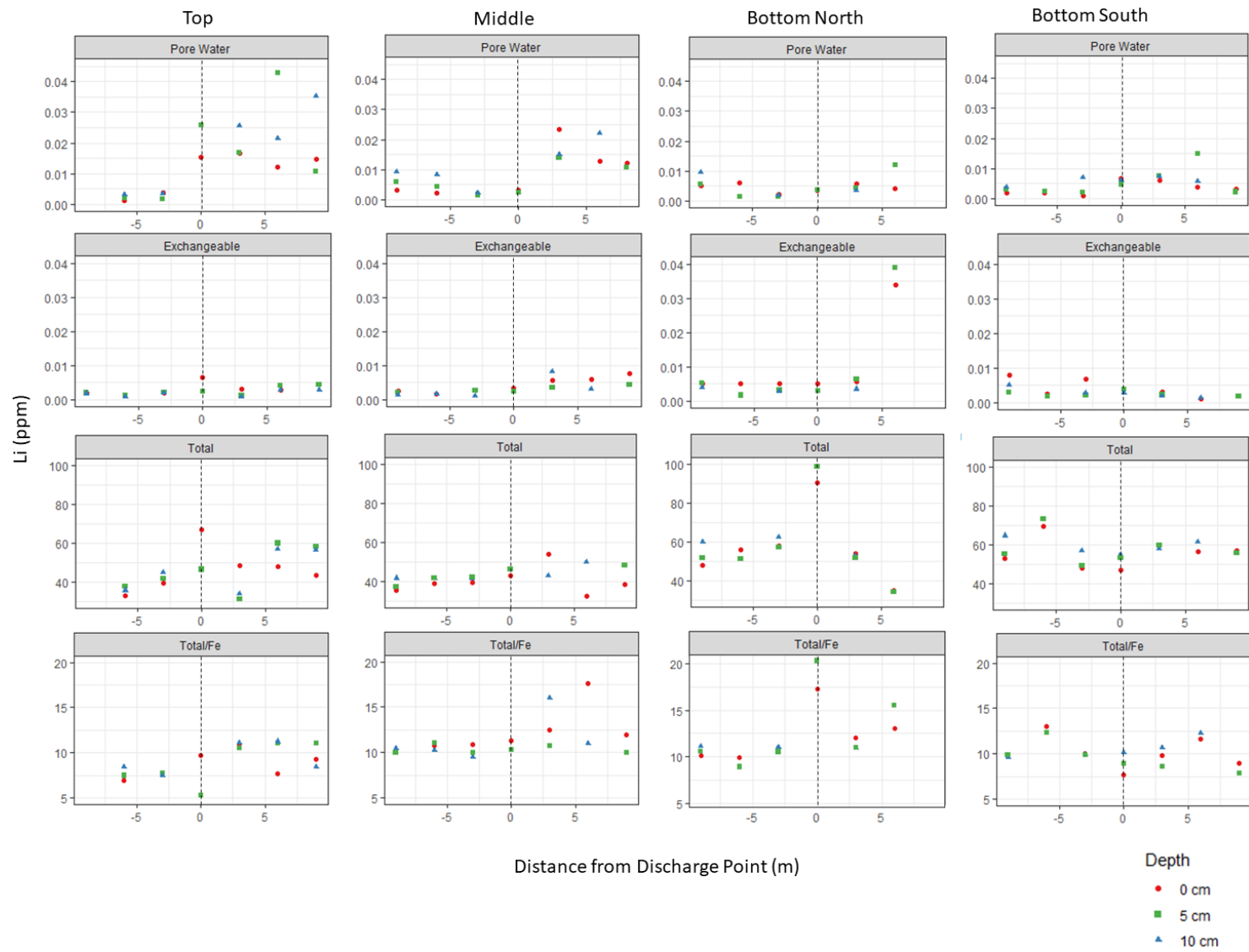


**Figure 4-4. Total, Fe-normalized, exchangeable, and pore water Li measured in soil cores collected along four transects intersecting groundwater springs. Black dotted lines indicate location of groundwater discharge along transect.**

### 4.3.3 Steel Alloy Metal Patterns

Table 4-3. Maximum, minimum, average, and coefficient of variation of pore water, Fe-normalized total, and exchangeable concentrations of Co, Cr, Ni, and V measured in soil cores across all transects

	Maximum (ppm)	Minimum (ppm)	Average (ppm)	Coefficient of Variation
<b>Co Pore Water</b>	0.07	0.0002	0.007	172%
<b>Co Exchangeable</b>	0.03	0.001	0.01	41%
<b>Co Fe-Normalized Total</b>	2.59	6.07	3.5	41%
<b>Cr Pore Water</b>	0.04	0.001	0.01	64%
<b>Cr Exchangeable</b>	0.07	0.04	0.06	9%
<b>Cr Fe-Normalized Total</b>	33.55	11.31	18.19	21%
<b>Ni Pore Water</b>	0.28	0.004	0.03	145%
<b>Ni Exchangeable</b>	0.04	0.003	0.01	57%
<b>Ni Fe-Normalized Total</b>	16.1	6.11	8.5	20%
<b>V Pore Water</b>	0.13	BDL	0.01	142%
<b>V Exchangeable</b>	0.02	0.0001	0.004	104%
<b>V Fe-Normalized Total</b>	41.83	15.04	18.73	23%

#### 4.3.3.1 Cobalt

The highest single concentration of pore water, Fe-normalized total, and exchangeable Co was observed at or downslope of spring discharge in all four transects (Figure 4-4). In general, concentrations were not consistently higher downslope of spring discharge. Instead, there is generally one point along the transect that is much higher in concentration than the other samples from the transect.

**Pore Water Co:** The highest concentration of pore water Co was measured in the Top transect (Figure 4-5). Although pore water Co in the Bottom North transect is highest at the spring, the highest concentration is almost an order of magnitude lower than the other transects (Top = 0.07 mg/L, Middle = 0.04 mg/L, Bottom South = 0.02 mg/L, Bottom North = 0.003 mg/L). When

all values from the four transect locations are combined, downslope concentrations are significantly higher than upslope values (Table 4-2)

**Exchangeable Co:** In the Top, Middle, and Bottom South transects, the exchangeable Co concentrations are relatively consistent across the transect other than a single sample in each transect with elevated exchangeable Co (3 m downslope in Top transect, 9 m downslope in Middle, and at the spring in Bottom South, Figure 4-5). In contrast, exchangeable Co concentrations in the Bottom North transect steadily increases along the transect from the core collected nine meters upslope to the highest concentration measured in the core three meters downslope. Further, the core collected six meters downslope of the Bottom North spring has the lowest concentration of exchangeable Co.

**Fe-Normalized Total Co:** The highest Fe-normalized total Co concentrations were measured in the Top transect, similar to pore water concentrations (Figure 4-5). Although the Bottom North transect had a much lower maximum pore water concentration relative to other transects, Fe-normalized total Co concentrations were more consistent across transects. The Middle, Bottom North and Bottom South transects all significantly increase in concentration downslope of spring discharge (Table 4-1)

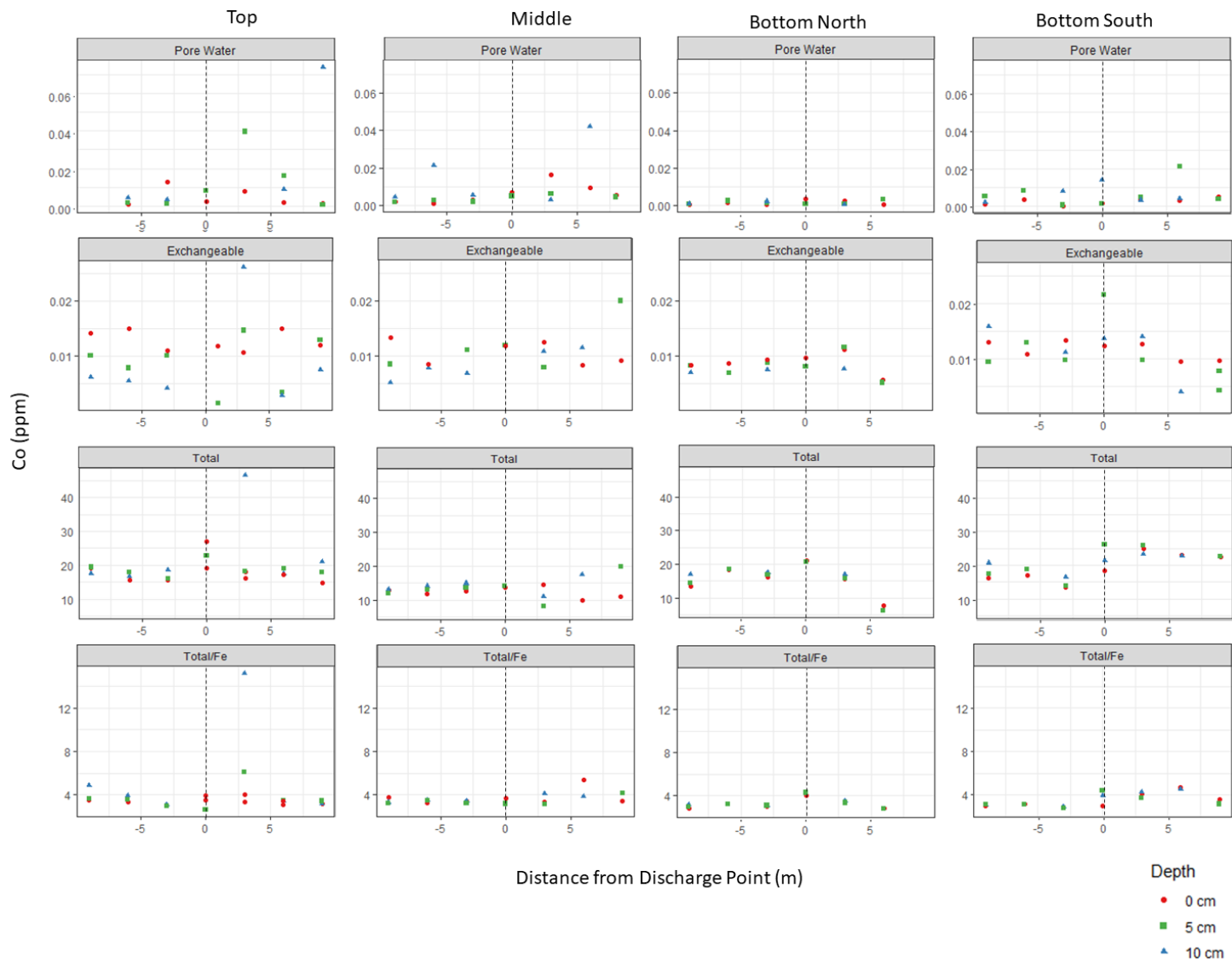


**Figure 4-5. Total, Fe-normalized, exchangeable, and pore water Co measured in soil cores collected along four transects intersecting groundwater springs. Black dotted lines indicate the location of groundwater discharge**

#### 4.3.3.2 Chromium

Almost all the elevated pore water, Fe-normalized total, and exchangeable Cr were observed at or downslope of spring discharge (Figure 4-6).

**Pore Water Cr:** Porewater Cr concentrations in the Middle and Bottom South transects both increase three meters downslope of the discharge point and remain elevated six meters downslope (Figure 4-6). In contrast, porewater Cr concentrations in the Top and Bottom North transect peak at the point of discharge. In these two transects, the cores collected three meters downslope have lower concentrations of Cr than those collected at the spring. Despite this variability, Cr concentrations in the Middle, Bottom North, and Bottom South transects all significantly increase in soils interacting with groundwater discharge (Table 4-1)

**Exchangeable Cr:** In general, exchangeable Cr concentrations are less variable than other metals considered in this study, with a coefficient of variation of 9% (Table 4-3). Concentrations of exchangeable Cr in the study transects were higher downslope in the Bottom North and Bottom South transects (Figure 4-6). In contrast, the top and middle exchangeable Cr concentrations are generally consistent across the sample transect. While Fe-normalized total Cr metal concentrations are lower down gradient in the Bottom South transect, exchangeable Cr concentrations are elevated downslope of the spring.

**Fe-Normalized Total Cr:** While the cores collected from the Top, Middle, and Bottom North transects all have elevated Fe-normalized Cr concentrations downslope of spring discharge, the Bottom South transect has the opposite pattern (Figure 4-6). Fe-normalized Cr concentrations in the Bottom South transect decrease at the point of discharge and remain lower than concentrations measured upslope of the spring throughout the downslope portion of the transect. The Top and Middle transects significantly increase downslope of spring discharge while the

Bottom North transect is trending toward significance (Table 4-1). When all transect measurements are combined, the downslope values are significantly higher than upslope concentrations (Table 4-2).

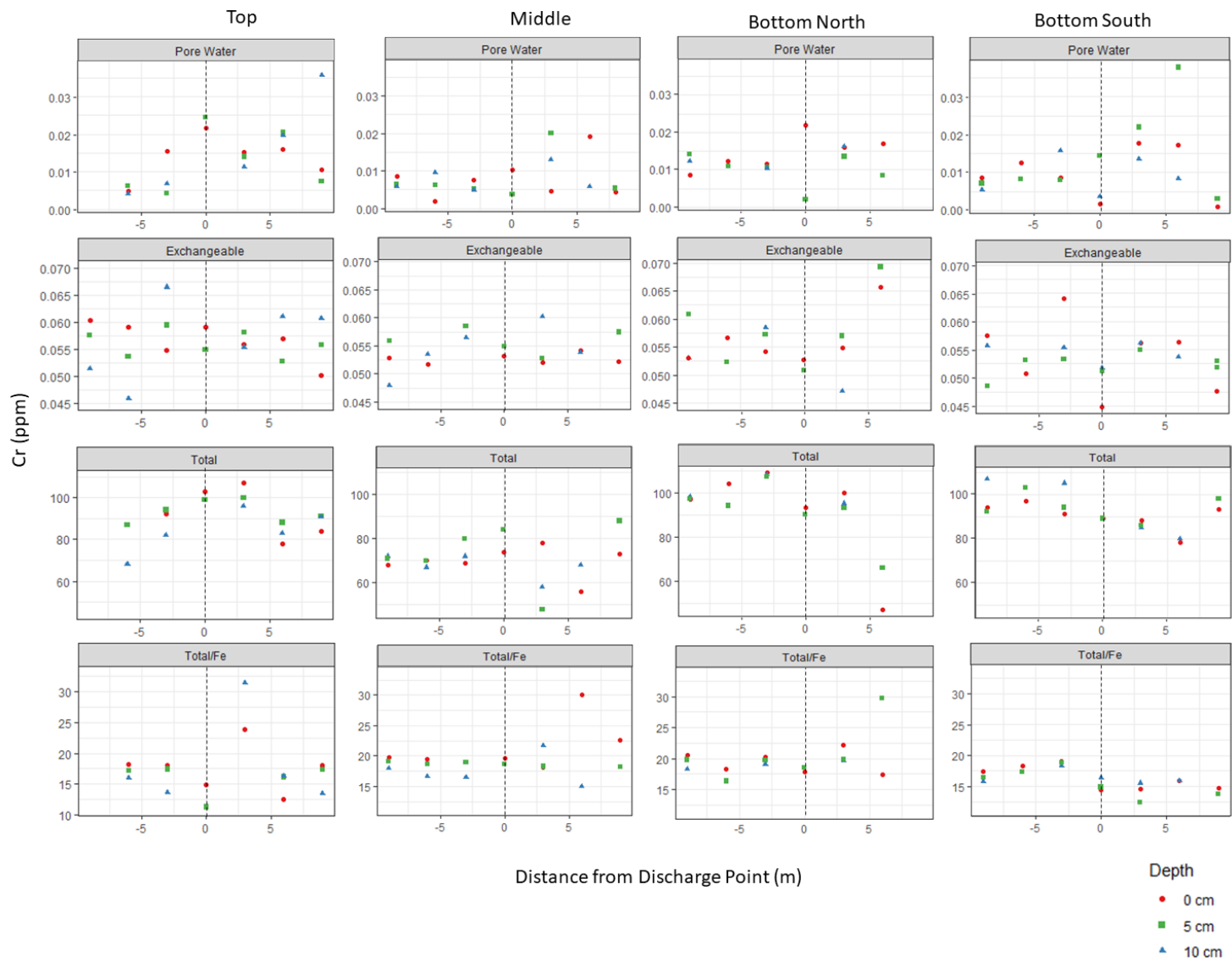


Figure 4-6. Total, Fe-normalized total, exchangeable, and pore water Cr measured in soil cores collected along four transects intersecting groundwater springs. Black dotted lines indicate the location of groundwater discharge

#### 4.3.3.3 Nickel

With two exceptions, the highest concentration of porewater, normalized total, and exchangeable Ni measured in the transects were measured at or downslope of spring discharge (Figure 4-7).

**Pore Water Ni:** Although the highest porewater Ni concentrations in the Middle transect were measured upslope of the spring, there is still a distinct increase in porewater Ni concentration between the core collected at the spring and the core collected three meters downslope (Figure 4-7). Dissolved Ni concentrations in the soil pore water of the Top transect vary widely with the highest concentration measuring two orders of magnitude higher than the lowest concentration. The Top and Middle transects increase significantly in pore water Ni concentrations downslope of spring discharge (Table 4-1). When all transect values are combined, there is a significant increase in pore water [Ni] in downslope soils (Table 4-2).

**Exchangeable Ni:** Top, Middle, and Bottom North transects all increase in exchangeable Ni concentration at or downslope of spring discharge (Figure 4-7). In contrast, the Bottom South transect has lower exchangeable Ni concentration in all cores collected at or downslope of the spring than concentrations measured in the upslope cores. The peak concentration of exchangeable Ni in the Top transect (at spring elevation) is the highest concentration measured, similar to patterns in porewater Ni and Fe-normalized total Ni.

**Fe-Normalized Total Ni:** Although the highest concentration of Fe-normalized total Ni was measured downslope of the point of discharge in all four transects, enrichment downslope is not as clear in the Bottom South transect (Figure 4-7). Ni concentrations at the spring and three meters downslope are lower than concentrations collected upslope of the spring. However, concentrations measured six meters downslope are the highest in the entire transect. The Top and

Middle transects have significantly higher concentrations in the downslope portions and the Bottom North transect is trending toward significance. However, the Bottom South transect decreases in Fe-normalized total Ni downslope of spring discharge (Table 4-1).

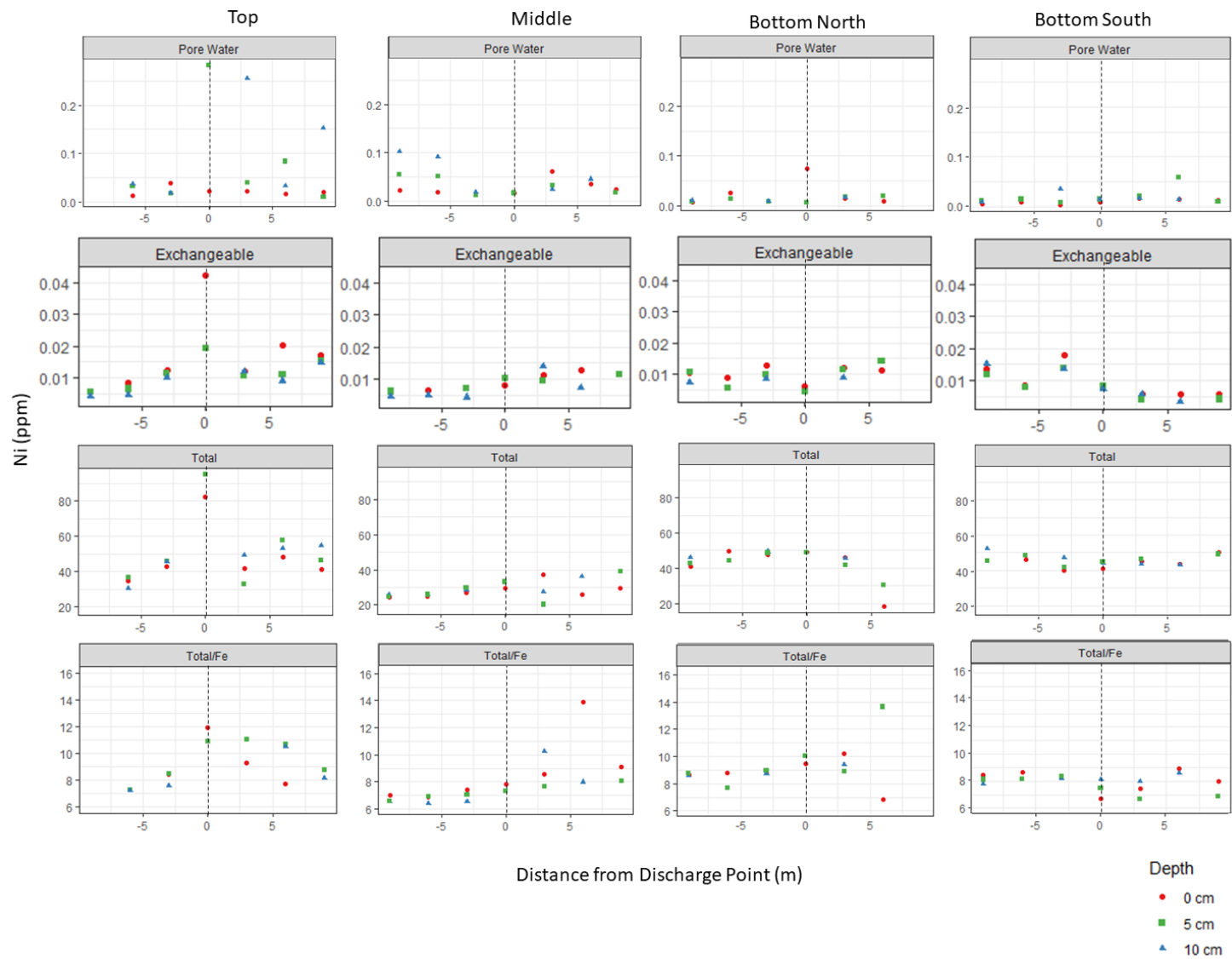


**Figure 4-7. Total, Fe-normalized total, exchangeable, and pore water Ni measured in soil cores collected along four transects intersecting groundwater springs. Black dotted lines indicate the location of groundwater discharge.**

#### 4.3.3.4 Vanadium

Like other trace metals, most concentrations of pore water, Fe-normalized total, and exchangeable V are highest at or downslope of spring discharge (Figure 4-8).

**Pore Water V:** V concentrations in the Bottom North transect are lower than the other three transects with several of the samples measuring at or below the detection limit. The highest concentration of dissolved V in the other three transects was measured at six meters below the spring (Figure 4-8). The highest concentrations of pore water V in the other three transects were measured in soil waters six meters below the springs. None of the individual transects were significantly different between the upslope and downslope pore water concentrations (Table 4-1). However, when all values from the transects were evaluated together, there was a significant increase in downslope pore water [V] (Table 4-2).

**Exchangeable V:** Unlike the other study transects, the highest concentration of exchangeable V in the Bottom South transect was measured three meters upslope of spring discharge (Figure 4-8). Three meters downslope of the spring in the Bottom South transect, exchangeable V concentrations are much lower than those measured at and upslope of the spring. This pattern is similar to exchangeable Ni concentrations in the Bottom South transect.

**Fe-Normalized Totals V:** The highest concentration of Fe-normalized V was measured in the deepest segment (10-15 cm) of the core in Top, Bottom North, and Bottom South transects (Figure 4-8). The Fe-normalized total [V] was significantly higher in the downslope portion of the Top, Middle, Bottom North and Bottom South transects (Table 4-1).

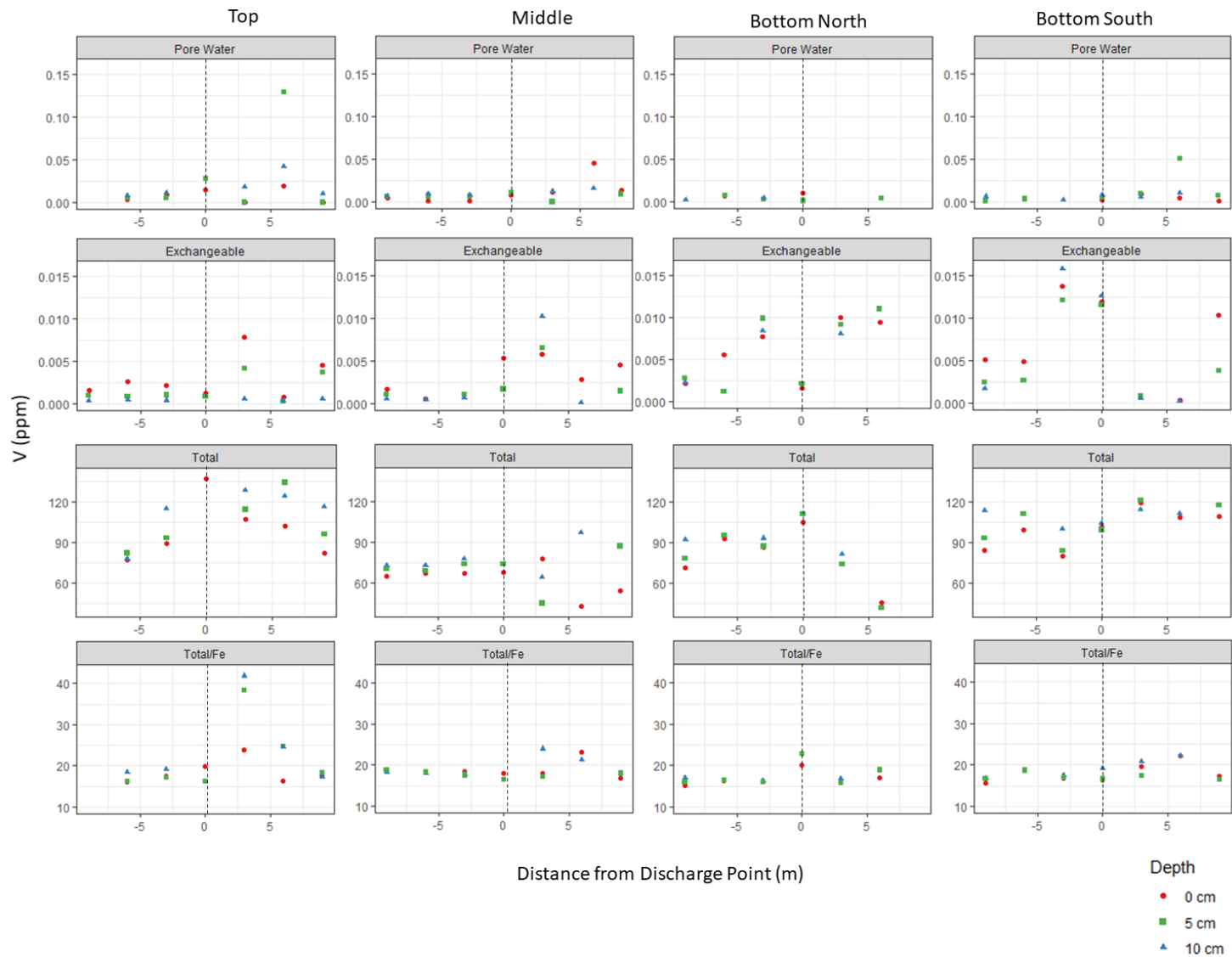


**Figure 4-8. Total, Fe-normalized total, exchangeable, and pore water V measured in soil cores collected along four transects intersecting groundwater springs. Black dotted lines indicate the location of groundwater discharge.**

## 4.4 Discussion

### 4.4.1 Lithium Concentrations

Lithium is enriched in urban water, especially as use has increased in the past two decades (Choi et al. 2019). Therefore, we interpret [Li] to indicate the influence of contaminated groundwater when compared to soil waters less impacted by human activities. When upslope values of pore water, exchangeable, and Fe-normalized total Li concentrations from all transects were compared to downslope values in all transects, downslope values were all significantly higher, suggesting enrichment of the soil environment in response to discharge of contaminated urban groundwater (Table 4-2). When exchangeable [Li] was evaluated at each transect, all of the downslope exchangeable Li concentrations were significantly higher. However, only in the top transect was downslope porewater [Li] significantly different from upslope values (Table 4-1). All within transect pore water concentration comparisons were likely affected by evaporation driven concentration in upslope soils. Spring water is not consistently introduced to upslope soils, so the soils dry out before downslope soils. The concentration of Li will increase as pore water is evaporated (Li has no obvious insoluble precipitate in these chemistries) and will therefore tend to be higher in upslope soils. This adds credence to the observation that down slope pore waters are elevated. These observations of [Li] across phases suggest contaminated groundwater is introduced by the spring and this water influences soil chemistry. Although Li concentrations indicate contributions of contaminated groundwater from urban sources, the legacy steel alloy

metals enter the groundwater through mobilization of soil contamination pools and may differ in contamination patterns at the point of groundwater discharge.

#### **4.4.2 Metal Concentrations in Soils Surrounding Groundwater Springs**

In general, Fe-normalized total concentrations are higher in soils downslope of groundwater springs, suggesting enrichment of metals from accumulated groundwater discharge. When evaluated separately by location and metal species, Fe-normalized total concentration was significantly higher downslope in 12 of 16 transects (Table 4-1). Of the four transects that were not significant most showed some evidence of enrichment (Figures 4-5 through 4-8). The heterogeneous nature of soils in general and the relatively small sample size at each transect may be insufficient to unambiguously reveal downslope enrichment. In particular, both Cr and Ni Fe-normalized total concentrations in the Bottom North transect had p-values trending towards significance (0.08 and 0.07 respectively). To evaluate groundwater-soil interactions across the study area, the metal concentrations at all of the transects were combined and upslope versus downslope patterns evaluated. Fe-normalized concentrations were significantly higher in soils downslope of discharging groundwater (Table 4-2). In general, all four transects seem to have been enriched in steel alloy metals over long time periods. Although this was predicted in the conceptual model, the distribution of metal contamination downslope of spring discharge was not as consistent as hypothesized in the model (Figure 4-1). For example, metal concentrations were not always highest right at the point of discharge and decreasing with distance downslope from the spring. Further, there was no consistent pattern with soil depth apparent in this study. Varying vegetation cover over the transect locations (i.e. forested vs grassy) and resulting soil carbon levels may impact the leaching of metals and contribute to the observed patterns. We are awaiting results to

analyze the impact of overlying vegetation. Despite these inconsistencies, spring discharge leads to elevated concentrations of trace metal contamination in downslope soils.

Pore water metal concentration patterns suggest that steel alloy metals are typically elevated in the spring discharges. However, pore water is more transient, increasing variability in the observations and is sensitive to soil moisture dynamics (see discussion above in the Li section). Only six of sixteen transect- metal combinations had statistically significant differences between soil waters above and below the spring discharge (Table 4-1). In particular, V pore water concentrations did not increase downslope of the springs. That said, V concentrations in pore water were often below detection limit and limited sample volume precluded the potential for re-measurement at lower dilutions. Nevertheless, when all transects were combined and evaluated pore water concentrations were higher for all metals in downslope soils (Table 4-2). Therefore, contaminated groundwater discharging from springs and seeps seems to create areas of elevated pore water contamination in soils receiving the discharge.

Steel alloy exchangeable metal concentrations did not systematically vary above/below the springs, potentially due to the exchangeability of transition metals relative to cations like Li and Na. Cation exchange sites in the soil tend to be better geochemical environments for these cations, introducing inconsistent patterns of exchangeable trace metal concentrations for these transition metals. For example, at the point of groundwater discharge in the Bottom North transect, the exchangeable concentrations of Cr, Ni, and V are lower than concentrations measured in the samples collected three meters upslope and downslope of the spring (Figures 4-6 through 4-8). Further, the highest concentration of pore water for all three of these metals was measured in the core collected at the point of discharge. As cations like Li and Na more readily bind to cation

exchange sites, trace metals may interact less with exchange sites. Therefore, transition metals may remain in the dissolved phase, resulting in more variable exchangeable concentrations.

Given the reliance on iron for Fe normalization, it's important to evaluate soil Fe patterns. Total Fe concentrations decrease downslope of spring discharge in the Middle and Bottom North transects (p-values = .001 and .007 respectively) while the Top and Bottom South transect are not significantly different in either direction (p-values = .162 and .445 respectively) (Figure 4-9). The concentration of Fe in the soil influences the amount of trace metals that accumulates in that soil as iron oxyhydroxides are a common binding site for trace metals. It is best to think of the Fe normalization as a measured rate of how trace metal interacts with available sorption sites. Higher normalized values suggest a stronger influence of the spring. Therefore, in the transects where iron decreases, while the total metal also decrease, it's generally at a slower rate, suggesting the spring water increases the total trace metal content.

**Table 4-4. Range of average total soil metal concentrations of Co, Cr, Ni, and V measured upslope and downslope of discharging springs divided by transect. Average total metal concentrations in other urban soil surveys. Maximum total concentrations measured in this study and maximum concentrations for ecological health.**

	<b>Co (ppm)</b>	<b>Cr (ppm)</b>	<b>Ni (ppm)</b>	<b>V (ppm)</b>
<b>Range of Upslope Means by Transect</b>	13-17	71-102	26-46	71-96
<b>Range of Downslope Means by Transect</b>	13-23	70-93	31-55	68-117
<b>Baltimore, MD mean (Yesilonis et al. 2008)</b>	15	72	27	37
<b>Chicago, IL mean (Cannon and Horton 2009)</b>	11	71	36	76
<b>Eco-SSL Plants</b>	13	N/A	38	N/A
<b>Eco-SSL Mammals</b>	230	34 (Cr III)	130	280
<b>EPA MSC Direct Contact Values</b>	66	190000 (Cr III)	4400	15

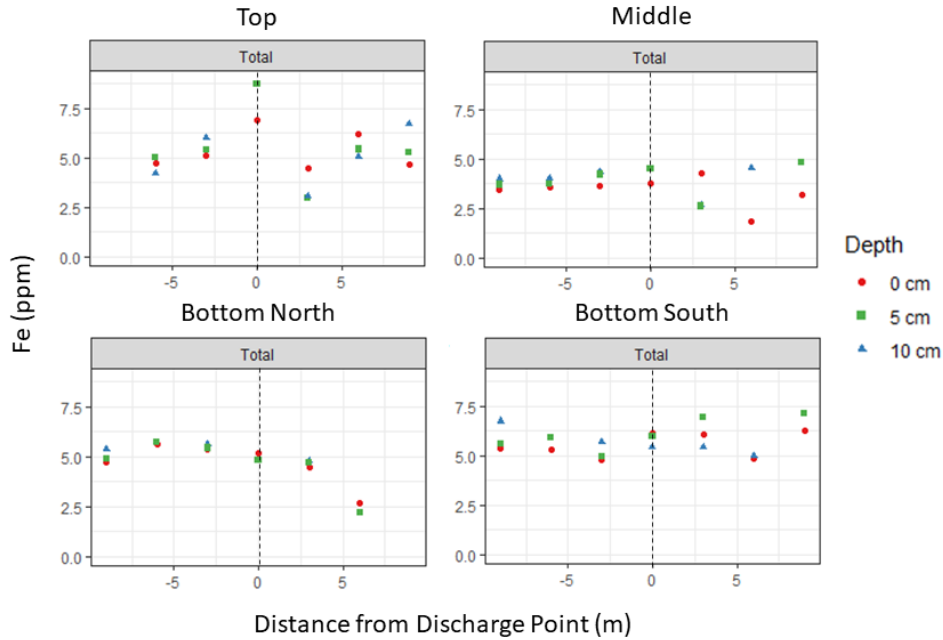


**Figure 4-9. Total Fe measured in soil cores collected along four transects intersecting groundwater springs. Black dotted lines indicated location of groundwater discharge.**

#### 4.4.3 Confounding Effects of Urban Soil Redistribution

There are several instances where Fe-normalized total concentrations decrease downslope, diverging from the conceptual model (Figure 4-1). In the Bottom South transect, Fe-normalized total Cr concentrations measured at or downslope of spring discharge are lower than concentrations measured upslope. While pore water Cr concentrations in the Bottom South transect are significantly higher, Fe-normalized total concentrations decrease (Table 4-1). Similarly, Fe-normalized total Ni concentrations in the downslope portion of the Bottom South transect are lower than upslope concentrations (Table 4-2). Further, Fe-normalized Ni concentrations measured in the deepest (10-15 cm), downslope core increments were highest. This pattern indicates the concentrations are diluted, particularly near the surface. Pore water concentrations are elevated at these locations, suggesting that relatively clean spring discharges do not cause the observed

decreases in Fe-normalized metals. However, this transect intersects a walking trail, and therefore soil disturbance or augmentation may cause this pattern.

The oxidation of metals as the groundwater moves downslope could potentially create the patterns observed in Cr in the Bottom South transect. The oxidation of Cr by manganese oxides in the soil could reduce the concentration of Fe-normalized total Cr in the transect (Fendorf and Zasoski 1992). However, Ni is not readily oxidized by manganese oxide compounds. As both Fe-normalized total Cr and Ni concentrations decrease downslope, the oxidation of Cr via manganese oxide seems less likely as the underlying mechanism.

Unlike [Cr] and [Ni], concentrations of Fe-normalized total Co and V are higher in the downslope portion of the Bottom South Transect (Table 4-1). One explanation for this is that materials introduced to the location during footpath construction were elevated only in Co and V. However, we cannot identify a source of contamination that would be elevated in [Co] and [V] but not [Ni] and [Cr]. Co and V may accumulate faster than Cr and Ni in downslope soils. However, this difference in accumulation rate is not obvious in any other transect. We do not have enough data to elucidate the causes of this pattern, but the footpath location suggests a role for some sort of soil disturbance.

#### **4.4.4 Total Metal Concentrations**

Average total concentrations tended to be higher in downslope soils than upslope soils, suggesting groundwater discharge driven enrichment. Despite variability in individual locations, the highest average concentrations of Co, Ni and V were measured in downslope soils. When compared to metal chemistries measured in other historically industrial cities, the highest downslope average concentrations of steel alloys are elevated (Table 4-4). The range of average

downslope concentrations for each metal generally spanned other city medians to higher values (Yesilonis et al. 2008; Cannon and Horton 2009). Therefore, the introduction of contaminated groundwater by springs seems to result in elevated areas of soil contamination.

The heavy metal enriched downslope soils often exceeded standards put in place to protect human and environmental health. Ecological soil screening levels (Eco-SSLs) are concentrations of contaminants in soil established to protect four different groups of ecological receptors (plants, soil invertebrates, birds, and mammals). The Eco-SSLs established by the EPA are a reasonable measure of the toxicity of heavy metals to ecological health (U.S. EPA 2005a, 2005b, 2005c, and 2007). The Pennsylvania Department of Environmental Protection also uses medium-specific concentrations (MSC) issued by the EPA as a point of compliance for soil metal concentrations. Medium-specific concentrations are concentrations that human populations could be directly exposed to on a daily basis without risk for the exposed population (35 P.S. Health and Safety). In the Top, Bottom North, and Bottom South transects, the downslope soil averages exceeded at least one Eco-SSL criteria or MSC for all four steel hardening agents, while the Middle transect exceeded standards for V and Cr concentrations (Table 4-4). Therefore, soils downslope of spring discharge in this study seem to be elevated in trace metal concentration and may pose a health risk to organisms that come into contact with them.

#### **4.5 Conclusions**

The spatial variability of legacy contamination associated with steel production in four soil transects straddling groundwater springs was assessed to evaluate the influence of contaminated groundwater discharge on surface contamination. Using multiple phases of metal concentrations,

the metal dynamics over multiple time scales were evaluated. When soils collected downslope of spring discharge were compared to soils collected upslope steel alloy metals were elevated downslope, particularly in the Fe-normalized total metal concentrations. This indicates that contaminated groundwater discharge enriches trace metal concentrations in downgradient soils. That said, patterns observed in the Fe-normalized Cr and Ni concentrations underline the inherent variability in urban soils. This enrichment has resulted in average downslope concentrations that exceed some EPA standards, creating regions of soil contamination that may pose risks to human and environmental health.

Further, this study suggests contaminated groundwater discharge at springs and seeps may redistribute soil contamination and create hot spots of soil metal contamination at predictable points along an urban landscape. Identification of this mechanism that concentrates soil metal contamination at specific hydrological locations, can improve predictions of trace metal exposures to humans and the ecosystem.

#### **4.6 Bibliography**

35 P.S. Health and Safety § 60626.303. Statewide health standard (Westlaw Edge)

Ajmone-Marsan F, Biasioli M. Trace elements in soils of urban areas. *Water Air Soil Pollut.* 2010 Nov;213(1-4):121–143.

Brooks PD, Chorover J, Fan Y, Godsey SE, Maxwell RM, McNamara JP, et al. Hydrological partitioning in the critical zone: Recent advances and opportunities for developing transferable understanding of water cycle dynamics. *Water Resour Res.* 2015 Sep;51(9):6973–6987.

- Cannon WF, Horton JD. Soil geochemical signature of urbanization and industrialization – Chicago, Illinois, USA. *Applied Geochemistry*. 2009 Aug;24(8):1590–1601.
- Choi H-B, Ryu J-S, Shin W-J, Vigier N. The impact of anthropogenic inputs on lithium content in river and tap water. *Nat Commun*. 2019 Dec 3;10(1):5371.
- Cobelo-García A, Prego R. Influence of point sources on trace metal contamination and distribution in a semi-enclosed industrial embayment: the Ferrol Ria (NW Spain). *Estuar Coast Shelf Sci*. 2004 Aug;60(4):695–703.
- Dieterich-Ward A. *Beyond rust: metropolitan pittsburgh and the fate of industrial america*. University of Pennsylvania Press; 2016.
- Effland WR, Pouyat RV. The genesis, classification, and mapping of soils in urban areas. *Urban Ecosystems*. 1997 Dec; 1(4):217-28.
- Essington ME. *Soil and water chemistry: an integrative approach*. CRC Press; 2004.
- Fendorf SE, Zasoski RJ. Chromium(III) oxidation by  $\delta$ -manganese oxide (MnO<sub>2</sub>). 1. Characterization. *Environ Sci Technol*. 1992 Jan;26(1):79–85.
- Gabor RS, Hall SJ, Eiriksson DP, Jameel Y, Millington M, Stout T, et al. Persistent urban influence on surface water quality via impacted groundwater. *Environ Sci Technol*. 2017 Sep 5;51(17):9477–9487.
- Luo X, Yu S, Zhu Y, Li X. Trace metal contamination in urban soils of China. *Sci Total Environ*. 2012 Apr 1;421-422:17–30.
- Mattielli N, Petit JCJ, Deboudt K, Flament P, Perdrix E, Taillez A, et al. Zn isotope study of atmospheric emissions and dry depositions within a 5 km radius of a Pb–Zn refinery. *Atmos Environ*. 2009 Feb;43(6):1265–1272.

PAMAP Program, PA Department of Conservation and Natural Resources, Bureau of Topographic and Geologic Survey, PAMAP Program LAS Files (LiDAR Data of Pennsylvania), Middletown, PA, 2006-2008

Pouyat RV, Yesilonis ID, Russell-Anelli J, Neerchal NK. Soil Chemical and Physical Properties That Differentiate Urban Land-Use and Cover Types. *Soil Sci Soc Am J.* 2007;71(3):1010.

Reay WG, Gallagher DL, Simmons GM. Groundwater discharge and its impact on surface water quality in a Chesapeake Bay inlet. *J Am Water Resources Assoc.* 1992 Dec;28(6):1121–1134.

Rivett MO, Ellis PA, Mackay R. Urban groundwater baseflow influence upon inorganic river-water quality: The River Tame headwaters catchment in the City of Birmingham, UK. *J Hydrol (Amst).* 2011 Mar;400(1-2):206–222.

Rozemeijer JC, Broers HP. The groundwater contribution to surface water contamination in a region with intensive agricultural land use (Noord-Brabant, The Netherlands). *Environ Pollut.* 2007 Aug;148(3):695–706.

Tarr JA, editor. *Devastation and renewal: an environmental history of Pittsburgh and its region.* University of Pittsburgh Press; 2004.

USEPA. Ecological Soil Screening Levels for Chromium; OSWER Directive 9285.7-66. 2005a.

USEPA. Ecological Soil Screening Levels for Cobalt; OSWER Directive 9285.7-67. 2005b.

USEPA. Ecological Soil Screening Levels for Vanadium; OSWER Directive 9285.7-75. 2005c.

USEPA. Ecological Soil Screening Levels for Nickel; OSWER Directive 9285.7-76. 2007.

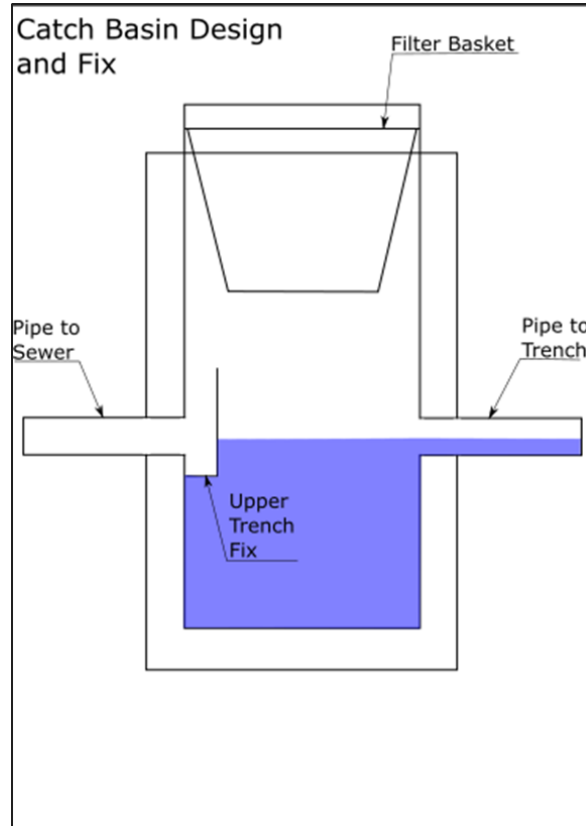
Vermillion B, Brugam R, Retzlaff W, Bala I. The sedimentary record of environmental lead contamination at St. Louis, Missouri (USA) area smelters. *J Paleolimnol.* 2005 Feb;33(2):189–203.

Wu W, Wu P, Yang F, Sun D-L, Zhang D-X, Zhou Y-K. Assessment of heavy metal pollution and human health risks in urban soils around an electronics manufacturing facility. *Sci Total Environ.* 2018 Jul 15;630:53–61.

Yesilonis ID, Pouyat RV, Neerchal NK. Spatial distribution of metals in soils in Baltimore, Maryland: role of native parent material, proximity to major roads, housing age and screening guidelines. *Environ Pollut.* 2008 Dec;156(3):723–731.

Yusuf M, Fariduddin Q, Hayat S, Ahmad A. Nickel: an overview of uptake, essentiality and toxicity in plants. *Bull Environ Contam Toxicol.* 2011 Jan;86(1):1–17.

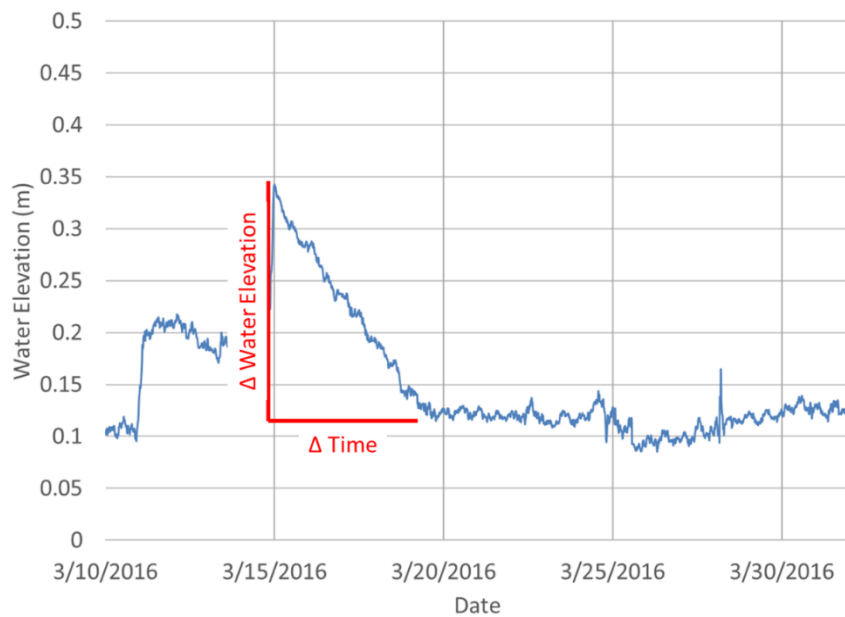
## Appendix A Chapter 2 Supporting Information



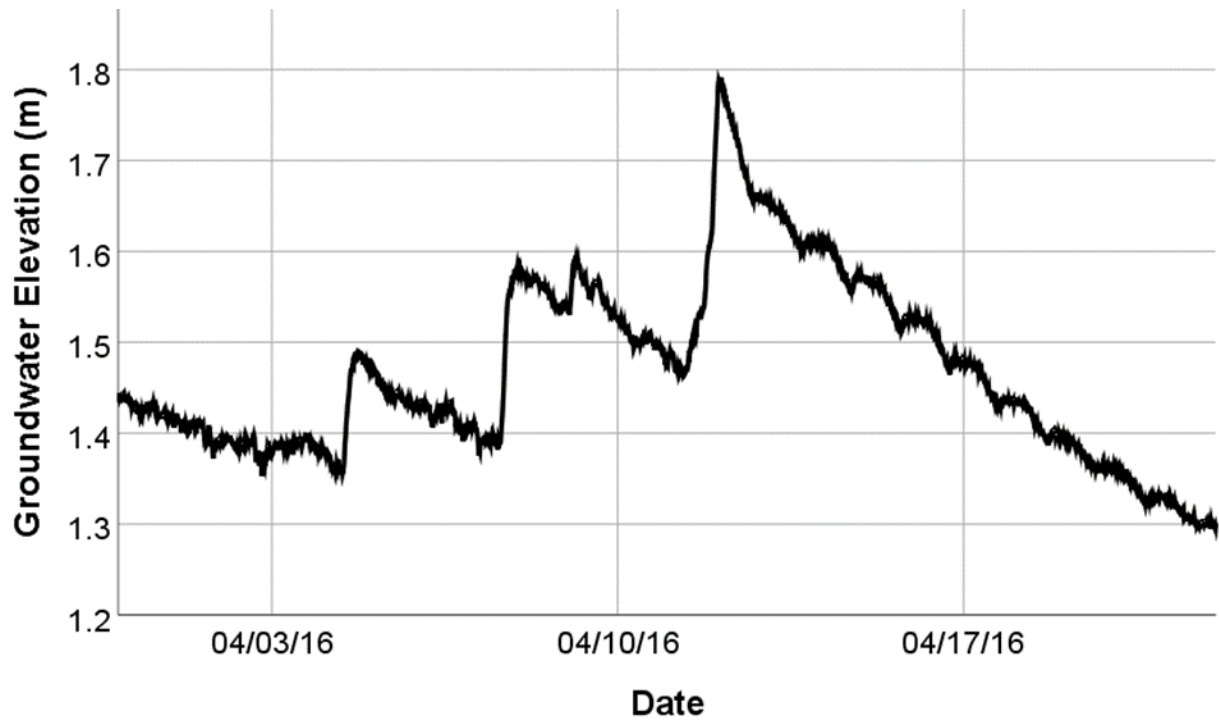
Appendix Figure A-1. Design of fix installed in the upper infiltration trench.



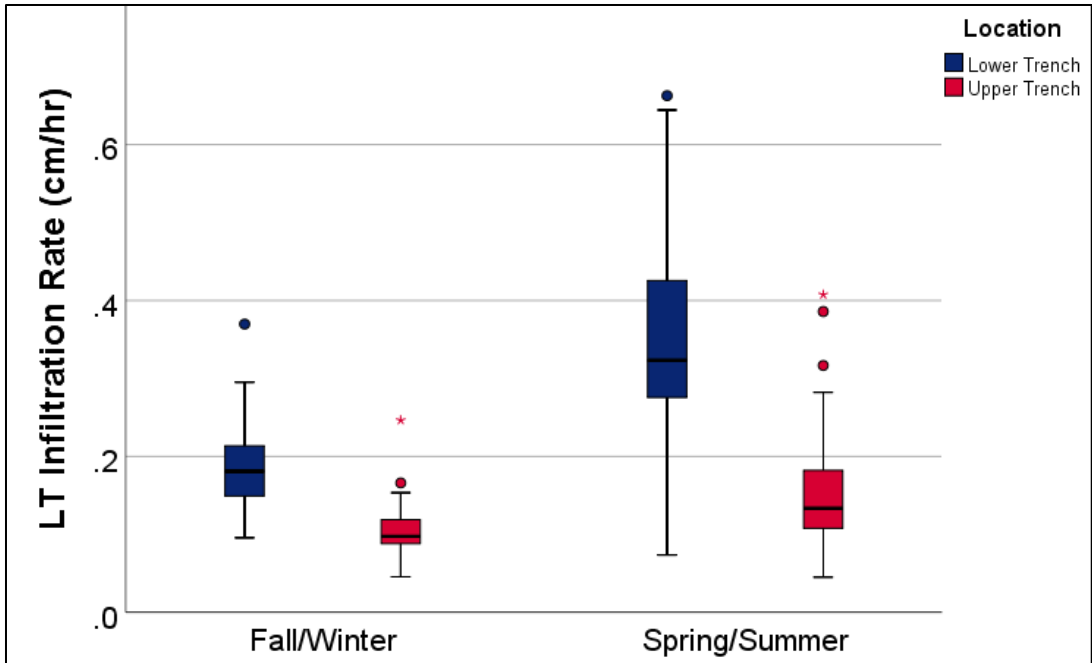
**Appendix Figure A- 2. Map of soil metal collection points for metal analyses surrounding infiltration trenches in Schenley Park, Pittsburgh, PA (Allegheny County Division of Computer Services Geographic Information Systems Group Allegheny County Imagery 2017).**



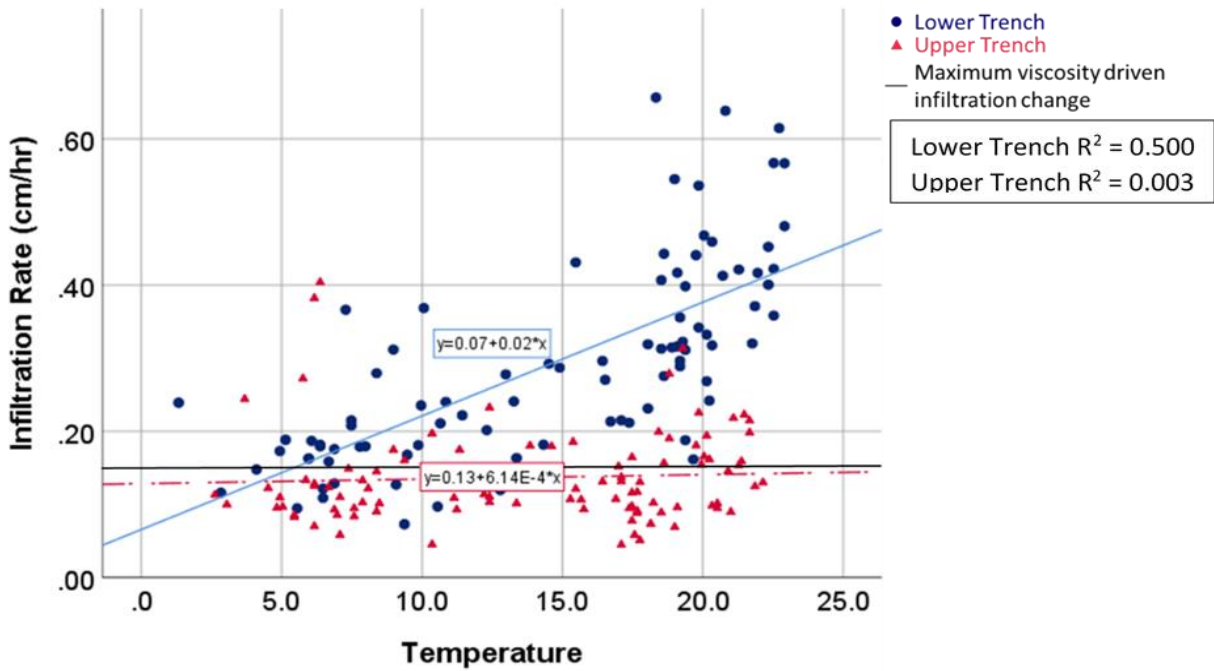
**Appendix Figure A-3. Example infiltration event measured to calculate infiltration rate from the lower trench.**



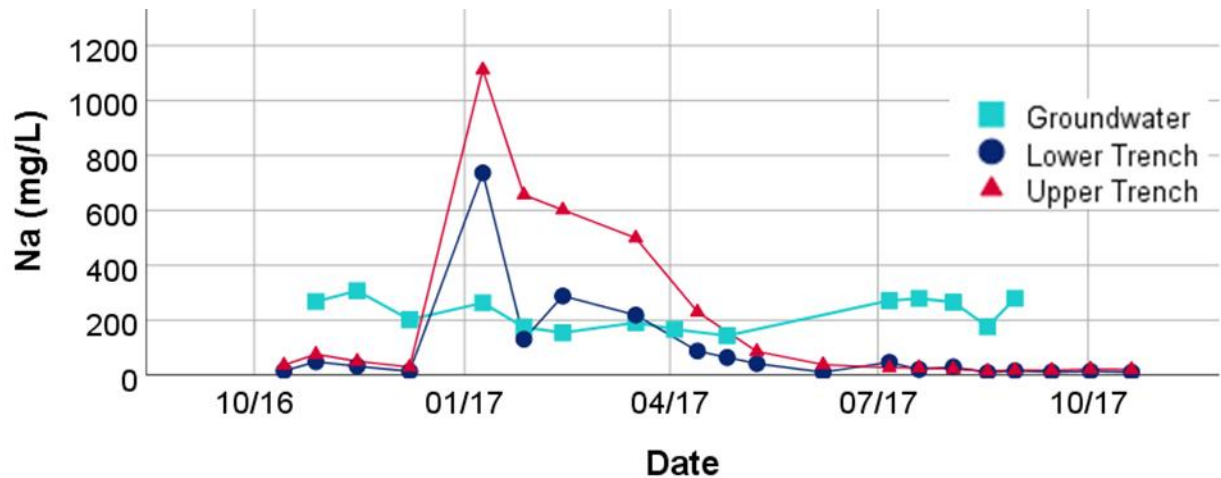
**Appendix Figure A-4. Groundwater table fluctuations showing the onset of evapotranspiration driven diurnal patterns starting on April 12, 2016.**



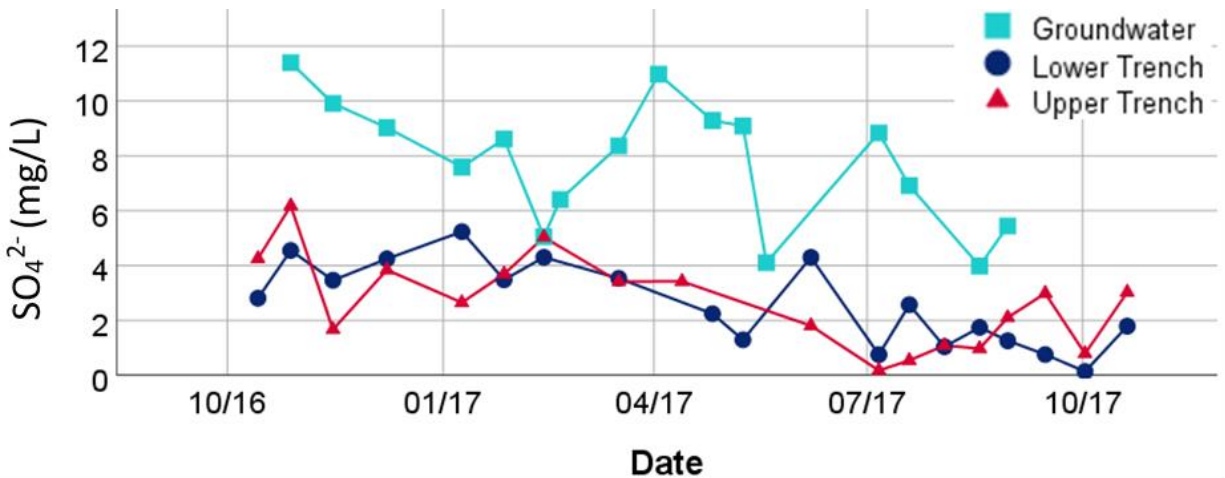
Appendix Figure A-5. Box plots showing seasonal distributions of infiltration rates for both infiltration trenches



Appendix Figure A-6. Comparison of change in infiltration rate compared to changes in temperature. Black line indicates highest possible infiltration rate calculated using temperature driven viscosity changes. The observed changes in infiltration rate are much higher than those expected of viscosity driven changes.



Appendix Figure A-7. Dissolved concentrations of sodium in infiltration trenches and nearby groundwater spring between January 2016 and October 2017.



Appendix Figure A-8. Dissolved concentrations of sulfate in infiltration trenches and nearby groundwater spring between October 2016 and October 2017.

Appendix Table A-1. Maximum, minimum, average, and standard deviation of concentrations of dissolved cations and anions in two infiltration trenches over the entire time of collection (January 2016 – January 2018).

(BDL = Below Detectable Limit)

(mg/L)	Na	Pb	Cu	Mn	Fe	Cd	Zn	NO <sub>3</sub>	SO <sub>4</sub>
<b>Lower Trench Max.</b>	737	0.0005	0.026	1.04	2.24	0.002	0.944	12.5	11.25
<b>Lower Trench Min.</b>	4.39	BDL	BDL	BDL	BDL	BDL	BDL	0.06	0.14

<b>Lower Trench Avg.</b>	123	0.0002	0.005	0.15	0.51	0.00007	0.168	3.86	3.57
<b>Lower Trench St. Dev.</b>	178	0.0002	0.006	0.21	0.46	0.0004	0.347	3.41	2.24
<b>Upper Trench Max.</b>	1280	0.002	0.046	1.92	4.28	0.002	0.884	16.0	9.32
<b>Upper Trench Min.</b>	14.2	BDL	BDL	0.003	BLD	BDL	BDL	0.05	0.17
<b>Upper Trench Avg.</b>	267	0.0003	0.008	0.585	0.75	0.00007	0.166	2.59	3.12
<b>Upper Trench St. Dev.</b>	359	0.001	0.009	0.481	0.90	0.0004	0.337	3.43	2.37

Appendix Table A-2. Comparison of total range of dissolved metal and nutrient concentrations measured in the upper infiltration trench (UT) and lower infiltration trench (LT) water between January 2016 – December 2017 and June 22, 2018 – June 28, 2018.

(Mg/L)	Na	Pb	Cu	Mn	Fe	Cd	NO <sub>3</sub>	SO <sub>4</sub>
<b>Total UT Range</b>	1270	0.002	0.05	1.92	4.28	0.002	16.0	9.14
<b>Total LT Range</b>	732	0.0005	0.026	1.04	2.24	0.002	12.4	11.12
<b>Daily UT Range</b>	20.4	0.0007	0.005	0.33	0.59	0.00004	0.68	0.67
<b>Daily LT Range</b>	15.7	0.0007	0.009	0.13	0.83	0.00003	0.91	0.81

Appendix Table A-3. Average bulk metal soil concentrations collected in Pittsburgh, PA compared to concentrations measured in previous studies of urban soil contamination.

Location Avg.	Cd (ppm)	Cr (ppm)	Cu (ppm)	Pb (ppm)	Zn (ppm)
<b>Albany (Amrhein et al. 1992)</b>	0.35	59	33	41.5	n/a
<b>Buffalo (Amrhein et al., 1992)</b>	1.4	63.5	42.5	151	n/a
<b>Cape Cod (Amrhein et al., 1992)</b>	0.43	14.5	4.3	6.2	n/a
<b>Donner (Amrhein et al., 1992)</b>	0.22	35.5	22	79.5	n/a
<b>Baltimore (Pouyat et al. 2007)</b>	0.11	72	45	231	141
<b>Gwynns Falls (Bain et al. 2012)</b>	0.17	31	30	76	120
<b>Pittsburgh Study Site</b>	1.4	100.3	44.3	195	137

## **Appendix A.1 Bibliography**

- Amrhein C, Strong JE, Mosher PA. Effect of deicing salts on metal and organic matter mobilization in roadside soils. *Environ Sci Technol*. 1992 Apr;26(4):703–709.
- Bain DJ, Yesilonis ID, Pouyat RV. Metal concentrations in urban riparian sediments along an urbanization gradient. *Biogeochemistry*. 2012 Feb;107(1-3):67–79.
- Pouyat RV, Yesilonis ID, Russell-Anelli J, Neerchal NK. Soil Chemical and Physical Properties That Differentiate Urban Land-Use and Cover Types. *Soil Science Society of America Journal*. 2007;71(3):1010.